Characterizing population pharmacokinetic / pharmacodynamic relationships in pulmonary tuberculosis infected adults using nonlinear mixed effects modelling

by

Wynand Anton Smythe

Division of Clinical Pharmacology, Department of Medicine

University of Cape Town

A thesis submitted in fulfilment of the requirements for the degree of Doctor of Philosophy (PhD)

Primary Supervisor: Prof Helen McIlleron

Co-supervisor: Dr Paolo Denti

June 2016

” If I can't picture it, I can't understand it”

Albert Einstein

” DEAR GOD - HELP ME BE THE PERSON MY DOG THINKS I AM”

Miscellaneous

Contributions to the field

This thesis has made a variety of contributions to the fields of pharmacology and pharmacometrics including but not limited to the following:

Peer reviewed publications

Smythe W, Khandelwal A, Merle CS, Rustomjee R, Gninafon M, Lo MB, Bah-Sow O, Olliaro PL, Lienhart C, Horton J, Smith P, McIlleron H, Simonsson USH. 2012. A semimechanistic pharmacokinetic-enzyme turnover model for Rifampin autoinduction in adult tuberculosis patients. Antimicrob. Agents Chemother. 56(4):2091. DOI: 10.1128/AAC.05792-11.

Smythe W, Merle CS, Rustomjee R, Gninafon M, Lo MB, Bah-Sow O, Olliaro PL, Lienhart C, Horton J, Smith P, McIlleron H, Simonsson USH. 2013. Evaluation of initial and steady-state Gatifloxacin pharmacokinetics and dose in pulmonary tuberculosis patients by using Monte Carlo simulations. Antimicrob. Agents Chemother. 57(9):4164. DOI: 10.1128/AAC.00479-13.

Conference presentations

Smythe W, McIlleron H, Smith P, Simonsson USH. Semi-Mechanistic pharmacokinetic enzyme model for the characterisation of rifampicin pharmacokinetics in South African pulmonary tuberculosis infected adults. *Annual Meeting of the Population Approach Group in Europe*. St Petersburg, Russia. June 2009.

Smythe W, McIlleron H, Smith P, Simonsson USH. Semi-Mechanistic pharmacokinetic enzyme model for the characterisation of rifampicin pharmacokinetics in South African pulmonary tuberculosis infected adults. *5th International Congress on Pharmaceutical and Pharmacological Sciences*. Potchefstroom, South Africa. September 2009.

Smythe W, McIlleron H, Merle C, Horton J, Smith P, Simonsson USH. A Semi-Mechanistic pharmacokinetic auto-induction model for the characterisation of rifampicin pharmacokinetics in African pulmonary tuberculosis infected adults. *Annual Meeting of the Population Approach Group in Europe*. Berlin, Germany. June 2010

Smythe W, Merle CS, Rustomjee R, Gninafon M, Lo MB, Bah-Sow O, Olliaro PL, Lienhart C, Horton J, Smith P, Simonsson USH, McIlleron H. Steady state Gatifloxacin pharmacokinetics in adult tuberculosis patients. *3rd International Workshop on Clinical Pharmacology of Tuberculosis Drugs*. Boston, USA. September 2010.

Smythe W, Merle CS, Rustomjee R, Gninafon M, Lo MB, Bah-Sow O, Olliaro PL, Lienhart C, Horton J, Smith P, McIlleron H, Simonsson USH. Population pharmacokinetics of gatifloxacin in African adults with pulmonary tuberculosis. *5th African Congress of Basic and Clinical Pharmacology* Accra, Ghana. July, 2012.

Smythe W, Pasipanodya JG., Merle CS, Olliaro PL, Gumbo T, Denti P, McIlleron H. Predictors of 2 month culture conversion in pulmonary tuberculosis. *46th Union World Conference on Lung Health* Cape Town, South Africa. December, 2015.

Declaration of work

Under the guidance of my supervisors, my role as the PhD student was as follows:

- Receive and store pharmacokinetic samples couriered from the study sites according to protocol specifications until drug concentration determination (-80℃).
- Assay pharmacokinetic samples for drug concentration using validated LCMS/MS methods in the ISO17025 compliant and accredited laboratory in the Division of Clinical Pharmacology, University of Cape Town, South Africa.
- Formulate the aims and design of the population pharmacokinetic (PK) models for rifampicin, isoniazid, pyrazinamide, ethambutol, and gatifloxacin.
- Formulate the aims and design of the pharmacokinetic and pharmacodynamic (PK/PD) analysis using classification and regression tree analysis.
- Analyse and interpret the results from population PK and PK/PD analysis.
- Write and submit the thesis for examination.

As the PhD student I had no role in the design or conduct of the clinical pharmacokinetic sub-study. Furthermore, Dr Khandelwal performed the linearized SCM method for covariate selection in chapter 4 of this thesis.

Abstract

Characterizing population pharmacokinetic / pharmacodynamic relationships in pulmonary tuberculosis infected adults using nonlinear mixed effects modelling

Wynand Anton Smythe

This pharmacokinetic sub-study was nested within the phase-III OFLOTUB study investigating the shortening of tuberculosis treatment. A total of 343 adults enrolled in Benin, Guinea, Senegal, and South Africa were randomized to receive rifampicin, isoniazid, pyrazinamide, and ethambutol in the standard 6-month control regimen or the 4-month test regimen where gatifloxacin replaced ethambutol. The pharmacokinetics of all drugs was described at first dose and steady-state using nonlinear mixed-effects modelling, and individual exposures were summarised as area under the concentration-time curve (AUC_{0-24}) and peak concentration. Autoinduction of rifampicin metabolism was characterized with a semi-mechanistic enzyme turn-over model. Gatifloxacin dose was evaluated using Monte Carlo simulations. Lastly, Classification & Regression Tree (CART) analysis techniques were used to identify factors predictive of 2-month culture conversion or 24-month long-term composite outcome.

Consistent with literature findings, approximately 73.0, 43.0, 0.3, 6.0 and 0.0% of patients failed to achieve previously reported target concentrations for rifampicin, isoniazid, pyrazinamide, ethambutol, and gatifloxacin, respectively. The rifampicin enzyme turn-over model showed similar reductions of 41% and 42% in AUC_{0-24} following daily 450 and 600 mg doses, suggesting that increasing rifampicin dose is unlikely to result in higher magnitudes of autoinduction. The median gatifloxacin steady-state AUC_{0-24} was 41.2 mg·h/L, 14.3% lower than the value after the first dose. Simulations reveal that 400 mg/day achieves effective exposure (>90% of patients) only for *Mycobacterium tuberculosis* strains with minimum inhibitory concentration <0.125 mg/L, suggesting higher gatifloxacin doses for optimal outcome. CART revealed test arm patients having better culture conversion rates while control arm patients had superior long-term outcome. In the control arm, increased rifampicin exposure improved the likelihood of successful culture conversion, while a negative effect of isoniazid concentration observed in the test arm suggested antagonism with the other drugs. Increased ethambutol and rifampicin exposure improved the long-term outcome in control arm patients, while in test arm a negative effect of pyrazinamide concentration was observed, partly overcome in patients who achieved higher rifampicin concentrations. Overall, drug exposure was a stronger outcome predictor compared to non-pharmacokinetic factors including baseline parasite burden, cavity, and HIV status.

Acknowledgements

This thesis could not have been undertaken without the generous funding received from a number of funders. The World Health Organization (WHO)/Special Programme for Research and Training in Tropical Diseases (TDR) and the Research Institute for Development (IRD) are gratefully acknowledged for support through grant ICA4-CT 2002-10057. I will always be grateful for the top-up bursary support provided by Professor Peter Smith and Professor Helen McIlleron.

I have had the privileged position of being supervised by a group of astute and stimulating academics. Professor Helen McIlleron is thanked for offering me this opportunity despite me not having had a modelling background. Her guidance and clinical insight are greatly appreciated and taught me a great deal. I am grateful to Professor Peter Smith, his support has enabled me to grow both academically and as a person. I am indebted to Dr Paolo Denti for all he has taught me. His mathematical insight has been invaluable. Thank you to you all for providing me with all the teaching opportunities during my many years at the department as well.

The contributions of the following co-authors of the papers emanating from this thesis are gratefully acknowledged: Prof Ulrika Simonsson and Dr Akash Khandelwal (Department of Pharmaceutical Biosciences, Uppsala University), Dr Corinne Merle (Department of Epidemiology and Population Health, London School of Hygiene and Tropical Medicine), Dr Roxana Rustomjee (Unit for Clinical and Biomedical TB Research, Medical Research Council), Prof Martin Gninafon (Programme National de Lutte contre la Tuberculose, Bénin), Dr Mame Bocar Lo (Programme National de Lutte contre la Tuberculose, Senegal), Prof Oumou Bah Sow (Service Pneumo-phtisiologie, Guinea), Dr Piero L. Olliaro (UNICEF/UNDP/World Bank/WHO Special Programme on Research and Training in Tropical Diseases (TDR), World Health Organization), Dr Christian Lienhardt (Institut de Recherche pour le Développement, France) and Dr John Horton (Tropical Projects, Hitchin Tropical Projects, Hitchin). Prof Tawanda Gumbo and Dr Jotam Pasipanodya are thanked for their input into the CART analysis presented in Chapter 7.

Many thanks go to the trial staff and patients involved in this study. The Service Laboratory of the Division of Pharmacology, headed by Professor Peter Smith and his amazing support

staff including Jenny Norman, Dr Dale Taylor, Dr Sandy Meredith, Afia Fredericks, and Alicia Evans, is thanked for the processing and analysis of pharmacokinetic study samples. The pharmacometric group within the Department of Pharmaceutical Biosciences, Uppsala University are thanked for hosting my multiple three month stints to Sweden, during which I learnt so much. Novartis Pharma, specifically Dr Collin Pillai, Dr Thomas Bouillion, and Dr Jean-Louis Steimer, are gratefully acknowledged for hosting and mentoring me during a three month internship undertaken during this degree. I hope to pass on the skills I learnt to others in the field.

I am grateful to the Pharmacometric Group at the University of Cape Town, headed by Dr Paolo Denti, for the many hours of stimulating discussion held during our weekly laboratory meetings with my fellow students including Dr Jan-Stefan Van Der Walt, Dr Emmanuel Chigutsa, Dr Simba Zvada, Dr Eddy Kimba Phongi, Andrzej Bienczak, Maxwell Chirehwa, Miné de Kock, and Retsilisitsoe Moholisa.

Lastly, but importantly, a special thanks must go to my family whom without their love and support none of this would have been possible. To my wife Tamara and children Kierha and Damian, you made this possible!

Table of Contents

Abbreviations

A_{ENZ}	amount of enzyme
AUC	area under the plasma drug concentration-time curve
$AUC_{0-\infty}$	AUC from 0 to infinity hours
AUC_{0-24}	AUC from 0 to 24 hours
CART	classification and regression tree analysis
CFR	cumulative fraction of response
CL	clearance
C_{MAX}	maximum concentration
DOT	directly observed therapy
EBA	early bactericidal activity
EBE	empirical Bayes estimates
EMB	ethambutol
FFM	fat-free mass
FOCE	first-order conditional estimation method
FOCE INTER	first-order conditional estimation method with interaction
GFX	gatifloxacin
HIV	human immunodeficiency virus
IIV	inter-individual variability
INH	isoniazid
IOV	inter-occasional variability
IPRED	individual predictions
k_a	absorption rate constant
k_{ENZ}	rate constant for the first-order degradation of the enzyme pool
LLOQ	lower limit of quantification
MDR-TB	multidrug-resistant tuberculosis

MIC	minimum inhibitory concentration
MTB	*Mycobacterium tuberculosis*
MTT	mean transit time
N	number of transit compartments
NFM	normal fat mass
NONMEM	Non-linear Mixed Effects Modelling
OFV	objective function value
OR	Odds Ratio
P-gp	P-glycoprotein
PsN	Pearl-speaks-NONMEM
PTA	probability of target attainment
PXR	pregnane X receptor
PZA	pyrazinamide
Q	inter-compartmental clearance
RMP	rifampicin
SCM	stepwise covariate model building
SD	standard deviation
TB	tuberculosis
TVP	typical value of parameter
V	apparent volume of distribution
V_c	apparent volume of distribution for central compartment
V_p	apparent volume of distribution for peripheral compartment
WHO	world health organization
XDR-TB	extensively drug-resistant tuberculosis
η	difference between population and individual parameter estimation
ω^2	variance of η

List of Figures

List of Tables

1. General Introduction

Tuberculosis is an infectious disease caused by the bacillus *Mycobacterium tuberculosis* (MTB) and was first described by Robert Koch in 1882 (Cambau and Drancourt 2014). Typically, these aerobic bacilli are spread through the air and affects the lungs, resulting in a disease diagnosed as pulmonary tuberculosis. Alternatively, this bacterium may affect other sites and is then recognised as extra-pulmonary tuberculosis. This infectious disease is a global health problem with an estimated 9.6 million people developing the disease and 1.5 million succumbing to it in 2014 (World Health Organization 2015). Notably though, approximately one third of the world's population infected with *M. tuberculosis* do not develop symptoms as the bacteria remain dormant (Zhang 2004). This condition is known as latent tuberculosis infection. However, the infection can become active, an occurrence often observed in people with a weakened immune defence such as those who become co-infected with the human immunodeficiency virus (HIV) (Torres-Gonzalez et al. 2013). Ultimately tuberculosis (TB) is the leading cause of death in many patients co-infected with HIV. This is exemplified in approximately a third of the estimated 1.2 million global deaths due to HIV being recorded in patients co-infected with tuberculosis in 2014 (World Health Organization 2015). In 2013, South Africa was reported as having the third highest incidence of tuberculosis worldwide with approximately 1% of the 50 million population developing active disease and approximately 60% of these cases co-infected with HIV (Kanabus 2016). *Mycobacterium bovis*, the primary causative agent of zoonotic tuberculosis (commonly known as bovine tuberculosis), infects humans primarily through close contact with infected animals or consumption of contaminated unpasteurized milk (Müller et al. 2013). Animal wildlife reservoirs (epically common in African countries having many national parks and nature reserves) ensure the persistence of zoonotic tuberculosis and likely increase the incidence of the disease (Müller et al. 2013). Although the reported incidence of bovine tuberculosis is low, surveillance activities remain insufficient, likely under predicting true prevalence in developing countries (Cosivi et al. 1998). As many diagnostics tests are unable to distinguish between zoonotic and human infections and are unable to detect the latent form of infection, treatment programs face challenges as they attempt to offer effective treatment to people afflicted with tuberculosis further impacting the burden of this disease African countries.

1.1. Challenges in optimizing current tuberculosis treatment

The majority of rapidly growing bacilli, known as log-phase or exponential-phase growth, are killed within the first 2 days of tuberculosis treatment, yet it takes 6 months of treatment to prevent relapse of the disease (Mitchison 2000; Hall et al. 2009). The primary goal of tuberculosis treatment is to rapidly kill metabolically active bacteria, minimize the emergence of drug resistance in the organisms and sterilize the host from metabolically inactive bacterium (persisting organisms) thereby preventing relapse (Mitnick et al. 2009). Bacilli not killed within first few days of treatment are likely bacteria in a dormant or non-replicating phase of development that have the capacity to revive and activate disease at a later time (Wayne and Hayes 1996; Shleeva et al. 2002). Alternatively, bactericidal activity may cease because of the emergence of drug resistance, and not necessarily the depletion of bacilli in log-phase growth (Gumbo et al. 2007a). Notably, Chigutsa et al, using a pharmacodynamic model, identified two rates of sputum bacillary burden decline (Chigutsa et al. 2015). The model firstly identified a rapidly declining rate (possibly indicative of metabolically active microorganisms declining rapidly under drug pressure) followed by a more slowly declining rate (possibly indicative of a population of persisting bacilli declining more slowly under drug pressure but which are not dormant or non-replicating). The World Health Organisation treatment guidelines (World Health Organization 2010) recommend that patients receive a 6-month rifampicin containing regimen comprised of 2-months daily rifampicin, isoniazid, pyrazinamide and ethambutol followed by 4-months of daily rifampicin and isoniazid for treatment of drug susceptible tuberculosis (World Health Organization 2010). One of the primary challenges for tuberculosis treatment is patient adherence to treatment (Mitchison and Davies 2012). To address this the WHO introduced a strategy of directly observed therapy (DOT) to help improve treatment adherence. However, in addition to the high cost and labour-intensity of the program, a systematic review established that this strategy is failing to improve treatment compliance relative to self-administered treatment (Karumbi and Garner 2015). As a result of treatment nonadherence, patients are more likely to fail treatment, or experience relapse, and the risk of emergence of drug-resistant bacterial strains is increased (World Health Organization 2006). Poor treatment compliance likely results in increased incidence of multidrug-resistant tuberculosis (i.e. MDR-TB; resistance to at least rifampicin

and isoniazid) and extensively drug-resistant tuberculosis (i.e. XDR-TB; MDR-TB resistance in addition to fluoroquinolone and aminoglycoside resistance). Between 0.5 and 3.7% of new cases of tuberculosis in Africa are estimated to be resistant to rifampicin and isoniazid (World Health Organization 2015). Unfortunately, drug resistance surveillance data are mostly lacking in Africa and as a result the proportion of MDR-TB is likely underestimated. WHO recommends patients diagnosed with MDR-TB receive twenty months of a second-line regimen comprised of, but not limited to, fluoroquinolones, aminoglycosides, capreomycin, ethionamide and cycloserine (World Health Organization 2015). Understandably, nonadherence to second-line regimens for MDR-TB treatment are poor due to lengthy and complicated treatment times with severe adverse events resulting once again in patients defaulting from treatment. The new standardized shorter MDR-TB regimen with seven drugs and a treatment duration of nine to twelve months may hopefully improve treatment compliance (World Health Organization 2016). HIV and tuberculosis co-infection is common in Africa and especially in southern Africa, where in 2012, more than half of all tuberculosis cases are co-infected with HIV (World Health Organization 2013). Following the general trend, patients with HIV and tuberculosis co-infection have poor treatment adherence due to high pill counts, regimen complexity and potentially severe adverse events resulting from drug-drug interactions between antiretroviral and anti-tuberculosis drugs (McIlleron et al. 2007a). Patients with confirmed latent tuberculosis infections are also treated with lengthy drug regimens, including daily isoniazid dosing of 6 or 9 months duration (World Health Organization 2014a). As could be expected, poor adherence to prophylactic treatment of an asymptomatic disease is frequently encountered (World Health Organization 2014a). As a result of the above mentioned problems, shortened treatment durations have been suggested as a method for improving compliance (Getahun et al. 2015; Rangaka et al. 2015). A recent 3-month WHO recommended regimen of weekly rifapentine plus isoniazid (World Health Organization 2014a) will hopefully improve treatment adherence. Such shortened treatment regimens could also reduce stock demands on highly burdened public health programs which often report insufficient stock of critical tuberculosis drugs (Bateman 2013). Furthermore, first line regimens, compatible with antiretroviral treatment regimens, need to be optimised in order to prevent the development of treatment resistance in the first place.

Shortening the duration of tuberculosis treatment is believed to improve patient adherence to treatment and reduce the risk of drug resistance (World Health Organization 2011), and could have financial benefits especially in resource-limited countries. Three large phase III studies investigated the addition of a fluoroquinolone as a substitute for either ethambutol or isoniazid to shorten the duration of drug susceptible tuberculosis treatment to 4 months (Gillespie et al. 2014; Jindani et al. 2014; Merle et al. 2014). Disappointingly, all three studies failed to show evidence in support of shortening of treatment and unexpectedly revealed greater risk of relapse in patients randomized to the fluoroquinolone regimen compared to the standard 6-month regimen. The Pan African Consortium for Evaluation of Anti-tuberculosis Antibiotics (PanACEA), are currently investigating the potential to shorten the duration of tuberculosis treatment by increasing rifampicin exposure in the MAMS-TB-01 study (World Health Organization 2014b). Results are promising given the favourable safety profile following increased rifampicin exposure relative to standard doses established in a 2-week dose ranging study (Boeree et al. 2015), and two phase II studies, namely RIFATOX (Clayden et al. 2014) and Ruslami et al (Ruslami et al. 2007). Furthermore, increased rifampicin concentration improved bacterial kill and prevented relapse in both hollow-fibre (Gumbo et al. 2007a) and murine studies (Jayaram et al. 2003; Hu et al. 2015). Lastly, TBTC Study 31 is similarly investigating the shortening of tuberculosis treatment from the standard 6-month regimen to the shortened 4-month regimen by substituting rifampicin with high dose rifapentine (Goldberg 2016).

The recent discovery of novel tuberculosis drugs, which appear to have good sterilizing ability, will likely aid in shortening the current duration of tuberculosis treatment (Zumla et al. 2013). Novel drugs, including bedaquiline, PA-824, delamanid, SQ109, PNU-100480, and AZD-5847, need to be combined either with old or repurposed drugs for effective regimen combinations and optimal doses. Examples of repurposed drugs include fluoroquinolones (moxifloxacin and gatifloxacin), linezolid and β-lactams (Meropenem and Clavulanate) that were originally developed to treat other infections but are now investigated for tuberculosis treatment. Additionally, higher doses of rifampicin is similarly being investigated (repurposed) to shorten the duration of tuberculosis treatment (Dutta and Karakousis 2015). Importantly, novel study designs and methods, such as those employed in the MAMS adaptive trial design (Zumla et al. 2013) will be required to investigate optimal regimen combinations and drug doses.

Murine studies have identified antagonism between isoniazid and the combination of rifampicin and pyrazinamide (Grosset et al. 1992), while the combination of rifampicin and moxifloxacin appeared synergistic for resistance suppression although antagonistic for microbial kill (Drusano et al. 2010). Furthermore, Srivastava et al has demonstrated the ability of induced *Mycobacterium tuberculosis* efflux pumps to reduce the effect of both ethambutol and isoniazid following previous exposure to ethambutol (Srivastava et al. 2010). Hence, there remain many challenges regarding the characterisation between drug exposure and treatment outcome particularly when you consider combined drug action synergism or antagonism within treatment regimens.

The OFLOTUB study

Prior to starting the phase III OFLOTUB study, *in vitro* (Sulochana et al. 2005; Singh et al. 2009), *in vivo* (Burman et al. 2006; Rustomjee et al. 2008; Conde et al. 2009; Dorman et al. 2009) and observational data (Tuberculosis Research Center 2002) strongly suggested the use of a fluoroquinolone as a mechanism to shorten the duration of tuberculosis treatment. Consequently, 1836 patients eligible for inclusion into the phase III trial were randomized to receive either the 6-month control regimen comprised of rifampicin, isoniazid, pyrazinamide and ethambutol or the 4-month test regimen where gatifloxacin replaced ethambutol. Patients in the control arm received the standard 4 drugs (rifampicin, isoniazid, pyrazinamide, and ethambutol) for 2 months followed by 2 drugs (rifampicin and isoniazid) for a further 4 months. In contrast, test arm patients received 3 drugs (rifampicin, isoniazid, and gatifloxacin) for 4 months with pyrazinamide for the first 2 months. The primary objective of the phase III OFLOTUB study was to establish the safety and efficacy of the 4-month gatifloxacin containing test regimen for treating patients with drug susceptible tuberculosis (Merle et al. 2014). The primary efficacy end point, measured 2 years post end of treatment, was the proportion of patients with an unfavourable outcome (defined as a composite of treatment failure, recurrence, death or drop out during study treatment). The study did not discriminate between relapse and re-infection but rather considered these patients having recurrence. Patients with 2 consecutive positive results for sputum cultures at least one day apart were considered having treatment failure or recurrence (post treatment cure). Patients with both negative sputum smear and culture outcomes at 2 months post treatment initiation were

considered having culture conversion (a secondary efficacy endpoint). The current pharmacokinetic sub-study investigated individual drug exposures and their associations with the primary (24-month unfavourable outcome) and secondary (2-month culture conversion) efficacy endpoints of the parent study stratified across treatment regimen.

1.2. Measuring of drug concentrations

Safety and efficacy of many drugs are optimised by measuring drug concentrations and performing therapeutic drug monitoring (TDM). TDM is unavailable to the vast majority of patients (especially those in developing countries) and only very rarely performed due to the high costs involved (Peloquin 2002; Alsultan and Peloquin 2014), however the extent to which drug concentrations predict outcome is unknown. A review investigating evidence for measuring drug concentrations of anti-tuberculosis drugs, revealed patients consistently failing target concentrations following standard dosing (Wilby et al. 2014). Notably, authors of the above mentioned review remain uncertain of the clinical implications of such findings given the extent to which drug concentrations predict outcome is yet unknown. Furthermore, the review highlighted factors responsible for pharmacokinetic variability in tuberculosis patients including obesity and HIV co-infection. Indeed, common sources for the variability in anti-mycobacterial drug concentration include body size (Anderson and Holford 2008), genetic variation such as N-acetyltransferase-2 (NAT2) genotype (Wilkins et al. 2011; Denti et al. 2015), factors affecting oral bioavailability including autoinduction of transport proteins and metabolising enzymes (Acocella 1978; Chen and Raymond 2006), food affects (Zvada et al. 2010), drug formulation (McIlleron et al. 2006) and malabsorption due to diarrhoea and/or HIV co-infection (Gurumurthy et al. 2004). Notably, Peloquin suggested that measuring drug concentration is only part of the solution, and that having simultaneous knowledge of both clinical and bacteriological data enables clinicians to successfully treat most tuberculosis patients receiving complex treatment regimens (Peloquin 2002). Indeed, several authors advocate the use of pharmacokinetic and pharmacodynamic (PK/PD) studies to define drug target concentrations for optimal therapeutic effect (Davies and Nuermberger 2008; Pasipanodya and Gumbo 2011). Drug target concentrations are, however, often optimized in patients from North America and Western Europe yet applied to patients in developing countries who are likely genetically and physiologically different. Consequently, Pillai and

colleagues have encouraged the use of pharmacometric studies to help characterise PK/PD relationships specifically in patients from developing countries (Pillai et al. 2013). Drug exposure is typically expressed in terms of area under the concentration time curve (AUC) or peak serum drug concentration (C_{MAX}) by means of computer software employing non-compartmental or compartmental methods. Non-compartmental analysis (NCA) and compartmental modelling approaches have their strengths and weaknesses (Gabrielsson and Weiner 1999; Dubois et al. 2012). However, compartmental modelling methods, specifically population pharmacokinetic modelling, using a non-linear mixed effects approach (NONMEM), is preferred under conditions where the kinetics of the drug are known to be non-linear, as is the case for rifampicin concentration (Acocella 1978; Chirehwa et al. 2015). Furthermore, population pharmacokinetic modelling enables the user to estimate covariate effects and perform simulations characterising exposure-response relationships predicting drug target concentrations optimal for therapeutic outcome (Pasipanodya and Gumbo 2011). Classification and regression tree analysis (CART), a technique which examines both linear and non-linear interactions simultaneously, has recently been recognised as an approach for investigating the role of several clinical variables, including drug concentrations, as predictors of therapeutic outcome (Pasipanodya et al. 2013). Additionally, recursive partitioning methods are ideal for exploring and identifying large numbers of predictor variables for outcome even in the presence of complex interactions (Strobl et al. 2009).

1.3. Pharmacology of antituberculosis drugs

Rifampicin

Rifampicin is a potent activator of the nuclear pregnane X receptor (PXR) which regulates the transcription of multiple drug metabolizing enzymes and drug transporters (Geick et al. 2001; Chen and Raymond 2006). Subsequent to PXR activation, hepatic and intestinal enzymes, along with many other metabolic pathways and transporters, are induced and result in increased clearance of many co-administered drugs including itself. Rifampicin is mainly cleared via the intestine and liver undergoing extensive first-pass metabolism which becomes saturated at higher doses yielding disproportionate increases in exposure (Acocella 1978). Although the exact mechanism is not known, following repeated intravenous or oral dosing,

rifampicin induces its own metabolism by increasing its systemic and pre-systemic clearance, a process known as autoinduction (Acocella 1978; Loos et al. 1985; Benedetti and Dostert 1994). Autoinduction of rifampicin's metabolism may, in part, be attributed to PXR-mediated induction of P-glycoprotein (P-gp), a trans-membrane efflux transporter expressed in enterocytes and hepatocytes (Faber et al. 2003; Lin 2003), organic anion-transporting polypeptide 1B (OATP1B1), a transporter aiding biliary uptake of rifampicin (Chigutsa et al. 2011), and beta-esterase's (Jamis-Dow et al. 1997; Staudinger et al. 2010) specifically arylacetamide deacetylase (AADAC) (Nakajima et al. 2011), responsible for biotransformation of rifampicin to its major metabolite 25-deacetyl rifampicin (Chen and Raymond 2006). A population pharmacokinetic model has previously characterised rifampicin exposure in African adults using a one-compartment model parameterized in terms of clearance and volume estimated respectively at 19.2 L/h and 53.2 L for the typical patient (Wilkins et al. 2008).

Rifampicin absorption, clearance and apparent volume of distribution display great inter-individual and inter-occasion variability (McIlleron et al. 2006; Wilkins et al. 2008). Rifampicin is estimated having 93% oral bioavailability following a single 10 mg/kg dose (Loos et al. 1985) which reduces to 68% following multiple doses (van den Boogaard et al. 2009). The average steady state area under the concertation-time curve over 24 hours (AUC_{0-24}) ranges between 25 and 80 mg·h/L following multiple 10 mg/kg doses (Peloquin et al. 1999a; McIlleron et al. 2006; Wilkins et al. 2008). Peak concentrations between 8 and 20 mg/L are observed approximately 1.5 to 2 hours post dose with an estimated half-life between 2 and 5 hours and is reported as demonstrating approximately 85% protein binding (van den Boogaard et al. 2009). The extent of rifampicin absorption is minimally influenced by food (6% reduction in AUC following a high fat meal), however peak concentration is reduced by 36% and the time taken to peak concentration almost doubled (Peloquin 1999). The relationship between rifampicin concentrations and HIV infection is currently not well understood with different studies reporting contrasting findings. Rifampicin peak concentrations have been reported as comparable across patients with and without HIV co-infection (Tappero et al. 2005; Chideya et al. 2009). However, HIV co-infected patients with CD4 counts <200 cells/μL had lower rifampicin peak concentrations compared to those with CD4 counts >200 cells/μL (Chideya et al. 2009), suggesting that the level of immune suppression (CD4 cell counts) influence

rifampicin peak concentrations. In contrast, rifampicin concentrations were found to be comparable between patients irrespective of the level of immune suppression in Kenyan and South African patients (Choudhri et al. 1997; McIlleron et al. 2012). Although similar peak concentrations were observed in Kenyan patients with or without HIV co-infection (Choudhri et al. 1997), McIlleron and colleagues observed low rifampicin concentrations in a cohort of HIV infected tuberculosis patients, especially in males with low total body weight (McIlleron et al. 2012). Furthermore, reduced rifampicin exposure (AUC and C_{MAX}) has been observed in tuberculosis patients with HIV co-infection when compared to those without HIV co-infection, with low concentrations thought to be due to malabsorption of the drug (Gurumurthy et al. 2004).

Rifampicin has good activity against drug susceptible *M. tuberculosis* with reports of a minimum inhibitory concentration (MIC) ranging between 0.125 and 1.0 mg/L on solid agar plates (Lee and Heifets 1987; Suo et al. 1988) and 0.016 to 0.5 mg/L in liquid broth (Lee and Heifets 1987; Rastogi et al. 1996; van Ingen et al. 2011; Chigutsa et al. 2015). Rifampicin applies its antimicrobial action through the inhibition of bacterial DNA-dependent RNA polymerase (Campbell et al. 2001). The drug binds the β-subunit of RNA polymerase in *M. tuberculosis* inhibiting the elongation of messenger RNA (da Silva and Palomino 2011). This mechanism allows rifampicin to retain its activity against relatively inactive or dormant bacilli (Dickinson and Mitchison 1981). The majority of *M. tuberculosis* clinical isolates achieve resistance to rifampicin through mutations in the gene rpoB encoding the B-subunit of RNA polymerase (Heep et al. 2000). Rifampicin demonstrates both excellent bactericidal and sterilizing activity in early bactericidal activity (EBA) studies conducted over 5 (Sirgel et al. 2000) and 14 days (Jindani et al. 2003). Blumberg and colleagues described sterilizing drugs as having the ability to eliminate dormant bacilli usually found in necrotic tissue and responsible for relapse of tuberculosis infection (Blumberg et al. 2003). During the 4-month continuation phase of standard therapy with isoniazid and rifampicin, persisting organism are likely eliminated via the sterilizing action of rifampicin (Mitchison 2000). Overall, rifampicin and pyrazinamide are the best sterilizing drugs preventing post treatment relapses (Alsultan and Peloquin 2014). Interestingly, *in vitro* and murine studies identified an antagonistic pharmacodynamic interaction between moxifloxacin and rifampicin with respect to bacilli elimination (Drusano et al. 2010; Balasubramanian et al. 2012). Experiments in the

tuberculosis hollow fiber system (HFS) model demonstrated the role of drug concentration to kill and prevent relapse of *M. tuberculosis* (Pasipanodya et al. 2013). In particular, rifampicin's microbial kill was linked to AUC/MIC while prevention of resistance and post antibiotic effect was associated with C_{MAX}/MIC (Gumbo et al. 2007a). Correspondingly, elevated rifampicin concentrations shortened treatment duration and reduced relapse rates in *in vitro* and murine studies (Hu et al. 2015). Similarly, clinical studies have demonstrated elevated rifampicin exposure (AUC and C_{MAX}), to significantly reduce the bacterial load and increase culture conversion rates in tuberculosis patients (Diacon et al. 2007; Boeree et al. 2015; Chigutsa et al. 2015). Moreover, elevated pyrazinamide, rifampicin and isoniazid exposure (AUC) predicted long term favourable outcome defined as the absence of microbiological failure or death or relapse 2 years post treatment completion (Pasipanodya et al. 2013). Gumbo and colleagues recently completed a review within HFS, murine and guinea pig models as well as clinical studies identifying PK/PD parameters applied to tuberculosis treatment (Gumbo et al. 2015). Their findings suggest increasing the ratio of rifampicin C_{MAX}/MIC for the suppression of resistance and rifampicin AUC/MIC for early microbial kill.

Isoniazid

A population pharmacokinetic model has previously characterised isoniazid concentrations in African adult patients using a two-compartmental model together with a mixture model characterising dual rates of elimination estimated respectively at 9.7 L/h and 21.6 L for slow and fast eliminators (Wilkins et al. 2011). Isoniazid displays large inter-individual pharmacokinetic variability (Peloquin et al. 1997; Wilkins et al. 2011) with the majority of its variable elimination explained by polymorphisms at the N-arylamine acetyltransferase type 2 (NAT2) locus (Bach et al. 1976; Weber and Hein 1979). There is wide-ranging diversity in NAT2 polymorphism across the world with patients with short elimination half-lives phenotyped as fast acetylators while patients with longer elimination half-lives are termed as slow acetylators. Isoniazid undergoes mostly hepatic and intestinal metabolism via the polymorphic NAT2 enzyme into metabolites eliminated via the kidney in a bimodal fashion (i.e. fast vs. slow acetylators) (Bach et al. 1976). Approximately 40% of black South Africans phenotyped as slow acetylators (Bach et al. 1976; Sabbagh et al. 2008). Recent studies conducted in South African patients identified trimodal distributions of isoniazid elimination

classifying patients as fast, intermediate or slow acetylators based on genotype (Parkin et al. 1997; Donald et al. 2007; Zhu et al. 2012). Notably, studies unable to statistically differentiate acetylator status, often due to lack of genotype data, dichotomize patients into slow versus fast phenotypes (McIlleron et al. 2006; Wilkins et al. 2011).

Isoniazid is rapidly absorbed on an empty stomach with C_{MAX} ranging between 3 and 6 mg/L approximately 1 to 2 hours post 300 mg daily dosing (Peloquin et al. 1997). Isoniazid exposures (AUC) of approximately 18 to 20 mg·h/L are observed following similar daily doses (Peloquin et al. 1999b). High fat meals reduce isoniazid C_{MAX} and AUC by 51% and 12%, respectively (Peloquin et al. 1999b). Furthermore, fast acetylators have approximately between 2 and 6-fold lower median AUC's compared to slow acetylators while isoniazid C_{MAX} is approximately between 1.2 and 4.4-fold lower in fast vs. slow acetylators (Parkin et al. 1997; Pasipanodya et al. 2012; Tostmann et al. 2013; Denti et al. 2015). Median isoniazid exposures observed in tuberculosis patients (irrespective of HIV or acetylator status) range between 2.5 to 5.9 mg/L for C_{MAX} and between 6.3 to 25.6 mg·h/L for AUC (Parkin et al. 1997; Choudhri et al. 1997; Tappero et al. 2005; McIlleron et al. 2006; Um et al. 2007; Chideya et al. 2009; Babalik et al. 2013; Fahimi et al. 2013; Tostmann et al. 2013; Denti et al. 2015; Chigutsa et al. 2015). These isoniazid exposures determined in patients were mostly in agreement with concentration ranges established in healthy individuals (Peloquin et al. 1997) with slight differences likely attributed to variances in study population, sampling schedules, drug formulations and dose.

The MIC for isoniazid on drug susceptible *M. tuberculosis* grown on solid Agar plates has reported as ranging between 0.1 and 0.5 mg/L while MIC's determined in liquid broth range between 0.02 and 0.125 mg/L (Lee and Heifets 1987; Suo et al. 1988; Rastogi et al. 1996; Chigutsa et al. 2015). A recent review described isoniazid entering the bacilli through passive diffusion whereupon the host enzyme KatG activates it by peroxidation (Timmins and Deretic 2006). In turn, the KatG activated intracellular reactive species inhibits lipid cell wall and nucleic acid synthesis together with respiratory inhibition yielding the drugs potent antituberculosis action. HFS model experiments suggested single point mutations in the bacterial katG gene, together with reserpine-inhibitable efflux pumps, confer isoniazid tolerance to stains of *M. tuberculosis* (Gumbo et al. 2007b). Isoniazid's rapid bactericidal action eliminates the majority of drug susceptible organisms within the first few days of

commencement of treatment (Mitchison 2000). Thereafter rifampicin and pyrazinamide take over the bactericidal role during the intensive phase of treatment while ethambutol, having a bacteriostatic action, protects against rifampicin resistance in the event of initial isoniazid resistance (Blumberg et al. 2003). Isoniazid bactericidal action is believed to diminish once log-phase bacilli are eliminated (Mitchison 2000). However, Gumbo and colleagues argue the cessation of drug action is due to emergence of isoniazid resistance (Gumbo et al. 2007b). Nevertheless a 14 day EBA study revealed fewer than 10% of patients developing isoniazid resistance (Jindani et al. 2003; Mitchison et al. 2007). A murine study established AUC/MIC followed by C_{MAX}/MIC correlating best with isoniazid's bactericidal activity over 6 days of monotherapy (Jayaram et al. 2004). Similarly, resistance suppression was linked to AUC/MIC as well as C_{MAX}/MIC (Gumbo et al. 2007c). A recent meta-analysis established similar PK/PD parameters correlating with isoniazid's bactericidal activity (Pasipanodya et al. 2012). Fast acetylators were determined having twice the risk of microbiological failure and acquired drug resistance compared to slow acetylators in patients receiving combination therapy (Pasipanodya et al. 2012). Furthermore, fast acetylators had significantly lower AUC and C_{MAX} compared to slow acetylators. Donald and colleagues demonstrated optimal early bactericidal activity, defined as 90% of the maximum EBA (EBA_{90}), associated with $AUC_{0-\infty}$ >10.52 mg·h/L and 2 hour concentrations post dose >2.19 mg/L (Donald et al. 2007). Fast acetylators achieved optimal outcome more often at higher doses, suggesting a dose increase from 3 to 6 mg/kg for optimal bactericidal activity (Donald et al. 2007). Conversely, slow acetylators only required a 3 mg/kg dose for optimal outcome and Donald and colleagues suggest the EBA of isoniazid plateaus following doses above 300 mg (Donald et al. 1997). Furthermore, EBA studies do not accurately reflect the sterilizing ability of drugs required for prevention of relapse typically observed over longer duration studies (Davies and Nuermberger 2008). Although isoniazid bactericidal action reduces after the first few days of treatment, *in vitro* studies suggest the drug conveys cumulative post-antibiotic inhibition on bacterial growth following repeated drug exposures (AUC) similar to that observed during daily dosing (Awaness and Mitchison 1973). Interestingly, murine studies have demonstrated bactericidal antagonism during the initial and continuation phase of treatment when isoniazid was added to the combination of rifampicin and pyrazinamide (Grosset et al. 1992). Subsequently, Almeida and colleagues repeated the findings of a dose dependent antagonism between isoniazid and the combination of rifampicin and pyrazinamide (Almeida et al.

2009a). Furthermore, the addition of isoniazid to rifampicin increases bactericidal activity while addition of isoniazid to pyrazinamide results in bactericidal antagonism (Almeida et al. 2009a). Consistently, Chigutsa and colleagues demonstrated elevated isoniazid concentration to antagonise culture conversion rates in patients receiving first-line antituberculosis treatment with low RIF exposure (Chigutsa et al. 2015).

Pyrazinamide

A population pharmacokinetic model has previously characterised pyrazinamide concentrations in African adult patients using a one-compartment model with first order absorption and elimination estimating clearance and apparent volume of distribution for the typical individual respectively at 3.42 L/h and 29.2 L (Wilkins et al. 2006). Pyrazinamide pharmacokinetics display limited variability and the drug is reliably absorbed, with simultaneous intake with food having little effect on C_{MAX} and AUC (Peloquin et al. 1997; Peloquin et al. 1998). Pyrazinamide concentrations have been reported as being mostly dependent on weight (McIlleron et al. 2006; Wilkins et al. 2006; Chirehwa et al. 2014; Denti et al. 2015). Typical pharmacokinetic profiles, determined in healthy individuals, established peak concentrations ranging between 21.7 and 42.64 mg/L while AUC varied between 303.55 and 541.36 mg·h/L following 20 mg/kg daily dosing (Peloquin et al. 1997). While some studies have reported significantly lower pyrazinamide concentrations in HIV co-infected tuberculosis patients as well as those with CD4 cell counts <200 cells/mL (Tappero et al. 2005; Chideya et al. 2009), several other studies failed to detect an effect of HIV status or immune status on pyrazinamide exposure (Choudhri et al. 1997; McIlleron et al. 2006; Wilkins et al. 2006; Zhu et al. 2012; Tostmann et al. 2013; Denti et al. 2015). The median pyrazinamide exposure observed in several patient studies ranges from 32.1 to 55.5 mg/L for C_{MAX} while AUC has been shown to vary between 219 and 499.7 mg·h/L irrespective of HIV or immune status (Choudhri et al. 1997; Tappero et al. 2005; McIlleron et al. 2006; Wilkins et al. 2006; Chideya et al. 2009; Zhu et al. 2012; Tostmann et al. 2013; Denti et al. 2015). Much of the variation in drug concentration observed in the above mentioned patient studies could be attributed to variable dose, with the median pyrazinamide dose ranging between 20 and 50 mg/kg. Notably, in these studies, all but one patient achieved pyrazinamide C_{MAX} above 20 mg/L (the lower limit of the reported reference range) (Alsultan and Peloquin 2014). Additionally, Zhu and colleagues reported a low pyrazinamide C_{MAX} of 18.8 mg/L (below 20 mg/L), but in this

case the associated dose range, which included a 15 mg/kg dose, was likely the culprit of such low exposure (Zhu et al. 2012). Interestingly, pyrazinamide concentrations are known to decrease with time due to an increase in clearance following multiple doses in combination with first-line tuberculosis drugs (Chirehwa et al. 2014; Denti et al. 2015).

Determining the susceptibility of *M. tuberculosis* to pyrazinamide is complex and requires an acidic environment as pyrazinamide is only active at low pH (Zhang et al. 1999). Pyrazinamide enters the bacterium via passive diffusion, thereafter host enzymes (PZase) covert it to pyrazinoic acid (POA) before excreting it via weak efflux pumps (Zhang and Mitchison 2002). Within an acidic environment (low pH), POA is reabsorbed into the bacilli and accumulates under conditions of poor efflux pump efficiency (e.g. low bacterial metabolic activity), causing cell damage and death (Zhang and Mitchison 2002). Point mutations in bacterial pncA gene encoding PZase, confers pyrazinamide tolerance to strains of M. tuberculosis (Zhang and Mitchison 2002). Salfinger and Heifets determined the MIC of pyrazinamide against drug susceptible MTB in liquid broth reporting concentrations ranging from <6.2 to 50 mg/L at pH 5.5 (Salfinger and Heifets 1988). Similarly, Werngren and colleagues suggest MIC's <64 mg/L in liquid broth be classified as drug susceptible bacilli (Werngren et al. 2012). *In vitro*, animal and EBA studies suggest pyrazinamide has little bactericidal activity on rapidly diving cells during the first 2 days of treatment, however, together with rifampicin, pyrazinamide exerts maximal sterilizing effect on metabolically inactive cells representative of persisting bacilli later on in therapy (Zhang and Mitchison 2002; Mitchison and Coates 2004). Gumbo and colleagues, using the hollow fibre system model, established that the sterilizing effect of pyrazinamide is dose dependent and driven by the AUC/MIC ratio while resistance suppression is linked to the proportion of time drug concentrations exceeded the MIC (Gumbo et al. 2009). Similarly, using murine and guinea pig models, Ahmed and colleagues demonstrated pyrazinamide's dose dependent action in reducing bacillary burden in the animals in a synergistic fashion with rifampicin (Ahmad et al. 2011). In line with this work, Chigutsa and colleagues established that pyrazinamide AUC/MIC >11.3 improves culture conversion rates in patients with rifampicin C_{MAX} >8.2 mg/L (Chigutsa et al. 2015). Furthermore, clinical studies have demonstrated that low pyrazinamide C_{MAX} (<35mg/L) is associated with poor outcome, when defined as the composite of treatment failure and death (Chideya et al. 2009). Similarly, Pasipanodya and colleagues revealed patients with

pyrazinamide C_{MAX} below 58 mg/L had lower 2-month sputum culture conversion (Pasipanodya et al. 2013). Overall, *in vitro*, animal and clinical studies suggest increased pyrazinamide concentrations for optimal outcome, but the safety of higher doses is unclear (Sahota and Della Pasqua 2012). However, a recent clinical study conducted on a cohort of 142 South African patients found no dose-dependent pyrazinamide liver toxicity subsequent to a median 36 (range, 20-53) mg/kg dose (Pasipanodya et al. 2013).

Ethambutol

A population pharmacokinetic model has previously described ethambutol concentrations in African adult patients using a two-compartment model with one transit compartment prior to first order absorption and allometric scaling by body weight on clearance and volume terms (Jönsson et al. 2011). Ethambutol time to peak concentration varies between 2 and 4 hours post dose displaying inconsistent absorption. This drug undergoes active renal secretion with most of the drug excreted unchanged in the urine (Lee et al. 1980; Peloquin et al. 1999a). Although food intake has minimal impact on ethambutol exposure, it is recommended that this drug be taken on an empty stomach (Peloquin et al. 1999a). Following a median single dose between 15 and 25 mg/kg, the typical C_{MAX} and AUC range between 3.25 & 5.62 mg/L and between 27.5 & 29.6 mg·h/L respectively in healthy volunteers (Lee et al. 1980; Peloquin et al. 1999a). Age, sex and HIV status are determinants of ethambutol exposure, with older, female, and HIV co-infected tuberculosis patients reported as having low concentrations (McIlleron et al. 2006; Jönsson et al. 2011; Denti et al. 2015). Clinical studies report 20 to 27% lower ethambutol C_{MAX} in HIV co-infected patients compared to those without HIV co-infection (Zhu et al. 2004; McIlleron et al. 2006). Similarly, HIV co-infected patients have been estimated as having approximately 15% lower ethambutol bioavailability compared to patients without co-infection (Jönsson et al. 2011). However, several other studies have found no significant effect of HIV status on ethambutol exposure (Tappero et al. 2005; Chideya et al. 2009; Tostmann et al. 2013; Prahl et al. 2014; Denti et al. 2015). In adult tuberculosis patients, following daily 15 to 32.6 mg/kg doses, the median (range) C_{MAX} was reported to be between 2.06 & 5.44 mg/L (0.2 & 11.21), while AUC was observed to be between 20.2 & 32 mg·h/L (6.9 & 73) (Zhu et al. 2004; Tappero et al. 2005; Perlman et al. 2005; McIlleron et al. 2006; Chideya et al. 2009; Tostmann et al. 2013; Prahl et al. 2014; Denti et al. 2015; Chigutsa

et al. 2015). These differences in drug concentration are likely explained by patient characteristics, pharmacokinetic evaluation, mg/kg dosing, and drug formulation. Several studies report between 39 and 69% of patients with ethambutol C_{MAX} below 2 mg/L (lower limit of the ethambutol reference range) (Zhu et al. 2004; Tappero et al. 2005; Perlman et al. 2005; Chideya et al. 2009; Alsultan and Peloquin 2014; Prahl et al. 2014). Conversely, other studies report no patients with ethambutol C_{MAX} below 2 mg/L (McIlleron et al. 2006; Tostmann et al. 2013). Variability in the proportion of patients achieving peak concentrations within the ethambutol reference range (2–6 mg/L after daily doses of 15–25 mg/kg), is likely due to variable absorption and/or pharmacokinetic evaluation (Lee et al. 1980; Peloquin et al. 1999a).

Ethambutol's role within the first-line regimen is to inhibit rifampicin resistance in the event of isoniazid primary resistance (Blumberg et al. 2003). The MIC for ethambutol on drug susceptible *M. tuberculosis* was reported between 1.9 and 7.5 mg/L using solid agar plates and between 0.50 and 5.0 mg/L in liquid broth (Lee and Heifets 1987; Suo et al. 1988; Rastogi et al. 1996; Chigutsa et al. 2015). Reserpine inhibited efflux pumps are suggested to confer ethambutol drug tolerance to strains of *M. tuberculosis* (Srivastava et al. 2010). Furthermore, both isoniazid and ethambutol are substrates to the reserpine inhibited efflux pumps (Srivastava et al. 2010). *In vitro* studies (i.e. Hollow Fibre System models) demonstrate ethambutol bactericidal action is best explained by AUC/MIC and C_{MAX}/MIC while resistance suppression is thought to be linked to the proportion of time ethambutol concentration exceeded the MIC (Srivastava et al. 2010). Interestingly, an EBA study demonstrates ethambutol monotherapy having less bactericidal activity compared to isoniazid and rifampicin (Jindani et al. 2003), however, when combined with either drug or with both, ethambutol antagonises the bactericidal activity of rifampicin and the combination of rifampicin and isoniazid (Jindani et al. 2003). Notably, ethambutol is believed to be bacteriostatic (Wallis et al. 2003) which may partially explain its bactericidal antagonism of isoniazid and rifampicin.

Gatifloxacin

Gatifloxacin has approximately 96% oral bioavailability and distributes widely throughout the body with an estimated apparent volume of distribution of 1.8 L/kg (Nakashima et al. 1995; Grasela 2000). Gatifloxacin has approximately 20% protein binding independent of concentration, with more than 80% of the drug eliminated unchanged in the urine (Nakashima et al. 1995; Grasela 2000; Gajjar et al. 2000; Mignot et al. 2002). Simultaneous intake with food has minimal effect on gatifloxacin exposure with only slight decreases in AUC and C_{MAX} reported (Nakashima et al. 1995). Co-administration of probenecid, prolongs the terminal half-life of gatifloxacin, while increasing its AUC and decreasing its total and renal clearance suggesting tubular secretion plays a role in the drugs renal elimination (Nakashima et al. 1995). Following multiple 200 to 800 mg/day dosing, gatifloxacin single dose pharmacokinetics has been reported as linear and time independent, with serum and urine concentrations reaching steady state within 2 to 3 days (Nakashima et al. 1995; Gajjar et al. 2000; Mignot et al. 2002). In healthy volunteers, following single and multiple 400 mg/day dosing, typical gatifloxacin C_{MAX} has been reported as between 3.35 and 4.56 mg/L, while the typical AUC has reported as ranging between 28.6 and 35.4 mg·h/L (Nakashima et al. 1995; Grasela 2000; Gajjar et al. 2000; Mignot et al. 2002; McIlleron et al. 2007b). Within adult patients, following multiple 400 mg/day dosing, gatifloxacin C_{MAX} has been found to vary between 3.4 and 6.4 mg/L, with AUC ranging between 30 and 73 mg·h/L (Grasela 2000; Schentag 2000; Ginsburg et al. 2003; Nuermberger et al. 2004; Johnson et al. 2006; Peloquin et al. 2008). Notably, when gatifloxacin is dosed together with rifampicin, isoniazid and pyrazinamide, a single-dose crossover study in healthy volunteers revealed a reduction in the elimination rate of gatifloxacin resulting in a 14% increase in the area under the concentration time curve to infinity ($AUC_{0-\infty}$) (McIlleron et al. 2007b). These findings raised concerns regarding the accumulation of gatifloxacin following multiple doses in tuberculosis patients in the then upcoming OFLOTUB phase III trial investigating the shorting of tuberculosis treatment to 4-months by replacing ethambutol with gatifloxacin (Merle et al. 2014). To the best of our knowledge, no prior population pharmacokinetic model characterised the population pharmacokinetics of gatifloxacin in African adult patients. Population pharmacokinetics of gatifloxacin has however, been described in 29 adult patients from Brazil using a single-compartment model estimating the typical clearance and apparent volume of distribution respectively at 10.42 L/h and 79 L (Peloquin et al. 2008). Fluoroquinolones

represent a promising class of drug for the treatment of tuberculosis. Gatifloxacin targets *M. tuberculosis* topoisomerase II or DNA gyrase, a tetramer consisting of 2 subunits (A and B) encoded by genes gyrA and gyrB (Ginsburg et al. 2003). Subsequently, point mutations in gyrA and gyrB encoding DNA gyrase, confer gatifloxacin resistance to *M. tuberculosis* (Pantel et al. 2011). Gatifloxacin MICs reported for drug susceptible *M. tuberculosis* observed *in vitro* vary between 0.031 to 0.5 mg/L (Tomioka et al. 1999; Rodriguez et al. 2002; Alvirez-Freites et al. 2002; Ginsburg et al. 2003; Singh et al. 2009). Microdialysis assays performed in rats suggest free gatifloxacin concentration as a good surrogate for drug concentration in the interstitial fluid of the lung (Tasso et al. 2008). Following a single 400 mg gatifloxacin dose in patients undergoing fibre-optic bronchoscopy, Honeybourne et al demonstrated the mean gatifloxacin concentration at 2, 4 and 12 hours post dose within epithelial lining fluid, alveolar macrophages and bronchial mucosa (Honeybourne et al. 2001) exceeded the MIC_{90} for *M. tuberculosis* (reported between 0.031 and 1.0 mg/L (Tomioka et al. 1999; Rodriguez et al. 2002; Alvirez-Freites et al. 2002; Peloquin et al. 2008; Singh et al. 2009)). Gatifloxacin demonstrates strong bactericidal activity in murine models and within human macrophages (Alvirez-Freites et al. 2002; Sato et al. 2003; Cynamon et al. 2007). Additionally, gatifloxacin displays excellent EBA, only slightly lower than that of isoniazid (Johnson et al. 2006), while in combination with isoniazid and rifampicin, it continues to display exceptional bactericidal activity on log phase cultures (Paramasivan et al. 2005). Gatifloxacin has been shown to improve the sterilizing activity of the standard tuberculosis treatment regimen when it replaced ethambutol in the phase II OFLOTUB study (Rustomjee et al. 2008). *In vitro* and *in vivo* studies suggest a target ratio of >125 for the free drug area under the concentration versus time curve to MIC (*f*AUC/MIC) for maximal bactericidal effect and prevention of resistance to fluoroquinolones (Forrest et al. 1993; Schentag 2000; Schentag et al. 2001). In contrast, reports of dysglycemia related to the use of gatifloxacin in elderly patients with renal insufficiency (Ambrose et al. 2003; Park-Wyllie et al. 2006; Mehlhorn and Brown 2007; LaPlante et al. 2008) have raised concerns that pharmacokinetic interactions may lead to an increased risk of toxicity related to higher gatifloxacin exposure. Nevertheless, multiple intravenous doses of up to 800 mg/day have been found safe following an oral glucose tolerance test with minimal mean changes in fasting serum glucose and insulin reported between patients randomised to receive placebo or gatifloxacin (Gajjar et al. 2000). Furthermore, in a phase III study, no evidence of increased risk of QT interval prolongation or

dysglycemia in patients randomized to receive the gatifloxacin containing regimen was found (Merle et al. 2014).

Overall there remains limited published data of antituberculosis drug pharmacokinetics at first dose and steady state within the same patient and especially in African populations. Additionally, the effect of dose on the extent of autoinduction of rifampicin metabolism was unknown at the onset of this study. The onset of the OFLOTUB study investigating the shortening of tuberculosis treatment to 4 months permitted an opportunity to investigate the pharmacokinetics of rifampicin, isoniazid, pyrazinamide, ethambutol, and gatifloxacin in African populations. Additionally, there remained the requirement to investigate potential drug-drug interactions across treatment regimen especially after a single dose study identified an increase in gatifloxacin exposure when it was given together with rifampicin, isoniazid, and pyrazinamide. Lastly, the requirement to study such interactions on the impact of treatment outcome would enable treatment regimen optimisation.

2. Aims

The overarching aim of this thesis is to characterizing population pharmacokinetic / pharmacodynamic relationships in African pulmonary tuberculosis infected adults. This was achieved through the following sub-aims:

1. Development of a semi-mechanistic pharmacokinetic-enzyme turn-over model describing rifampicin pharmacokinetics after first dose and steady state in adult patients with tuberculosis. In addition, four different structural basic models were explored in order to assess whether different scaling methods or no scaling affects the final covariate selection procedure.
2. Evaluate the population pharmacokinetics of gatifloxacin after a first dose and steady state (28 days) when given in combination with rifampicin, isoniazid and pyrazinamide in African adult patients newly-diagnosed with pulmonary tuberculosis. In addition, the probability of target (*f*AUC/MIC$\geq$125) attainment and the cumulative fraction of response across the MIC distribution of *Mycobacterium tuberculosis* for 400, 600 and 800 mg once daily of gatifloxacin at steady-state in combination with rifampicin, isoniazid and pyrazinamide were investigated with Monte Carlo simulations using the final model.
3. Characterisation of the population pharmacokinetics of rifampicin, ethambutol, isoniazid and pyrazinamide in African patients and investigate potential drug-drug interactions.
4. Identification of predictors of culture conversion at 2 months and a composite long term outcome by 24 months using classification and regression tree analysis (CART).

3. Methodology

3.1. Clinical methodology

This pharmacokinetic-pharmacodynamic study was nested within the phase III OFLOTUB randomized controlled trial (clinical trial identifier NCT00216385) undertaken at study clinics in South Africa, Senegal, Guinea, and Benin (Merle et al. 2014). Ethical approval was granted to all 4 sites (Benin (Cotonou), Guinea (Conakry), Senegal (Dakar) & South Africa (Durban)) participating in the pharmacokinetic sub-study of the parent OFOTUB phase III study.

Patient population

Patients with newly diagnosed pulmonary tuberculosis were invited to participate in this nested pharmacokinetic study. Informed consent was obtained prior to the commencement of the study. A total of 343 patients including 230 males and 113 non-pregnant females were included in this analysis. Patients were aged 18 to 65 years, weighed between 38 and 80 kg and were antiretroviral naïve with demographic and clinical characteristics summarized in Table 3.1.

Patient treatment

During the 2-month intensive phase of treatment, control arm patients below 50 kg received 450 mg rifampicin together with 225 mg isoniazid, 1200 mg pyrazinamide and 825 mg ethambutol, 6 days a week. Patients with body weight >50 kg received 600 mg rifampicin together with 300 mg isoniazid, 1600 mg pyrazinamide and 1100 mg ethambutol for 6 days of the week. In the test arm of the study, ethambutol was replaced by gatifloxacin, which was continued with rifampicin and isoniazid until the end of the 4-month regimen in a daily 400 mg dose, 6 days a week, irrespective of weight. All doses were given orally (rifampicin, isoniazid, pyrazinamide and ethambutol in fixed dose combination tablets, and gatifloxacin in 400 mg tablets given separately to those in the test arm) and supervised using DOT performed

either by health centre staff or designated representatives, for the duration of the study. All tablets were provided by Lupin Pharmaceuticals Pvt Ltd, Mumbai, India.

Blood sampling

Three venous blood samples per patient were taken after the first dose and repeated at steady state (after approximately 28 days) for the determination of pharmacokinetics. Samples were drawn between 1 to 2 hours and 2.5 to 3.5 hours post dose in each patient on both occasions. Patients were block randomized to a time for the third sample. After the first dose, the third sample was taken 4 to 6 hours, or 8 to 10 hours post dose. At steady-state, the third sample was either taken pre-dose, 4 to 6 hours post dose, or 8 to 10 hours post dose.

Drug quantification

Each 4 mL blood sample was drawn into heparinized blood collection tubes at each pharmacokinetic sampling time point. Samples were centrifuged immediately (within 30 minutes) at 750 g for 10 minutes using a bench-top centrifuge to separate the plasma. While awaiting centrifugation, blood samples were kept on crushed ice. Three plasma aliquots from each sample were divided between polypropylene tubes (at least 0.5 ml in each) and stored at -80°C prior to drug concentration quantification. Plasma samples were shipped on dry ice as arranged by an international courier company. Plasma drug concentrations were quantified using validated methods (McIlleron et al. 2006; McIlleron et al. 2007b) in the ISO17025 accredited laboratory in the Division of Clinical Pharmacology, University of Cape Town, Groote Schuur Hospital.

Plasma drug concentrations were quantified by tandem high-pressure liquid chromatographic (HPLC)-tandem mass spectrometric (MS-MS) methods (Applied Biosystems API 2000). A 20x2.1 mm Hypersil Gold C18 column (Thermo, MA, USA) was used for rifampicin and the racemic mixture of gatifloxacin, a 20x2.1 mm Betasil silica column (Thermo) for isoniazid and pyrazinamide, and a 50x4.6 mm Hypersil silica column (Thermo) for ethambutol. The mobile phase for gatifloxacin and rifampicin comprised a gradient from 10% to 90% acetonitrile in

0.1% formic acid with a 5 min run time. For isoniazid and pyrazinamide, an isocratic elution using 80% acetonitrile in 0.1% formic acid was used. For ethambutol, an isocratic elution using 80% acetonitrile in 4 mM ammonium acetate and 0.1% trifluoroacetic acid was used. The flow rate was 0.3 mL/min and the injection volume was 5 mL. Moxifloxacin served as internal standard for gatifloxacin, rifapentine for rifampicin, neostigmine and propranolol for ethambutol and sulfamethoxazole for isoniazid and pyrazinamide.

The multiple reaction monitor scanning mode for monitoring transitions of [M-H]+ precursor ions to product ions was set at the following conditions: gatifloxacin m/z 376.2–261.3; moxifloxacin m/z 402.1–261.4; rifampicin m/z 823.5–791.4; rifapentine m/z 877.2– 845.3; ethambutol m/z 205-116; neostigmine m/z 209-71; isoniazid m/z 138.0–121.2; pyrazinamide m/z 124.1–81.1 and sulfamethoxazole m/z 254.0–92.2. Plasma protein was precipitated with three volumes of acetonitrile containing the internal standard. Samples were vortexed and centrifuged for 5 minutes at 750 g. Supernatant (5 mL) was injected into the column. Standard curves were linear in the ranges 0.1–30 mg/L for rifampicin, 0.1–15 mg/L for gatifloxacin and isoniazid, 0.1–10 mg/L for ethambutol and 0.2–70 mg/L for pyrazinamide.

Quality control samples covering the ranges were included in each run. The mean percentage accuracies reported for low, medium and high quality control samples were respectively, 97.81%, 99.42%, and 101.05% for isoniazid, 105.82%, 95.91%, and 99.65% for pyrazinamide, 98.45%, 97.81%, 97.18% for ethambutol, 97.49%, 92.85%, 96.26% for gatifloxacin and 98.91%, 101.80%, and 106.50% for rifampicin (Table 3.2). The precision coefficient of variation for determination at low, medium, and high quality control level for pyrazinamide and isoniazid was less than 14% and for rifampicin, ethambutol and gatifloxacin less than 7%. The lower limit of quantification (LLOQ) was set at 0.2 mg/L for pyrazinamide and 0.1 mg/L for rifampicin, gatifloxacin, ethambutol and isoniazid. Concentrations below the validation range of the assay were reported as below the lower limit of quantification (BLQ).

3.2. Population pharmacokinetic modelling

Software

Data analysis was performed applying a nonlinear mixed-effects approach, as implemented in NONMEM software, version 7.3 (Icon Development Solutions, Ellicott City, MD, USA) (Beal et at al. 2009), using ADVAN 13 and the first-order conditional estimation method with interaction (FOCE INTER). R (version 3.2.1) was used for graphical analysis and data management. Xpose (version 4.5.0) was used for data exploration and visualization as well as model diagnostics and model comparison (Jonsson and Karlsson 1998). The software tool Pearl-speaks-NONMEM (PsN) version 3.7.6 (Lindbom et al. 2005) was used to produce diagnostics such as non-parametric bootstrap, visual predictive checks (VPCs), (Holford 2005; Holford and Karlsson 2008) and prediction-corrected VPCs (pcVPCs) (Bergstrand et al. 2011) of the models.

A semimechanistic pharmacokinetic-enzyme turnover model to explain rifampicin autoinduction

All drugs were administered as oral doses in our study, thus preventing the estimation of absolute bioavailability. As such relative bioavailability was estimated fixing first dose bioavailability to 1 and estimating the relative change in bioavailability at steady state. One- and two-compartment distribution models were tested on the data. An enzyme turnover model, as described previously by Hassan et al. (1999) was adapted to characterize rifampicin's autoinductive properties. The change in amount of enzyme in the enzyme pool over time was expressed as follows (Eq. 1):

$$\frac{dA_{ENZ}}{dt} = k_{ENZ} \cdot (1 + EFF) - k_{ENZ} \cdot A_{ENZ} \qquad (1)$$

A_{ENZ} is the amount of enzyme in the enzyme pool. k_{ENZ} is the rate constant for the first-order degradation of the enzyme pool. At pre-induced state the amount in the enzyme pool was set to 1, and the steady-state equation balanced by constraining the zero-order production rate of the enzyme to be equal to k_{ENZ}. EFF is the relationship between the rifampicin concentration and the induction of the enzyme through an increased enzyme production rate. Linear and nonlinear relationships for *EFF* were tested. Induction was modelled as an increase in the enzyme production rate and not as a decrease in the enzyme elimination rate, assuming that rifampicin activates nuclear PXR (Chen and Raymond 2006). Rifampicin plasma

concentrations drive the enzyme pool, which in turn affects the clearance (*CL*) of the drug (Eq. 2):

$$CL = CL_{BASE} \cdot A_{ENZ} \quad (2)$$

where *CL* is the typical values of clearance after including the effect of autoinduction, which depends on CL_{BASE}, the typical *CL* in the pre-induced state and A_{ENZ} the model-predicted amount in the enzyme pool.

A transit absorption compartment model described by Savic et al. (2007) and already applied to rifampicin pharmacokinetics by Wilkins et al. (2008) for multiple dosing was used to capture the drug's highly variable absorption characteristics. The absorption model uses hypothetical transit compartments to mimic a delay in absorption onset and produces a gradual increase in absorption rate in a physiologically plausible manner. Drug transfer from the final transit compartment (in this case the absorption compartment) to the central compartment occurs via the rate constant k_{tr} (Eq. 3):

$$k_{tr} = \frac{N+1}{MTT} \quad (3)$$

Inter-individual variability (IIV) and inter-occasional variability (IOV) in the pharmacokinetic parameters was explored and modelled exponentially as in the case for *CL* (Jonsson and Karlsson 1998) (Eq. 4):

$$CL_{ij} = TV(CL) \cdot \exp\left(\eta_i + \kappa_{ij}\right)_{CL} \quad (4)$$

CL_{ij} is the oral clearance for individual *i* on occasion *j*. $(\eta_i)_{CL}$ is the IIV, normally distributed with mean 0 and variance ω^2_{CL}. $(k_i)_{CL}$ is the IOV, normally-distributed with mean 0 and variance $\omega^2_{IOV\_CL}$. Correlations between variability components were also tested. Different residual error models were investigated including proportional and slope-intercept models. Shrinkage was calculated for the random effects as (Eq. 5)

$$1\text{-}SD(\eta)/\omega \quad (5)$$

where η are the individual- (or occasion-) specific estimates of the random effects obtained from the post-hoc step (or empirical Bayes estimates) and ω is the population model estimate of the standard deviation in η.

Model selection was guided by using the NONMEM objective function value (OFV is proportional to minus twice the log likelihood of the data), standard error of parameter estimates, scientific plausibility, and goodness-of-fit plots together with VPC and when indicated, pcVPC.

Once the structural model was evaluated a covariate analysis was performed using 4 different basic pharmacokinetic-enzyme turn-over models: no scaling (Model 1), allometric scaling using body weight as the size descriptor applied to *CL* and apparent volume of the central compartment *V* (Holford 1996; West et al. 1997; West et al. 1999; Anderson and Holford 2008) (Model 2), allometric scaling using normal fat mass (*NFM*) as the size descriptor applied to *CL* and *V* and with $Ffat\text{-}_{CL}$ (estimated contribution of fat-free mass (*FFM*) and body weight to *CL*) or $Ffat\text{-}_{V}$ (estimated contribution of *FFM* and body weight to *V*) being estimated (Anderson and Holford 2009) (Model 3), and allometric scaling using *FFM* as the size descriptor applied to *CL* and *V* (Anderson and Holford 2008; Anderson and Holford 2009) (Model 4). *CL* and *V* were scaled allometrically standardized to a 70 kg patient using equations 7 (Eq. 6) and 8 (Eq. 7) respectively:

$$TV(CL) = CL_{STD} \cdot \left(\frac{MASS_i}{70} \right)^{\frac{3}{4}} \quad (6)$$

$$TV(V) = V_{STD} \cdot \left(\frac{MASS_i}{70} \right)^{1} \quad (7)$$

MASSi denotes individual values of the 3 size descriptors; body weight (Model 2), *NFM* (Model 3) and *FFM* (Model 4), used in the respective basic models. CL_{STD} is the typical oral clearance at pre-induced state in a patient weighing 70 kg. V_{STD} is the typical volume of distribution in a patient weighing 70 kg.

Creatinine clearance CL_{CR} was estimated from serum creatinine using the Cockcroft-Gault formula (Cockcroft and Gault 1976) (Eq. 8):

$$CL_{CR} = \frac{(140 - age) \cdot MASS \cdot K}{Serum\ \ creatinine} \quad (8)$$

where CL_{CR} is in ml/min, serum creatinine is in nmol/mL, age is recorded in years, *K* represents a constant of 1.23 for men and 1.04 for women, and *MASS* is the total body weight recorded in kilograms.

Individual *FFM* values FFM_i were calculated as follows (Eq. 9):

$$FFM_i = \frac{WHS_{MAX} \cdot HT^2 \cdot WT}{WHS_{50} \cdot HT^2 + WT} \quad (9)$$

where WHS_{MAX} is 42.92 kg/m^2 and WHS_{50} is 30.93 kg/m^2 in men. WHS_{MAX} is 37.99 kg/m^2 and WHS_{50} is 35.98 kg/m^2 in woman. *HT* is height in meters and *WT* is weight in kg.

NFM is obtained as the weighted average of the contributions of fat and non-fat body mass to the size predictor. This was estimated separately for *CL* (Eq. 10) and *V* (Eq. 11) as described by (Anderson and Holford 2009), with the equations below:

$$NFM_i = FFM_i + Ffat_{\_CL} \cdot (WT_i - FFM_i) \quad (10)$$

$$NFM_i = FFM_i + Ffat_{\_V} \cdot (WT_i - FFM_i) \quad (11)$$

where $Ffat_{\_CL}$ and $Ffat_{\_V}$ denotes the estimated unique contribution of fat mass (i.e. *WT* minus *FFM*) to *CL* and *V*, respectively.

Various parameter-covariate relationships were tested on each of the four different basic models. Sex, age and HIV status were tested on *CL*, *V*, F, *MTT* and EC_{50}, whereas CL_{cr} was only explored on *CL* (Models 2-4). The covariate effect of study site, tested as South Africa versus West Africa, was explored on *CL*, *V* and *F*. *WT* was investigated as a covariate on *CL* and *V* but only in Model 1. A fast method to build covariate models in population pharmacokinetic/ pharmacodynamic analysis based on linearization of the first-order conditional estimation (Khandelwal et al. 2011) was performed by Dr. Khandelwal as an initial step to screen for significant parameter-covariate relationships (Smythe et al. 2012). Briefly, the linearization method consisted of three steps. First the individual predictions (IPRED) and first partial derivatives of the IPREDs with respect to etas were extracted from each of the four non-linear

basic pharmacokinetic-enzyme models. Thereafter each of the four basic models was linearized and further developed using derivatives and prediction from each respective non-linear basic model. Lastly, covariates were tested using each of the four linearized basic models. The linearization method has many advantages compared to methods based on empirical Bayes estimates (EBE) or generalized additive models as it does not depend on the accuracy of the EBE's.

The covariate analysis using the linearized basic models was performed by Dr. Khandelwal (Smythe et al. 2012) via forward addition and backward elimination using stepwise covariate model building (SCM) as implemented in PsN (Harling et al. 2010). In the SCM, initially each covariate relationship was tested in a univariate fashion within NONMEM. The covariate model that resulted in the lowest significant drop in OFV was carried forward. In the forward step, statistically significance was defined as a decrease in OFV by more than 3.84 (Chi-square distribution, $p<0.05$, one degree of freedom). This step was repeated for the remaining parameter-covariate relations until no more covariate where eligible for inclusion based on the selected criterion. Thereafter, a backward deletion was performed to determine the best covariate model for each of the four basic models. In the backward deletion step, each parameter covariate relationship was then left out one at a time and tested using a statistical significance criterion of 1% (an increase in OFV of at least 6.635 for 1 degree of freedom). This step was repeated until no more covariates could be excluded.

The continuous covariates were included as linear functions (Eq. 12):

$$TVP = \theta_1 \cdot \left(1 + \theta_{COV} \cdot \left(COV - COV_{MEDIAN}\right)\right) \quad (12)$$

where θ_1 is the covariate parameter estimate in a typical patient with the median covariate value (COV_{median}). θ_{COV} is the fractional change in the parameter with each unit change in the covariate (COV) from COV_{median}. For the categorical covariates (sex and HIV status), the covariate model was expressed as follows (Eq. 13):

$$TVP = \theta_1 \cdot \left(1 + \theta_{COV} \cdot COV\right) \quad (13)$$

where, θ_1 is the typical value of parameter (*TVP*) and θ_{COV} is the fractional change in *TVP* for the covariate (*COV*). Dichotomous covariates are coded as 0 or 1 with the reference covariate coded as 0.

The best covariate model for each of the four basic models, as identified from the linearization method, were subsequently run in non-linear mixed effect models in order to generate parameter estimates, standard errors and VPC.

Simulations exploring a dose effect (450 and 600 mg) on the magnitude of rifampicin autoinduction were performed in the typical male patient with and without HIV infection weighing 55 kg (or *FFM*= 47.67) and subsequent drug exposure (expressed as the area under the concentration versus time curve from 0 to 24 hours [$AUC_{0\text{-}24}$]) was predicted for pre-induced and induced-state. In addition, *CL* was simulated over time from pre-induced CL_{BASE} to induced-state CL_{IND}.

The original data set was replicated generating 1000 new individuals retaining the original covariate distribution, except for HIV status, and the simulation repeated assuming all patients HIV co-infected or not to explore the effect of co-infection. In the simulation, rifampicin was administered daily until steady state of autoinduction and dosed like in the study (450 mg if body weight <50 kg and 600 mg otherwise). Median and 90% prediction intervals for $AUC_{0\text{-}24}$ and maximal rifampicin concentrations (C_{MAX}) according to HIV status and dose (at pre- and induced-state) were derived.

Population pharmacokinetic modelling of first dose and steady-state gatifloxacin

One- and two-compartment distribution models with first-order elimination were fitted to the data. Potential differences in gatifloxacin pharmacokinetic parameters were evaluated after initial and multiple doses. Similar to the rifampicin model described above, a transit absorption compartment model described gatifloxacin absorption characteristics, however, drug transfer from the final transit compartment to the central compartment occurs via the first-order rate constant k_a rather than the rate constant k_{tr}.

As gatifloxacin is primarily renally excreted (Nakashima et al. 1995), the typical value of clearance *TV*(*CL*) was parameterised as the sum of $TV(CL)_{GFR}$ accounting for the drug passively filtered by the kidneys, and $TV(CL)_{other}$ accounting for the remaining clearance (Eq. 14):

$$TV(CL) = TV(CL)_{GFR} + TV(CL)_{OTHER} \quad (14)$$

$TV(CL)_{GFR}$ was assumed to depend on CL_{CR} using Eq.15:

$$TV(CL)_{GFR} = (CL_{GFR})_{STD} \cdot \left(\frac{CL_{CR,i}}{CL_{CR(MEDIAN)}} \right) \quad (15)$$

where $(CL_{GFR})_{STD}$ is the clearance in a typical patient with a median CL_{CR} of 94 mL/min and $CL_{CR,i}$ is the individual CL_{CR}. $TV(CL)_{OTHER}$ was scaled to a body size descriptor (*MASS*) and reported for a typical 70 kg patient $(CL_{OTHER})_{STD}$ following Eq.6.

Allometric scaling with either *WT*, *NFM* or *FFM* was applied to *CL* and *V* terms as described in equations 7 (Eq. 6) and 8 (Eq. 7) respectively.

Creatinine clearance (CL_{CR}) was estimated from serum creatinine using the Cockcroft-Gault formula (Cockcroft and Gault 1976) as described by Eq. 8.

FFM and *NFM* for all *CL* and *V* terms was calculated using equations 9, 10 and 11 respectively.

IIV and IOV were modelled exponentially for all parameters as described in equation 4. Correlation between random effects was also tested. Different residual error models were investigated including proportional and slope-intercept models. Shrinkage was calculated for the random effects as described previously.

Once the basic model (structural and stochastic) was developed, a covariate analysis was performed using SCM as described previously for the rifampicin autoinduction model. Sex, age, HIV status and study site (South Africa versus West Africa), were investigated as covariate effects on the following parameters; CL_{GRF}, CL_{OTHER}, *V*, k_a, *MTT* and bioavailability (*F*). Continuous covariates were firstly introduced in a linear fashion (fractional change) and centred on the median covariate value. If a continuous covariate was included in a linear fashion, inclusion according to a nonlinear fashion (i.e. piece-wise linear, exponential, and

power equation) was also tested. For categorical covariates, models were expressed as fractional change from the typical value.

Based on the final model, the AUC from zero hours to infinity ($AUC_{0-\infty}$) was derived to describe exposure after the first dose while the AUC from 0 to 24 hours (AUC_{0-24}) described exposure at steady-state (Day 28). Total oral clearance was simulated for 10 000 virtual patients and the appropriate exposure for first dose and steady state derived through (Eq. 16):

$$AUC = F \cdot \frac{Dose}{CL} \qquad (16)$$

The individual percentage change in AUC between first dose and steady state was calculated and reported as median (5^{th}-95^{th} percentiles). 10 000 virtual patients were derived by re-sampling the sets of individual covariate values from the original subjects.

As a pharmacokinetic / pharmacodynamic (PK/PD) index, the ratio of the day 28 free gatifloxacin AUC for a 24 hour-dosing interval over the minimum inhibitory concentration (*f*AUC/MIC) was used, as this has been shown to correlate to clinical outcome (Pasipanodya and Gumbo 2011). The PK/PD target was defined as *f*AUC/MIC$\geq$125 which corresponds to a surrogate for maximal bactericidal effect and reduced probability of resistance (Forrest et al. 1993; Schentag et al. 2001). The probability of target attainment (PTA) (Mouton et al. 2005b), i.e. the proportion of patients expected to achieve effective exposure, at different MIC levels was investigated with Monte Carlo simulations. The final model describing the pharmacokinetics in our study population was used together with the MIC distribution from an *in vitro* study investigating the activity of gatifloxacin against 234 clinical strains of MTB isolated in the Southeast of Spain published by (Rodriguez et al. 2002) with a MIC range of 0.06 to 16 mg/L. The median MIC_{50} from the aforementioned study was 0.125 mg/L while the median MIC_{90} was 0.25 mg/L with only 6 strains (2.5%) having MIC >0.25 mg/L. Unfortunately MIC distributions for gatifloxacin in local tuberculosis infected patients were not available at the time of the study although the MIC_{90} in the Rodriguez study compared favourably with other studies (Perry et al. 1999; Nuermberger and Grosset 2004).

The acceptable level for the PTA is still under debate as is the most appropriate value for the target ratio of *f*AUC/MIC for optimal activity of gatifloxacin against MTB. Therefore, the target ratio of *f*AUC/MIC as a function of the MIC, with the 80% and 90% confidence intervals (CI)

were derived. The lower boundary in the 80% and 90% CI's of the total probability function is equivalent to 90% and 95% PTA (Mouton et al 2005). The PK/PD breakpoint was defined as the MIC at which the calculated PTA was 90%.

Ten thousand individual *f*AUC's were simulated based on the final model by integrating predicted drug concentrations from 0 to 24 hours at steady state and thereafter correcting for serum protein binding, which was assumed to be 20% (Nakashima et al. 1995; Gajjar et al. 2000). The PTA, i.e. the probability of *f*AUC/MIC≥125 across the range of MIC's described (Rodriguez et al. 2002), was derived. The cumulative fraction of response (CFR) (Mouton et al. 2005b) was calculated representing the proportion of the population achieving *f*AUC/MIC≥ 125, given Monte Carlo simulation and the MIC distribution of MTB for 400, 600 and 800 mg once daily of gatifloxacin at steady-state in combination with rifampicin, isoniazid and pyrazinamide. The CFR was calculated using Eq. 17:

$$\sum_{i=1}^{n} PTA_i \cdot F_i \qquad (17)$$

where i indicates the MIC category ranked from lowest to highest MIC value, PTA_i is the PTA at each MIC level and *F* is the fraction of the MTB population at each MIC category. *F* was calculated at each MIC as the number of isolates divided by the total number of isolates (n=234) yielding the frequency for each MIC.

Population pharmacokinetics of first-line tuberculosis drugs

The following analysis utilised simple models quantifying drug exposure in all study participants to be used in subsequent PK/PD analysis (Chapter 7). Concentration-time observations for rifampicin, isoniazid, pyrazinamide, and ethambutol were analysed separately. Observations falling below the LLOQ for gatifloxacin (<8%), isoniazid (<7%), rifampicin (<5%), pyrazinamide (<1%) and ethambutol (<1%) were imputed as LLOQ/2. Series of BLQ values were handled by including in the analysis the first value and excluding all trailing ones in the elimination phase, and the converse during absorption phase, (Beal 2001). All BLQ and excluded values were included for simulation-based diagnostics, such as VPC's.

Visual inspection of the data revealed several profiles that appeared physiologically implausible, possibly due to sample swaps or other experimental issues. To try and identify such profiles in an objective manner, it was decided to explore how the individual contributions to the objective function value (iOFV) from each profile compared to the levels expected from a simulation. Once a reasonably well fitting pharmacokinetic model had been developed for each drug, this was used on the data assuming each pharmacokinetic sampling occasion as a separate individual. A simulation-re-estimation procedure was implemented using the stochastic simulation and estimation (SSE) tool in PsN. Briefly, this procedure simulates data based on the model, and then applies the same (or an alternative) model to fit the simulated data. This procedure was repeated 10 times and iOFV's were obtained for each pharmacokinetic profile. The values from the simulation and the original values of iOFV were compared for each profile, and the profiles in the original data characterised by and iOFV larger than all values generated in the simulations were flagged and further inspected for exclusion. The idea behind this procedure is that a pharmacokinetic profile with a value of iOFV conspicuously larger than the ones obtained by re-simulation is characterised by poor model fit, and was then inspected to identify the potential presence of data errors.

Various residual error models were investigated including combinations of additive and proportional error models. One- and two-compartment distribution models with first-order elimination were fitted to the data. A transit absorption compartment model described the absorption characteristics of each drug. Drug transfer between transit compartments occurred via the rate constant k_{tr} (Eq. 3). Drug transfer from the final transit compartment to the central compartment occurred via the first-order rate constant k_a. IIV and IOV were modelled exponentially using equation 4. Correlations between variability components were tested.

Allometric scaling using either *WT*, *FFM* or *NFM* was applied to clearance and volume of distribution terms as described in equations 6 and 7. Clearance and apparent volume of distribution terms were reported on the median patient body size descriptor. *FFM* was calculated using (Eq. 9) while *NFM* was estimated uniquely for *CL* and *V* terms using equations 10 and 11 respectively. *NFM* was similarly estimated for inter-compartment clearance (Q) and peripheral compartment volumes (V_p) in 2-compartment distribution models.

Covariate relationships were identified by clinical and statistical significance. Continuous covariates were regarded as clinically significant (and hence retained in the final model) if the fractional change in the typical parameter was greater than 10% when comparing the typical parameter value to either the minimum or maximum value of the covariate. Covariate relationships were tested in the model using stepwise addition (forward step) applying a 5% significance level (i.e. difference in the NONMEM objective function value of >3.84) as the cut-off for inclusion. After identification of the full forward model, a backward deletion step was performed to determine the final model. In the backward deletion step each parameter covariate relationship was left out 1 at a time and tested using a statistical significance criterion of 1% (i.e. difference in the NONMEM objective function value of >6.635). The backward deletion step was repeated until no more covariate could be excluded and the resulting model was referred to as the final model. Continuous covariates were introduced in a linear fashion as fractional changes and centred on the median covariate value (COV_{median}) according to Eq. 12. If a continuous covariate was included in a linear fashion, inclusion according to a nonlinear fashion (i.e. piece-wise linear, exponential, and power equation) was also tested. When investigating categorical covariates e.g. sex, HIV status, and site effect, covariate models were represented as fractional changes from *TVP* (Eq. 13). When investigating continuous covariates potentially affecting both k_a and *MTT*, we used the same parameter to simultaneously affect the proportional change in both absorption parameters using respective Eq. 18 and 19:

$$TVk_a = \theta_2 \cdot \left(1 + \theta_{COV} \cdot \left(COV - COV_{MEDIAN}\right)\right) \quad (18)$$

$$TVMTT = \theta_2 \cdot \frac{1}{\left(1 + \theta_{COV} \cdot \left(COV - COV_{MEDIAN}\right)\right)} \quad (19)$$

where θ_2 is the covariate parameter estimate in a typical patient with the median covariate value (COV_{median}). θ_{COV} is the fractional change in the parameter with each unit change in the covariate (*COV*) from COV_{median}. For categorical covariates (sex, site, and HIV status), the covariate model was expressed as follows for k_a and *MTT* using respective Eq. 20 and 21:

$$TVk_a = \theta_2 \cdot \left(1 + \theta_{COV} \cdot COV\right) \quad (20)$$

$$TVMTT = \theta_1 \cdot \frac{1}{\left(1 + \theta_{COV} \cdot COV\right)} \quad (21)$$

where, θ_2 is the typical value of parameter of the absorption rate constant (TVk_a) or mean absorption transit time (*TVMTT*) and θ_{COV} is the fractional change in either typical value for the covariate (*COV*). Dichotomous covariates are coded as 0 or 1 with the reference covariate coded as 0. Under conditions were the covariate model did not support simultaneous effect on k_a and *MTT*, equations 12 and 13 were applied to respective continuous and categorical covariates on either absorption parameter individually. Categorical covariates were regarded clinically significant (and hence retained in the final model) if the fractional change from the typical covariate was greater than 10%.

Pharmacokinetic models incorporating separate fixed effects for the typical values of bioavailability and clearance at single dose and steady state were implemented, enabling the investigation of the effect of multiple dosing on drug concentrations. Similarly, regimen effect parameters were estimated to investigate the potential effect of drug-drug interactions when the drug was dosed either in control or test regimens of the study. AUC was estimated using Eq. 16 both at first dose (from 0 to infinity hours) and steady state (from 0 to 24 hours). Similarly, peak concentration (C_{MAX}) at first dose and steady state was estimated within NONMEM applying the final pharmacokinetic model.

3.3. Classification and Regression Tree Analysis (CART)

Classification & regression tree (CART) analysis was used to identify factors predictive of treatment outcome (Breiman et al. 1984; Steinberg and Colla 1995). CART identifies important patterns and relationships even in highly complex data. Optimal predictor cut-off values or class assignment for continuous and categorical variables respectively, are identified at each node of the decision tree. CART builds a regression tree with the root node as the most significant predictor of the outcome variable and daughter nodes trying to maximize homogeneity in the two groups. This process is repeated automatically and hence known as a binary recursive partitioning technique. Additionally, CART generates a variable importance

score, based on how much each subsequent daughter node improves the primary predictor. The score of the root node is 100%, with the improvement by the predictors identified in daughter nodes scored relative to the root node. Battery options within CART were employed to select both optimal parent (Atom) and daughter (Minchild) node sizes. Goodness-of-fit for each tree was assessed by 10-fold cross-validation and receiver operating curves. In the cross-validation, the data are randomly split into 2 datasets, with one used for training and the other as the test data, and CART analysis performed. This was repeated 10 times, so that 10 randomly split datasets were tested, for 10 CART analyses. True predictive power is defined as performance of the training set–derived tree on the test dataset. Pruning was used to select optimal trees, based on relative misclassification costs, complexity, and parsimony. The optimal tree was chosen based on the lowest cross-validated relative error.

In this study two outcomes were considered: short and long-term outcomes. The short-term outcome (culture conversion at 2 months) was defined in the OFLOTUB study as when patients were culture and smear negative at two months post treatment initiation (Merle et al. 2014). The long-term outcome was defined as a composite of treatment failure, or relapse, or death, up to two years (24 month) post treatment completion (Merle et al. 2014). Potential predictors for both outcomes included steady state C_{MAX} and AUC for rifampicin, isoniazid, pyrazinamide, ethambutol & gatifloxacin, age (in years), sex, body mass index (BMI), HIV status, baseline cavitation (defined as presence or absence) and number of lung zones affected (defined as scores ranging from 0 to 6, with 0 indicating that no lung regions are affected and 6 indicating that all lung regions are affected), baseline sputum smear (defined as scores ranging from 1+ to 3+, with higher numbers indicating more severe disease), and regimen (i.e. “control arm” including rifampicin, isoniazid, ethambutol & pyrazinamide vs. versus “test arm” with gatifloxacin replacing ethambutol). As the target variable for 2 and 24-month outcomes was binary, we employed the Gini splitting rule within CART (Breiman et al. 1984). We assumed equal probability of class distribution within the population sampled using the Priors Equal procedure in CART.

Point estimates and confidence intervals for the odds ratio (OR) were calculated using the OR calculator within STATA version 13 (Stata Corp. 2013. Stata Statistical Software: Release 13. College Station, TX: Stata Corp LP). Confidence intervals were calculated for the OR applying a 95% confidence level using the Woolf approximation. 2-sided Fisher's exact P, rather than

the chi-squared, and its significance level was calculated when individual cell counts were <5. Where cell counts of zero were encountered, 0.5 was added to each cell.

Table 3. 1 *Demographics and clinical characteristics of 343 patients within the OFLOTUB phase III pharmacokinetic sub-study stratified by study site and treatment regimen. Unless stated otherwise, data variables given as median (5th & 95th percentile).*

	All sites (n=343)		**South Africa (n=200)**		**Benin (n=52)**		**Guinea (n=38)**		**Senegal (n=53)**	
	Test	**Control**	**Test**	**Control**	**Test**	**Control**	**Test**	**Control**	**Test**	**Control**
No. of patients (%)	169 (49)	174 (51)	99 (51)	101 (49)	25 (42)	27 (58)	19 (50)	19 (50)	26 (49)	27 (51)
No. of females (%)	53 (31)	60 (34)	37 (37)	42 (42)	5 (20)	6 (22)	8 (42)	7 (37)	3 (12)	5 (19)
No. of HIV^+ (%)	54 (32)	54 (31)	51 (52)	49 (49)	3 (12)	3 (11)	2 (11)	0 (0)	0 (0)	0 (0)
Age (years)	29 (20-49)	28 (20-49)	30 (20-49)	28 (20-51)	30 (21-55)	34 (19-52)	25 (18-42)	25 (18-53)	28 (20-46)	27 (19-48)
[a]CL_{CR} ($mL \cdot min^{-1}$)	91 (60-132)	91 (59-140)	100 (70-138)	94 (58-145)	75 (50-101)	73 (55-123)	89 (57-117)	94 (48-141)	87 (71-178)	91 (53-146)
[b]*FFM* (kg)	45 (30-56)	45 (32-55)	45 (31-55)	43 (31-54)	46 (26-54)	46 (29-55)	45 (30-62)	45 (32-54)	49 (32-57)	48 (31-60)
Bodyweight (kg)	55 (42-70)	55 (43-70)	56 (44-75)	55 (43-69)	53 (36-64)	56 (40-72)	52 (40-76)	52 (45-80)	55 (43-67)	55 (39-70)

[a]CL_{CR}, creatinine clearance; [b]FFM, fat free mass; Test, test regimen comprised of rifampicin, pyrazinamide, isoniazid and gatifloxacin; Control, control regimen comprised of rifampicin, pyrazinamide, isoniazid and ethambutol.

Table 3. 2 *Summary of quality control samples included in each run during concentration quantification by tandem high-pressure liquid chromatographic tandem mass spectrometric methods for rifampicin, isoniazid, pyrazinamide, ethambutol, and gatifloxacin. The mean percentage accuracies, together with standard deviation and precision estimates are reported for high, medium and low quality control samples.*

Quality control sample	**High**	**Medium**	**Low**
Rifampicin [µg/mL]	25	12	0.3
Mean % accuracy	106.5	101.80	98.91
STDEV	6.28	6.78	6.92
RSD (%)	5.90	6.66	7.00
Gatifloxacin [µg/mL]	25	12	0.3
Mean % accuracy	96.26	92.85	97.49
STDEV	5.48	2.78	6.88
RSD (%)	5.69	2.99	6.85
Ethambutol [µg/mL]	2.5	0.9	0.3
Mean % accuracy	97.18	97.81	98.45
STDEV	6.08	5.79	6.04
RSD (%)	6.25	5.92	6.14
Pyrazinamide [µg/mL]	60	30	0.6
Mean % accuracy	96.73	98.90	98.46
STDEV	5.42	4.37	3.15
RSD (%)	5.61	4.42	3.20
Isoniazid [µg/mL]	15	7.5	0.3
Mean % accuracy	94.23	98.36	94.14
STDEV	4.56	5.43	5.77
RSD (%)	4.84	5.52	6.13

STDEV, standard deviation; RSD (%), percent relative standard deviation. The lower limit of quantification (LLOQ) for rifampicin, gatifloxacin, ethambutol, and isoniazid was 0.1 µg/mL while for pyrazinamide it was 0.2 µg/mL.

4. A semimechanistic pharmacokinetic-enzyme turnover model to explain rifampicin autoinduction in adults with tuberculosis

Rifampicin is a central constituent of first-line therapy used in the treatment of drug-susceptible MTB. During the 2-month intensive phase of standard short-course antituberculosis treatment, patients receive rifampicin in combination with isoniazid, pyrazinamide and ethambutol. Rifampicin and isoniazid are given for a further 4-month continuation phase, completing the 6-month treatment regimen. Isoniazid is responsible for killing the majority of organisms within the first 2 days of treatment. From the third to the seventh day of treatment, rifampicin and pyrazinamide continue the bactericidal function (Mitchison 2000), while ethambutol protects against the development of rifampicin resistance in the event of pre-existing isoniazid resistance (Blumberg et al. 2003). The ability of rifampicin to eradicate persisting mycobacteria has enabled the shortening of treatment from 12 to 6 months (WHO 2003).

Rifampicin is a potent activator of the nuclear PXR, which regulates the transcription of multiple drug metabolizing enzymes and drug transporters (Geick et al. 2001; Chen and Raymond 2006). Although the exact mechanism has not been elucidated, following chronic intravenous or oral dosing, rifampicin has been shown to induce its own metabolism and/or elimination by increasing its systemic and pre-systemic clearances (Loos et al. 1985; Niemi et al. 2003). This effect might, in part, be attributed to the PXR-mediated induction of P-gp, a trans-membrane efflux transporter expressed in enterocytes and hepatocytes (Faber et al. 2003; Loos et al. 1985), and the class β-esterase's (Staudinger et al. 2010; Nakajima et al. 2011) which are responsible for the biotransformation of rifampicin to its major metabolite, 25-deacetyl rifampicin (Jamis-Dow et al. 1997).

While steady-state population pharmacokinetics of rifampicin has been described for adult African patients (Wilkins et al. 2008), to date there has been no simultaneous characterisation of first dose and steady state kinetics. Thus the aim of this chapter was to develop a semimechanistic pharmacokinetic enzyme turnover model describing rifampicin pharmacokinetics after first dose and steady state in adult patients with tuberculosis.

Additionally, four different structural basic models were explored in order to assess whether scaling affects the final covariate selection procedure.

4.1. Results

A total of 946 rifampicin concentration-time observations from 174 patients were included in the analysis. All pre-dose observations (54 out of 1004) following an unobserved dose at the induced state and all observations falling below the LLOQ (4 of 950 samples; LLOQ = 0.1 mg/L) were excluded. The final rifampicin pharmacokinetic-enzyme model is shown in Figure 4.1.

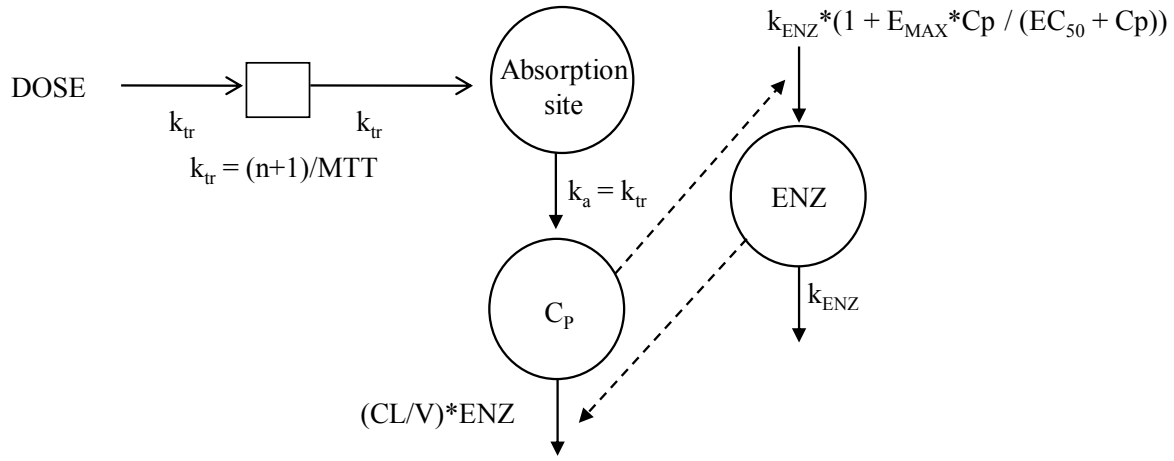

Figure 4. 1 *Rifampicin pharmacokinetic-enzyme model including a one-compartment disposition model and a transit absorption compartment model. Drug is transferred from the absorption compartment into the central compartment via the rate constant k_{tr}. Rifampicin autoinduction was modelled with an enzyme turn-over model, where rifampicin plasma concentrations (CP) increase the enzyme production rate (k_{ENZ}) which in turn increases the enzyme pool (ENZ) in a non-linear fashion by means of an E_{MAX} model. ENZ in turn increases rifampicin's clearance.*

Demographics and covariates of patients included in the rifampicin pharmacokinetic-enzyme turn-over model are described in Table 4.1. The final model included a nonlinear relationship between rifampicin concentration and induction of the enzyme through an increased enzyme production rate as shown in the equation below:

$$\frac{dA_{ENZ}}{dt} = k_{ENZ} \cdot (1 + EFF) - k_{ENZ} \cdot A_{ENZ}$$

EFF is the relationship between the rifampicin concentration and the induction of the enzyme through an increased enzyme production rate. The nonlinear E_{MAX} model best described (OFV dropped by approximately 13 points compared to the linear method) the relationship between rifampicin concentration and the induction of the enzyme (*EFF*) shown in the equation below:

$$EFF = \left(\frac{E_{MAX} \cdot C_p}{EC_{50} + C_p} \right)$$

where EC_{50} is the rifampicin concentration that causes half of the maximum induction (E_{MAX}) and C_p is the plasma drug concentration.

Table 4.1 *Demographics and covariates of patients included in the rifampicin pharmacokinetic-enzyme turn-over model.*

	Values for patients from			
Parameter [a]	**South Africa**	**Senegal**	**Benin**	**Guinea**
Total no. of patients	101	27	19	27
No. of patients on 450 mg dose	23	5	7	3
No. of male/female patients	59/42	22/5	12/7	21/6
No. of HIV^+ patients	49	0	2	3
Median *FFM* (IQR)	44 (37-49)	48 (42-50)	45 (39-47)	46 (43-50)
Median body weight (kg) (IQR)	56 (50-61)	55 (52-61)	53 (50-58)	56 (51-60)
Median age (years) (IQR)	28 (24-37)	26 (23-32)	25 (23-31)	34 (25-44)
Median CL_{CR} (mL/min) (IQR)	98 (85-115)	91 (81-106)	95 (81-124)	75 (67-88)

[a] *Continuous covariates are given as median (interquartile range, IQR). FFM, fat free mass; CL_{CR}, creatinine clearance.*

The four basic models and their respective best covariate model are described in Table 4.2. The underlying structural model with or without allometric scaling did not influence the final covariates. The best covariate model for Model 1 (no scaling) included body weight and sex on clearance and volume, and HIV on volume. For Model 2 (scaling with body weight), HIV

and sex on volume were selected. For Model 3 (scaling with *NFM*) and Model 4 (scaling with *FFM*), HIV on volume described the best covariate relationship. The best covariate model for all four basic models was very similar as all models contained influence of body weight, sex and HIV infection either as part of the allometric scaling or estimated as a covariate relationship. Of the four basic models, Models 1, 2 and 4 contained fewer parameters than Model 3. The highest ΔOFV (OFV_{best} – OFV_{basic}) was for Model 1 (ΔOFV=-46.72), followed by Model 4 ((ΔOFV=-26.03). Both Model 1 and 4 were able to describe the data but Model 4 was considered better since it contained fewer parameters. Model 4 and 1 cannot be compared based on likelihood ratio tests since these models are not nested. Model 4 was also not selected as the final model since the estimate of k_{ENZ} was not regarded as plausible. The ΔOFV for Model 3 between basic model and best covariate model was -21.09 and was larger than for Model 2. Model 3 included allometric scaling using *NFM* i.e. WT minus *FFM*. Hence, in keeping with allometric scaling theory (Anderson and Holford 2008), Model's 3 and 4 were candidates for best covariate model. Ultimately, even with added complexity with respect to Model 4 (2 parameters), Model 3 was chosen as the final model based on precision of parameter estimates, scientific plausibility and ΔOFV.

The parameters of the induction process, k_{ENZ} and EC_{50} were both well estimated with relative standard errors of approximately 6% (Table 4.3). The application of linearization approximation for covariate screening made it possible to explore the effect of covariate screening for different basic models with different approaches with and without allometric scaling. The parameter estimates from the final pharmacokinetic-enzyme turn-over model are shown in Table 4.3, with HIV infection associated with a 29.6% increase in the typical value of apparent volume of distribution.

Table 4.2 *Comparison of the four different basic models and their subsequent best covariate models.*

Model	Basic model (no. of fixed-effect parameters)[a]	Best covariate model (no. of fixed-effect parameters)	OFV		ΔOFV [b]	%IIV decrease (s)
			Basic model	Best covariate model		
1	No scaling (10)	WT & SEX-*CL*, WT & SEX-*V*, HIV-*V* (15)	2169.17	2122.45	-46.72	2.65[c], 48.03[d]
2	Allometric scaling with WT (10)	HIV-*V*, Sex-*V* (12)	2154.90	2133.56	-21.34	16.30[d]
3	Allometric scaling with *NFM* (12)	HIV-*V* (13)	2145.89	2124.80	-21.09	2.90[d]
4	Allometric scaling with *FFM* (10)	HIV-*V* (11)	2157.44	2131.41	-26.03	5.86[d]

[a] *Allometric scaling was applied to clearance (CL) and the apparent volume of the central compartment (V) using body weight (WT), fat free mass (FFM), or normal fat mass (NFM).*

[b] *ΔOFV is the difference in the objective function value (OFV) between the basic model and the best covariate model ($OFV_{best} - OFV_{basic}$).*

[c] $\%IIV\_decrease = \frac{\omega^2_{CL}base - \omega^2_{CL}final}{\omega^2_{CL}base} \cdot 100$

[d] $\%IIV\_decrease = \frac{\omega^2_{V}base - \omega^2_{V}final}{\omega^2_{V}base} \cdot 100$

Table 4.3 *Parameter estimates based on the final rifampicin pharmacokinetic-enzyme turn-over model.*

Parameter [a]	**Estimate**	**% RSE**
CL (L/h)	10.0	3.7
$Ffat\text{-}_{CL}$	0.311	40.2
V (L)	86.7	2.3
$Ffat\text{-}_{V}$	0.188	49.1
V-HIV (%)	29.6	17.2
MTT (h)	0.713	1.6
N	1 FIX	1 FIX
E_{MAX}	1.04	2.6
EC_{50} (mg/L)	0.0705	6.3
k_{ENZ} (1/h)	0.00369	5.6
Correlation *CL*-*V* (%)	91.1	20.7
IIV_{CL} (%)	30.0	12.3
IIV_{V} (%)	19.2	14.8
IIV_{EC50} (%)	493.0	19
IOV_{MTT} (%)	68.0	7
IOV_{F} (%)	16.2	11.2
Additive error (mg/L)	0.965	2.8
Proportional error (%)	9.9	4.7

[a] *IIV, inter-individual variability expressed as coefficient of variation; IOV, inter-occasion variability expressed as coefficient of variation; RSE, relative standard error computed from NONMEM reported on the approximate standard deviation scale; CL, the typical clearance at pre-induced state in a patient weighing 70 kg; V, the typical apparent volume of distribution in a patient weighing 70 kg; MTT, absorption mean transit time; N, number of transit compartments;* E_{MAX}*, maximal increase in the enzyme production rate;* EC_{50}*, rifampicin concentration at*

which half E_{MAX} is reached; k_{ENZ}, rate constant for first-order degradation of the enzyme pool; Correlation CL-V, correlation between CL and V; $Ffat_{-CL}$, estimated contribution of fat mass to scaling of CL; $Ffat_{-V}$, estimated contribution of fat mass to scaling of V; V-HIV, increase in apparent volume of distribution in HIV infected patients; 1 FIX, number of transit compartments fixed to 1. F (bioavailability) was fixed to 1. Shrinkage estimates for IIV_{CL}=23.3%, IIV_{V}=22.7%, IIV_{EC50}=60.1%, IOV_{MTT}=36.5% and IOV_{F}=47.3%.

The final pharmacokinetic-enzyme turn-over model described the rifampicin concentration-time data both at pre- and induced-state as shown in the pcVPC (Figure 4.2). The rate constant for the first-order degradation of the enzyme pool (k_{ENZ}) was estimated to 0.00369 /h. As such, the turn-over of the inducible process was estimated with a corresponding half-life of approximately 8 days in a typical patient. Assuming 5 half-lives to steady-state, this is equivalent of approximately 40 days to induced-state for rifampicin autoinduction. Hence, full induction occurred before the end of the two-month intensive phase of antituberculosis treatment.

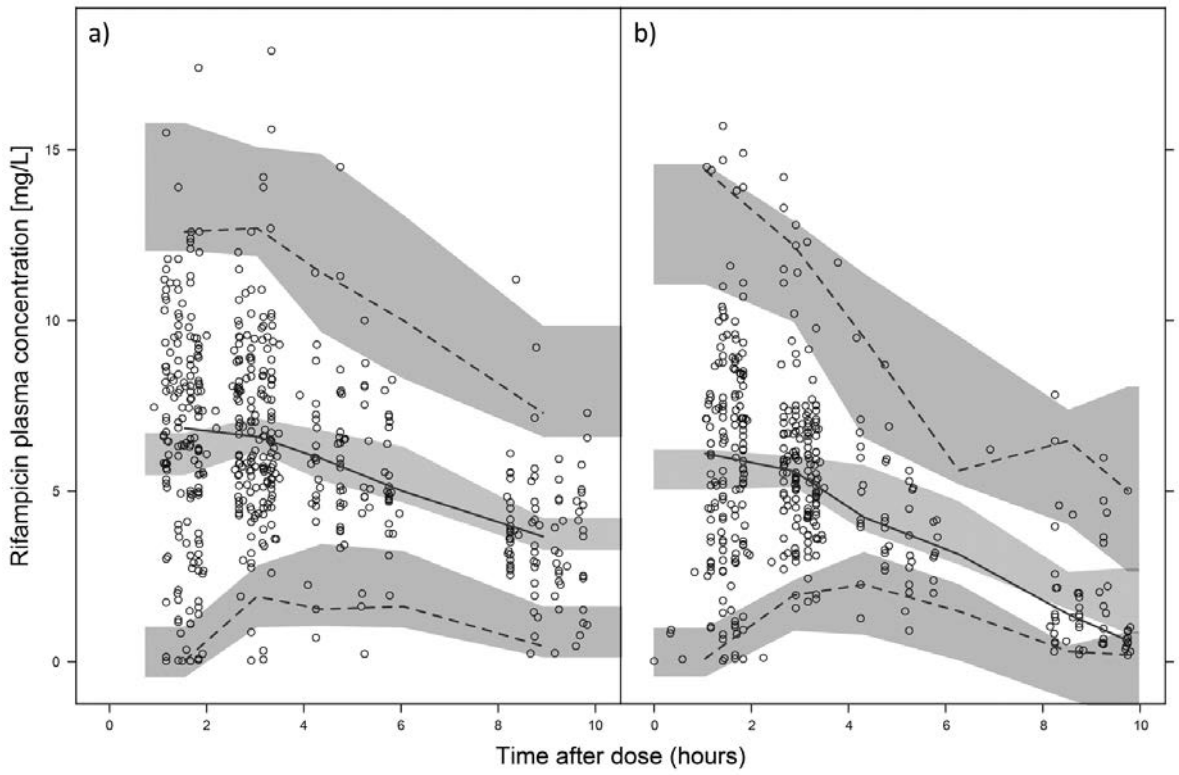

Figure 4. 2 *Prediction-corrected visual predictive check (pcVPC) of the final rifampicin pharmacokinetic-enzyme turn-over model stratified by occasion. (a) Occasion 1, pre-induced state and (b) occasion 2, after at least 28 days of RMP administration. The solid and dashed lines are the medians and 5th and*

95th percentiles of the observed rifampicin plasma concentrations, respectively. Shaded areas are the 95% prediction intervals for the medians and 5th and 95th percentiles of simulated data. The open circles are observed patient concentration-time data.

Simulated clearance and $AUC_{0\text{-}24}$ values for a typical 55 kg male patient with and without HIV infection following daily doses of 450 and 600 mg are shown in Table 4.4. Simulated clearance from first dose to steady-state of autoinduction in a typical patient is illustrated in Figure 4.3. Model-based simulations of oral clearance in the typical patient without HIV infection increased from 7.76 L/h at pre-induced state to induced-state clearance values of 14.16 and 14.37 L/h following respective 450 and 600 mg doses. Hence, autoinduction resulted in similar increases of 1.82-and 1.85-fold in clearance from pre-induced to induced-state corresponding to 41 and 42% reductions in $AUC_{0\text{-}24}$ following multiple 450 and 600 mg doses, respectively.

Table 4.4 *Predicted CL and $AUC_{0\text{-}24hr}$ values for typical 55 kg male patients with and without HIV infection at pre-induced and induced states following daily rifampicin doses of 450 and 600 mg.*

Parameter [a]	**450 mg** **TB**	**450 mg** **TB+HIV**	**600 mg** **TB**	**600 mg** **TB+HIV**
CL_{BASE} *(L/h)*	7.76	7.76	7.76	7.76
CL_{IND} *(L/h)*	14.16	14.62	14.37	14.82
CL fold increase	1.82	1.88	1.85	1.91
$AUC_{0\text{-}24hr,\ BASE}$ ($mg \cdot h/L$)	53.86	51.01	71.80	68.01
$AUC_{0\text{-}24hr,\ IND}$ ($mg \cdot h/L$)	31.70	30.80	41.80	40.50
$AUC_{0\text{-}24hr}$ reduction (%)	41.14	39.62	41.78	40.45

[a] *BASE, first dose; IND, induced-state; TB, patients infected with tuberculosis; TB+HIV, patients infected with tuberculosis and HIV; CL, clearance; fold increase in CL, CL_{IND} / CL_{BASE}; $AUC_{0\text{-}24hr}$, area under the concentration-time curve from 0 to 24 hours; $AUC_{0\text{-}24hr}$ reduction, reduction in $AUC_{0\text{-}24hr}$ from pre-induced to induced state.*

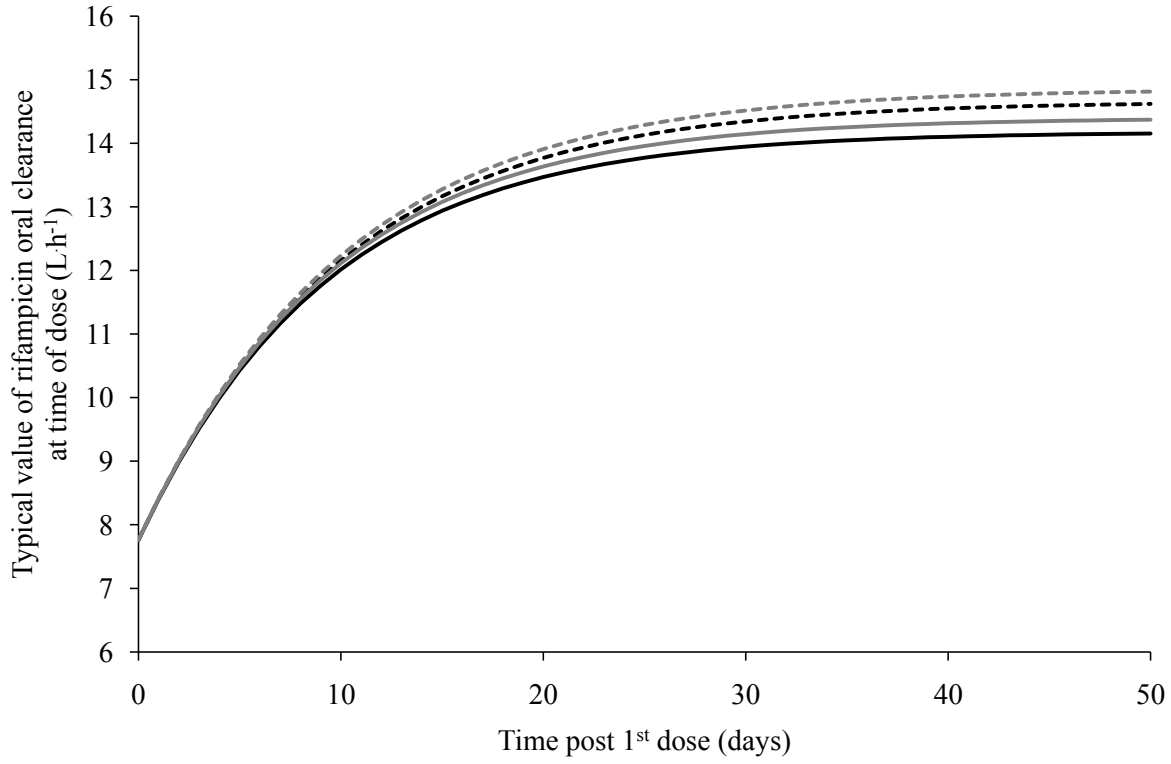

Figure 4. 3 *Simulated oral rifampicin clearance versus time on treatment in a typical 55 kg male patient with HIV (450 mg/day grey solid line; 600 mg/day grey dashed line) and without HIV (450 mg/day black solid line; 600 mg/day black dashed line). In the simulations, rifampicin was given 7 days/week.*

Table 4.5 shows the simulated $AUC_{0\text{-}24}$ and C_{MAX} values for patients with or without HIV infection, receiving 450 or 600 mg daily doses of rifampicin according to body weight. Patients weighing less than 50 kg and receiving the 450 mg dose had a median $AUC_{0\text{-}24}$ approximately 10% lower than patients weighing 50 kg or above and receiving the 600 mg dose. These differences in $AUC_{0\text{-}24}$ can be accounted for by differences in body weight. Figure 4.4 illustrates simulated C_{MAX} for different subgroups using the final pharmacokinetic-enzyme turn-over model. The median C_{MAX} was lower in HIV infected patients compared to patients without HIV irrespective of dose and duration of dosing. Notably, less than a third of all patients, irrespective of dose and HIV status, achieved a C_{MAX} above the target 8 mg/L (Peloquin 2002) at induced-state.

Table 4.5 *Median and 90% prediction interval values of simulated $AUC_{0\text{-}24hr}$, C_{MAX}, and normal fat mass in patients with (n=1000) or without (n=1000) HIV infection at pre-induced and induced states following daily rifampicin doses of 450 (body weight of <50 kg) or 600 mg (body weight of ≥50 kg).*[a]

	450 mg **TB**	**450 mg** **TB+HIV**	**600 mg** **TB**	**600 mg** **TB+HIV**
Median *NFM*	43	37	49	48
$AUC_{0\text{-}24hr,\ BASE}$ (mg·h/L)	65.84 (38.38 – 116.60)	63.46 (39.08 – 113.39)	71.24 (41.50 – 123.81)	72.39 (42.56 – 121.04)
$AUC_{0\text{-}24hr,\ IND}$ (mg·h/L)	42.00 (20.98 – 87.39)	43.30 (23.27 – 91.80)	47.40 (24.66 – 92.10)	48.40 (25.52 – 95.36)
$C_{MAX,\ BASE}$ (mg/L)	7.45 (4.34 – 12.55)	6.24 (3.95 – 10.41)	7.89 (4.80 – 12.66)	6.89 (4.37 – 11.01)
$C_{MAX,\ IND}$ (mg/L)	6.65 (3.77 – 11.24)	6.10 (3.33 – 10.54)	7.24 (4.12 – 21.21)	6.45 (3.64 – 10.61)

[a] *The 90% prediction interval was obtained from the 5th and 95th percentiles of simulated data. The original data set was replicated, generating 1000 new individuals retaining the original covariate distribution. NFM, normal fat mass; BASE, after single dose; IND, induced-state; TB, patients infected with tuberculosis; TB+HIV, patients infected with tuberculosis and HIV;* $AUC_{0\text{-}24hr}$*, area under the concentration-time curve from 0 to 24 hours;* C_{MAX}*, maximum plasma concentration.*

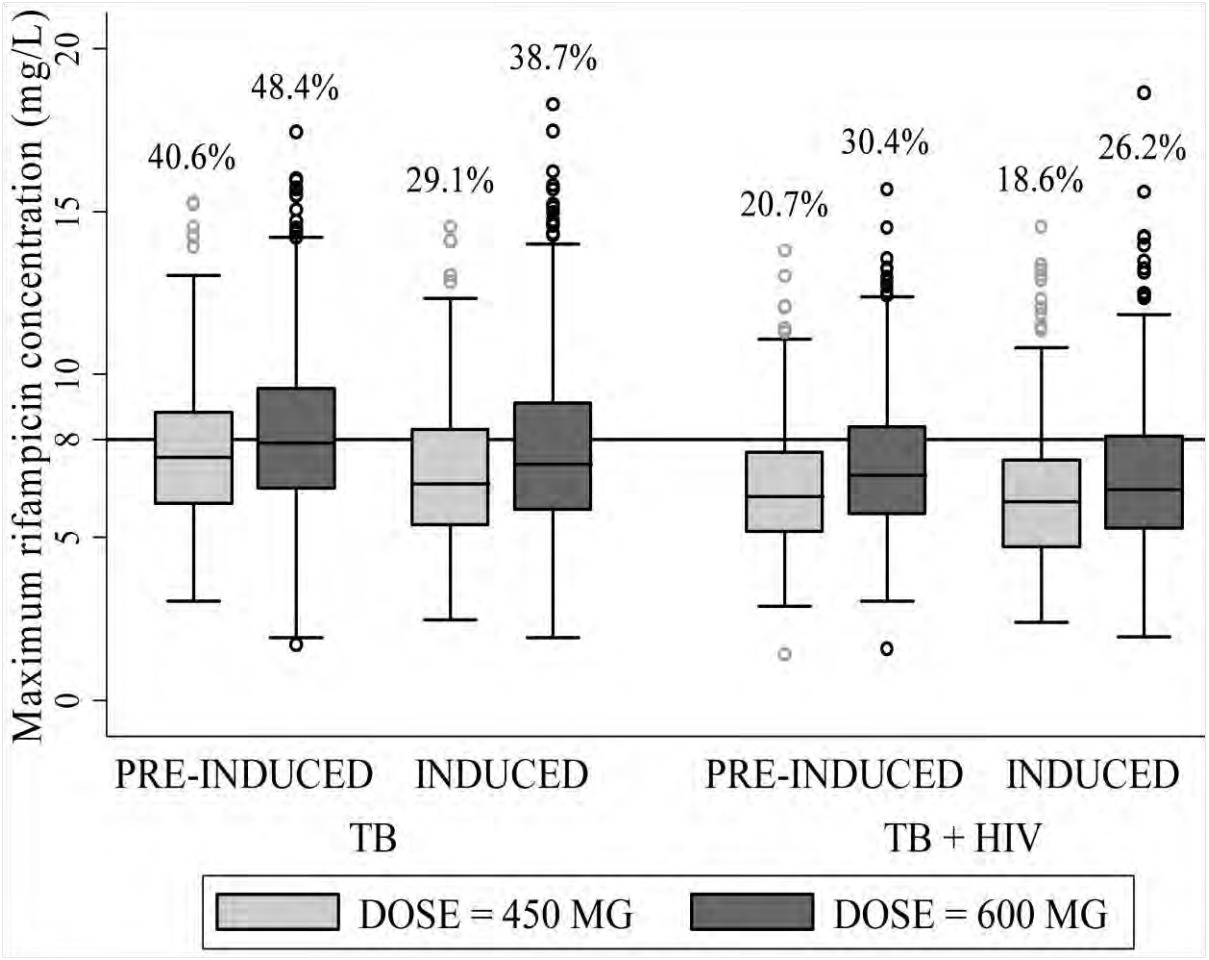

Figure 4. 4 Box plots of simulated rifampicin maximal concentrations (C_{MAX}) in tuberculosis patients with (TB + HIV, n=1000) or without HIV infection (TB, n=1000) following daily doses of either 450 or 600 mg at pre-induced (treatment initiation) and induced-state. The original data set was replicated generating 1000 new individuals retaining the original covariate distribution. Percentage values represent the fraction of patients in each category falling above 8 mg/L (Peloquin 2002) denoted by the horizontal line.

4.2. Discussion

The model developed in this chapter shows rifampicin autoinduction yields similar increases in rifampicin oral clearance with daily doses of 450 and 600 mg, resulting respectively in decreases in $AUC_{0\text{-}24}$ at induced-state of 41% and 42%. Although HIV infection was associated with a 30% increase in apparent volume of distribution, simulations demonstrated the effect of HIV on rifampicin exposure was not of clinical significance as similar induced state $AUC_{0\text{-}24}$ were observed between the two patient populations. The turn-over half-life for the induction process was estimated to be approximately 8 days. This corresponds to attainment of full

induction of rifampicin metabolism in a typical patient after 40 days of treatment, assuming five half-lives to steady-state.

There are several reports of autoinduction of rifampicin pharmacokinetics (Acocella 1978; Acocella 1983; Benedetti and Dostert 1994; Peloquin 2003). Loos and colleagues demonstrated rifampicin systemic clearance to increase 1.6-fold (from 5.69 to 9.03 L/h) following 3 weeks of multiple oral or intravenous 600 mg daily dosing (Loos et al. 1985; Loos et al. 1987). This finding is similar to our estimates of 1.82-and 1.85-fold increases in clearance following daily doses of 450 and 600 mg respectively in the typical patient. Loos et al. (1987) observed that rifampicin bioavailability decreased from 93% to 68% during 3 weeks of drug administration. As this is unlikely attributable solely to an increase in hepatic clearance, it suggests the existence of an inducible pre-systemic pathway. As P-gp is expressed on the apical surface of enterocytes (Lin 2003), these cells are able to eliminate rifampicin into the luminal space enabling the excretion of the drug along with faeces, in an inducible fashion. In the present pharmacokinetic-enzyme turn-over model, the induction process was expressed as a change in clearance over time. The inclusion of a change in bioavailability by time or by dose (mg/kg) was tested, but not supported by the data. The predicted clearance over time by this model is therefore a description of both hepatic and pre-systemic processes, although their relative contributions are not known. Of the 174 patients, 162 were sampled on two occasions; at the first day of treatment (occasion 1) and again approximately one month after (occasion 2). The median sampling day on occasion 2 was 29 days with a range spanning from 26 to 50 days. As such, the data collected in this study included information on the PK from prior to rifampicin-mediated induction to beyond 5 induction half-lives (40 days), thus allowing us to characterise the induction process. This is reflected by good precision of the parameters characterising induction i.e. the enzyme production rate (k_{ENZ}), EC_{50}, and E_{MAX}, which all had relative standard errors of <6%.

No significant covariate relationship was found between clearance and HIV infection. Therefore, clearance at first dose in the two patient populations was predicted to be the same (Table 4.4). Despite the absence of an association between HIV infection and clearance, a clinically non-relevant higher steady state clearance was seen in HIV infected patients. HIV infection was associated with a 29.6% increase in volume compared to patients without HIV infection resulting in lower C_{MAX} in HIV infected patients. Sahai and colleagues (Sahai et al.

1997) similarly found HIV infected patients to have lower rifampicin plasma concentrations compared to patients without HIV infection. The basis for an increased volume of distribution in HIV patients is not known, although it has been shown that HIV causes morphological and physiological changes that may alter the pharmacokinetics of drugs. In our study, increased volume in HIV infected patient leads to smaller oscillations in the concentration versus time profile. In the pharmacokinetic-enzyme turn-over model, this results in an increased enzyme production rate compared to patients without HIV infection, which is observed as a slightly higher predicted induced state clearance in HIV infected patients. HIV infection was, however, not shown to be of clinical significance, since similar induced-state AUC_{0-24} were simulated in the typical patient with and without HIV infection (Table 4.4). In the simulations using the same covariate distribution as observed in the study (Table 4.5), induced-state AUC_{0-24} in HIV infected patients were slightly higher compared to patients without HIV infection, and this was due to a relatively higher dose in HIV infected patients (median dose of 11.7 mg/kg (median body weight of 51 kg) in HIV+ as opposed to a median dose of 10.7 mg/kg (median body weight of 56 kg) in HIV-).

The three different models used to adjust for the effect of body size using allometric scaling were selected, based on work by (Anderson and Holford 2009). Clearance and volume parameters were scaled using various size descriptors (body weight in Model 2; *NFM* in Model 3; *FFM* in Model 4). Model 3 scaled using *NFM* was selected as the final model, based on the parameter estimates and the drop in OFV. *NFM* includes *FFM* and an estimated fraction of fat mass (*Ffat*). Fat mass contributes to overall body size and may have an indirect influence on both metabolic and renal clearance, although it has minimal metabolic activity. On the other hand, a drug may have distribution properties that are more directly linked to fat mass, hence the effect on volume of distribution. Notably, although the estimates of *Ffat* for clearance and volume were significant, they were relatively small. This suggests that *FFM* plays the dominant role as the size descriptor for allometric scaling on rifampicin pharmacokinetics compared to total weight. Current dose regimens based on total weight result in patients dosed with 600 mg (weight $\geq$50 kg) having marginally higher rifampicin exposure (AUC) when compared to those dosed with 450 mg (weight <50kg). Notably, patients receiving the 600 mg dose had significantly higher median fat mass (weight minus FFM) compared to those dosed with 450 mg (z=-2.495, p=0.0126) suggesting the need to dose rifampicin based on *FFM*

rather than total weight, although the clinical relevance of this finding remains to be established. Overall, using allometric scaling with total body weight, sex and HIV status had significant effect on volume (Model 2). However, scaling with *FFM* improved the fit and explained the effect of sex on volume while the effect of HIV status on volume remained (Model 4). Lastly, estimating *Ffat* (using NFM, Model 3) provided further improvement while HIV effect on volume remained significant.

The currently recommended daily doses of rifampicin (8-12 mg/kg) are believed to be at the lower end of the dose-response curve (Peloquin 2003; van Ingen et al. 2011). In light of several ongoing studies exploring the activity of increased doses of rifampicin and other rifamycins, pharmacokinetic studies aimed to explore the magnitude of autoinduction for higher doses are required. Rifampicin pharmacokinetics has been shown to display a non-linear relationship between dose and exposure, with higher doses resulting in more than proportional increases (Acocella 1978; Ruslami et al. 2006; Diacon et al. 2007; Chirehwa et al. 2015). In this analysis, this dose/exposure non-linearity was not supported by the data, possibly due to the limited dose range included. For this reason, exposure with doses higher than 600 mg could not be reliably simulated with our model, since neglecting this effect will result in under-prediction of the concentrations. However, simulations in this study found that close to maximum induction was already achieved after 450 mg daily, with a negligible increase in clearance observed following the 600 mg/day regimen. Therefore, should the assumptions of our model apply to higher doses, increasing the dose beyond 600 mg would not result in autoinduction of higher magnitude than that observed with daily doses of 450 to 600 mg.

The pharmacokinetic-pharmacodynamic relationships for rifampicin are not well characterised and a robust target exposure is yet to be identified. However, simulations in the present work showed less than a third of all patients achieving the minimum recommended peak concentration of 8 mg/L (Peloquin 2002) at induced-state. The C_{MAX} to MIC ratio has been suggested as important for activity of rifampicin against MTB (Gumbo et al. 2007a). Notably, in the patient group with body weight <50 kg receiving the 450 mg dose, a lower median C_{MAX} was seen compared to the patient group with body weight ≥50 kg receiving the 600 mg dose, suggesting inappropriate dosing by body weight could play a role in the selection for rifampicin resistance. McIlleron et al have similarly demonstrated low

rifampicin concentration in low weight male patients, however, the authors suggest review of treatment outcome in these patients to inform future dosing guidelines (McIlleron et al. 2012). Indeed, studies have revealed patients with low body weight, bilateral pulmonary disease and cavitary lesions more likely having poor outcome (Alsultan and Peloquin 2014).

The application of SCM (the linearization method for the covariate search) made it possible to explore the effect of covariate screening for different basic models with different scaling approaches. This was exemplified by the time required to fit the final model with one parameter-covariate relationship which was 26 seconds using the FOCE linearization covariate search (Khandelwal et al. 2011) compared to 37 hours with FOCE INTER estimation. The base model used for the covariate search (different scaling approaches) did not influence the covariate selection procedure, as the same covariates were selected in all cases. In the final model, HIV infection was associated with a volume 30% higher than HIV negative patients. The volume – HIV covariate relationship resulted in lower first dose and steady state peak concentrations and slightly higher steady state clearance predicted in the HIV infected population, but these differences were judged not to be of clinical importance. As the HIV infected patients in our study were antiretroviral naive, the volume – HIV covariate relationship could not be attributed to co-treatment and is most likely related to the disease.

4.3. Conclusion

This analysis developed a semi-mechanistic pharmacokinetic-enzyme turn-over model for rifampicin autoinduction in adult tuberculosis patients. Neither different allometric scaling approaches nor the absence of scaling influenced the covariate selection. Although HIV infection was associated with a 30% increase in volume for a typical patient, this was shown not to be of clinical significance as simulations in the typical patient demonstrated similar induced-state exposures (AUC_{0-24}) in patients with and without HIV infection. Maximum induction is likely achieved after 450 mg daily dosing as negligible increases in clearance were observed following the 600 mg/day regimen. This suggests that dose increases beyond 600 mg/day are unlikely to result in autoinduction of higher magnitude than observed in this study. The turn-over of the inducible process was estimated to a corresponding half-life of

approximately 8 days in a typical patient. Assuming 5 half-lives to steady-state, this is equivalent of approximately 40 days to induced-state for rifampicin autoinduction.

5. Assessment of first dose and steady-state gatifloxacin pharmacokinetics and dose in patients with pulmonary tuberculosis through the use of Monte Carlo simulations

Fluoroquinolones represent a promising class of drug for the treatment of tuberculosis. Gatifloxacin distributes widely throughout the body (Nakashima et al. 1995) and achieves the *in vitro* determined MICs for MTB (i.e. 0.031 – 0.5 µg/mL) (Rodriguez et al. 2002; Alvirez-Freites et al. 2002; Singh et al. 2009) and demonstrates strong bactericidal activity in the mouse model (Alvirez-Freites et al. 2002; Cynamon et al. 2007). Additionally, gatifloxacin displays excellent EBA (0.35 $\log_{10}$ cfu/mL/day), only slightly lower than that of isoniazid (0.67 $\log_{10}$ cfu/mL/day) (Johnson et al. 2006) and replacing ethambutol with gatifloxacin in the standard first-line regimen resulted in accelerated killing of MTB in the sputum of patients with pulmonary tuberculosis (Rustomjee et al. 2008). A single dose cross-over study in healthy volunteers showed a reduction in the elimination rate of gatifloxacin resulting in a 14% increase in $AUC_{0-\infty}$ when it was given together with rifampicin, isoniazid and pyrazinamide (McIlleron et al. 2007a). Reports of dysglycemia related to the use of gatifloxacin in elderly patients with renal insufficiency (Ambrose et al. 2003; Park-Wyllie et al. 2006; Mehlhorn & Brown 2007; LaPlante et al. 2008) have raised concerns that pharmacokinetic interactions resulting in higher gatifloxacin exposure may lead to an increased risk of toxicity. *In vitro* and *in vivo* studies suggest a target ratio $\geq$125 for the free drug area under the concentration versus time curve to minimum inhibitory concentration (*f*AUC/MIC), for maximal bactericidal effect and prevention of resistance to fluoroquinolones (Forrest et al. 1993; Schentag et al. 2001).

This chapter aims to evaluate the population pharmacokinetics of gatifloxacin after first dose and steady state (more than 28 days) when given in combination with rifampicin, isoniazid and pyrazinamide in African adult patients with newly-diagnosed pulmonary tuberculosis. In addition, the probability of target (*f*AUC/MIC$\geq$125) attainment and the CFR (Mouton et al. 2005a) across the MIC distribution of MTB for 400, 600 and 800 mg once daily of gatifloxacin at steady-state in combination with rifampicin, isoniazid and pyrazinamide were investigated with Monte Carlo simulations using the final model.

5.1. Results

A total of 954 gatifloxacin concentration observations from 169 patients were included in this analysis. Observations from 12 individuals fell below the LLOQ (0.1 mg/L) and were replaced with LLOQ/2, no consecutive BLQ values were present. The characteristics of the 169 patients contributing to this analysis are described in Table 5.1. More than half (59%) of study participants were recruited at the South African study site, which also happened to have the highest frequency of HIV infected patients (i.e. 52% vs. 12% in Benin and none in Guinea or Senegal).

Table 5.1 *Demographics and covariates of patients included in the gatifloxacin population pharmacokinetic model. Continuous variables are given as median (interquartile range).*

	All sites	**South Africa**	**Senegal**	**Benin**	**Guinea**
Total no. of patients	169	99	26	25	19
male/female	116/53	62/37	23/3	20/5	11/8
No. of HIV^+ patients	54	51	0	3	0
FFM[a] (kg)	45 (39-49)	45 (38-48)	49 (46-52)	46 (41-48)	45 (35-46)
bodyweight (kg)	55 (51-60)	56 (51-61)	55 (52-59)	53 (46-57)	52 (50-55)
AGE (years)	29 (24-35)	30 (24-35)	28 (25-31)	30 (26-37)	25 (20-34)
CL_{CR}[b] (mL/min)	94 (81-110)	100 (85-111)	87 (82-102)	75 (63-87)	89 (78-99)

[a]FFM= fat free mass; [b]CL_{CR}= creatinine clearance

The final gatifloxacin pharmacokinetic model was a one-compartment with first-order elimination. Including an absorption transit compartments model to account for the delay in absorption resulted in a drop in OFV of 125 points when compared to simple first-order absorption. The relationship between gatifloxacin clearance and creatinine clearance was described using equations 14 and 15 based on the prior knowledge that gatifloxacin is largely

eliminated by the kidneys (Nakashima et al. 1995), and resulted in OFV reductions of 19 and 24 points respectively compared to models not accounting for creatinine clearance or not allowing for a combination of GFR mediated- and non-GFR clearance. In a 70 kg patient with a typical creatinine clearance of 94 ml/min, gatifloxacin total clearance was estimated to be 11.28 L/h, of which 55% (6.17 L/h) of clearance was accounted for by renal filtration (a route scaled with creatinine clearance). Allometric scaling was applied to the non-GFR clearance (5.11 L/h) and to volume (141 L) using *FFM* as the optimal size descriptor, and the estimates were reported for a 70 kg patient (Table 5.2). *F* was 11.7% lower at steady-state (Day 28) than at the first dose. Age, sex and HIV status had significant effects on the absorption rate constant (Table 5.2).

The final model adequately described plasma concentration-time data at single dose and at steady state as shown by the VPC in Figure 5.1. Shrinkage for random effects between individuals and occasions had the range of 17-25% and 35-99% respectively. Shrinkage in IIV and IOV for clearance was 25% and 41%, respectively. The epsilon (residual error) shrinkage was 40%.

Table 5.2 *Parameter estimates based on the final gatifloxacin pharmacokinetic model.*

Parameter	**Estimate**	**% RSE**
$CL_{GFR,\ STD}$ (L/h)	6.17	9.7
$CL_{OTHER,\ STD}$ (L/h)	5.11	15.4
V_{STD} (L)	141	2.7
$F_{First\ dose}$	1 FIX	-
$F_{Steady\ State}$ (% change from $F_{First\ dose}$)	-11.7	17.4
k_a (h^{-1})	4.13	13.5
AGE-k_a (% per year above 29)	3.2	15.2
SEX-k_a (% for female)	-54.8	10.7
HIV^+-k_a (% for HIV+)	61.9	38.4
MTT (h)	0.65	8.1
N	12.6	19.7
Inter-individual variability (IIV)		
IIV_{CL} (%)	33.0	7.7
IIV_V (%)	22.1	10.9
Inter-occasional variability (IOV)		
IOV_{CL} (%)	33.0	5.7
IOV_V (%)	13.2	13.9
IOV_{MTT} (%)	44.9	12.3
Residual variability		

Parameter	Estimate	% RSE
Additive error (µg/mL)	0.341	5.1
Proportional error (%)	7.35	12.5
Pre-dose additive error (µg/mL)	0.0418	40.7

IIV= inter-individual variability expressed as coefficient of variation; IOV= inter-occasion variability expressed as coefficient of variation; RSE= relative standard error computed from NONMEM reported on the approximate standard deviation scale; $CL_{GFR, STD}$= clearance in a typical patient with a median CL_{CR} of 94 mL/min, representing drug cleared via glomerular filtration (GFR); $CL_{OTHER, STD}$= clearance not due to GFR in a typical 70 kg male patient and with a Fat Free mass (FFM) of 55 kg. V_{STD}= typical apparent volume of distribution scaled to FFM and reported for a 70 kg male patient; F= bioavailability; MTT= absorption mean transit time; N= number of transit compartments; AGE-k_a= % increase in k_a for every year change from the median AGE of 29 years; SEX-k_a= % decrease in k_a for female patients relative to male patients; HIV^+-k_a (%)= % increase in k_a for patients with HIV relative to patients without HIV; Pre-dose additive error (µg/mL)= additive error estimated uniquely for the pre-dose concentrations following an unobserved dose in addition to Additive error.

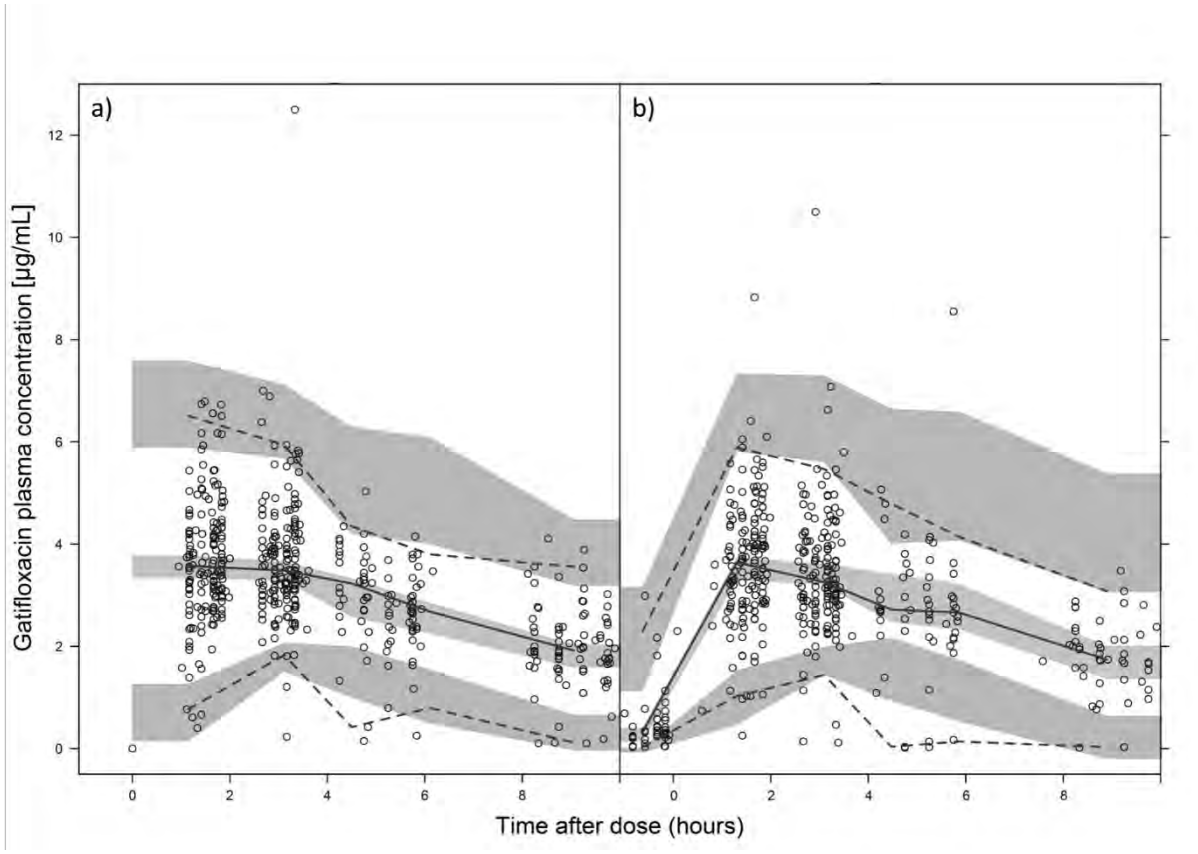

Figure 5.1 *Visual predictive check (VPC) of the final gatifloxacin pharmacokinetic model stratified by occasion i.e. a) first dose and b) steady-state (Day 28). The solid and dashed lines are the median, 5th and 95th percentiles of the observed gatifloxacin plasma concentrations, respectively. Shaded areas are the 95% prediction intervals for the median, 5th and 95th percentiles of simulated data. The open circles are observed concentrations.*

Based on 10 000 Monte Carlo patient simulations using the covariate values from the patients in the study cohort the median $AUC_{0-\infty}$ at first dose was 41.2 µg·h/mL, while the AUC_{0-24} at steady-state was 35.4 µg·h/mL, following multiple 400 mg/day doses (Figure 5.2). The median decrease in AUC was 14.3%, but this difference was small compared to the inter-individual and -occasion differences in exposure, as in our simulations the individual differences between single dose and steady state had a 90% range spanning from -90.4% to +61.5%.

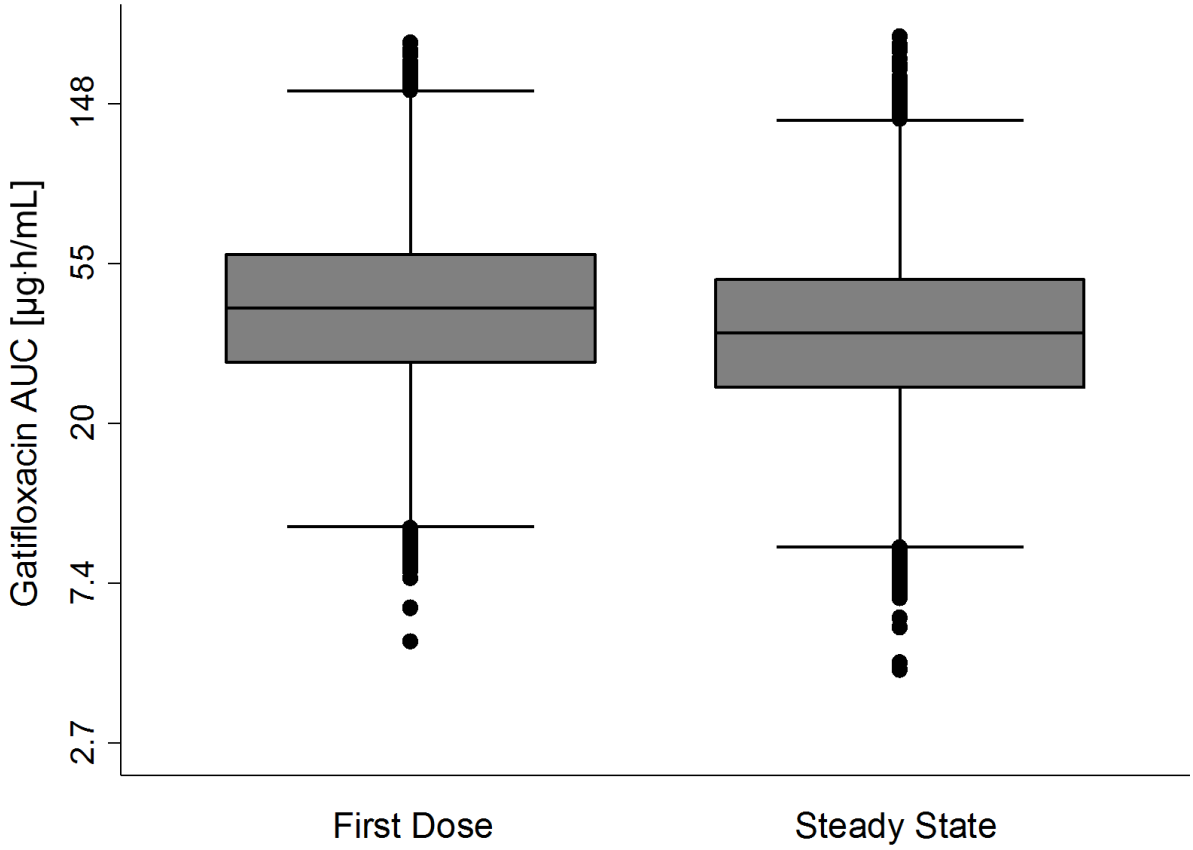

Figure 5.2 *Box plot of gatifloxacin area under the concentration-time curve from 0 hours to infinity ($AUC_{0-\infty}$), at first dose and from 0 to 24 hours (AUC_{0-24}) at steady state (Day 28) based on 10 000 virtual patients and Monte-Carlo simulations of 400 mg gatifloxacin daily together with rifampicin, isoniazid and pyrazinamide. In this population, the median gatifloxacin $AUC_{0-\infty}$ of 41.2 µg·h/mL (5-95% percentiles: 17.9 and 93.8) after first dose was reduced to an AUC_{0-24} of 35.4 µg·h/mL (5-95% percentiles: 15.2 and 80.4) at steady-state (Day 28).*

The probability of patients achieving or exceeding the target ratio of *f*AUC/MIC of 125 (at steady-state) for each MIC level, is shown in Figure 5.3. Additionally, the figure shows the frequency distribution of MICs reported from 234 clinical isolates of MTB. The CFR (i.e. the proportion of the population achieving a *f*AUC/MIC≥ 125 for the given MIC distribution) for daily 400 mg doses of gatifloxacin in combination with rifampicin, isoniazid and pyrazinamide was calculated to be 61.4%. The respective CFR for 600 and 800 mg doses of gatifloxacin were 79.3% and 88%. The PK/PD breakpoint, defined as the MIC at which the calculated PTA was <90%, was 0.125 µg/mL for daily gatifloxacin doses of 400 mg, and 0.25 µg/mL for 800 mg doses of gatifloxacin (long dash dot dot line in Figure 5.3). The *f*AUC/MIC as a function of the MIC is shown for 400, 600 and 800 mg doses in Figure 5.4.

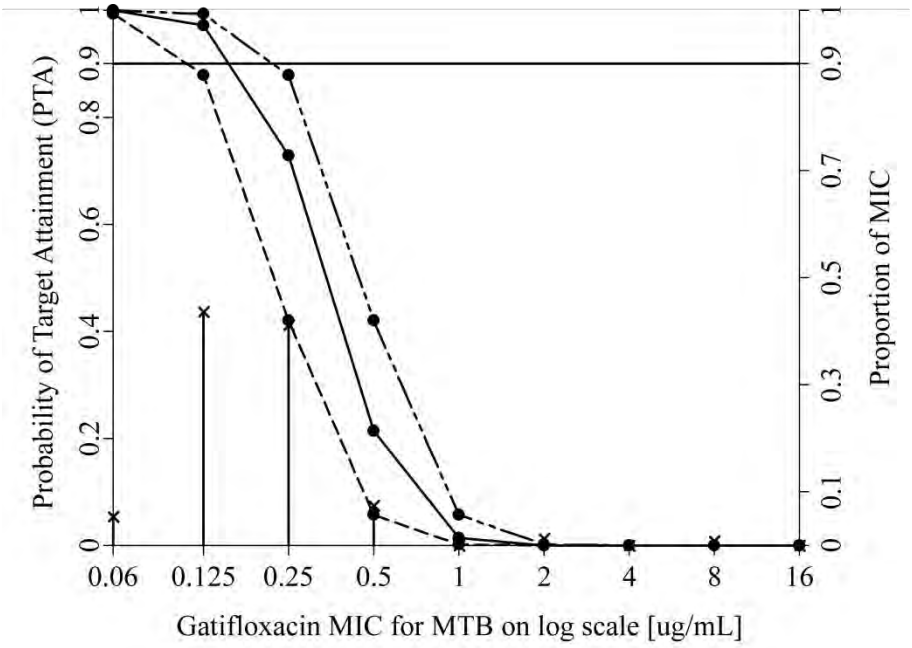

Figure 5.3 *The probability of target attainment (PTA) versus Mycobacterium tuberculosis minimum inhibitory concentration (MIC) following daily administration of 400 (dashed line), 600 (solid line) and 800 mg (long dash dot dot line) gatifloxacin together with rifampicin, isoniazid and pyrazinamide based on 10 000 virtual patients and Monte Carlo simulations (y-axis on left hand side). The PTA was defined as the probability of achieving the target PK/PD index ratio of fAUC/MIC≥125. The solid horizontal line indicates the reference line of 90% PTA. The solid drop lines with crosses (x) represent the frequency distribution for MIC of gatifloxacin (y-axis on right hand side) obtained from 243 clinical isolates of MTB (Gajjar et al. 2000).*

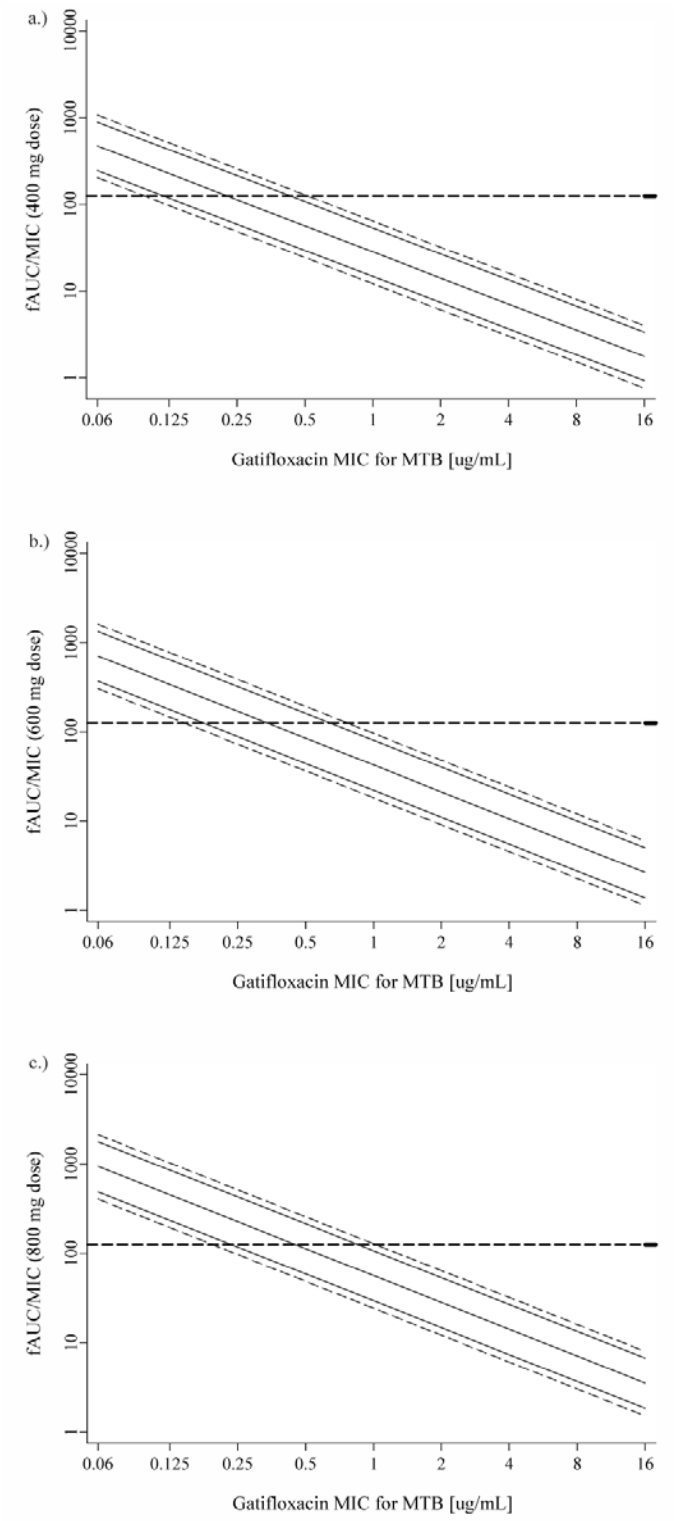

Figure 5.4 *The median (solid thick line) total probability function, irrespective of the target, as a function of the Mycobacterium tuberculosis minimum inhibitory concentration (MIC), with the 80% (solid lines) and 90% (dashed lines) percentiles following daily administration of (a) 400, (b) 600 and (c) 800 mg of gatifloxacin together with rifampicin, isoniazid and pyrazinamide. The lower boundary in the 80% percentile of the total probability function is equivalent to 90% PTA. The dashed horizontal line indicates the target of fAUC/MIC=125.*

5.2. Discussion

In this study, we found that gatifloxacin exposure was reduced following multiple doses when given together with rifampicin, isoniazid and pyrazinamide. Our model attributed this effect to lower bioavailability. This effect goes in the opposite direction of that detected in a single dose study in healthy volunteers, where increased gatifloxacin exposure ($AUC_{0-\infty}$) was observed when co-administering rifampicin, isoniazid and pyrazinamide (McIlleron et al. 2007). It is possible that the increase in gatifloxacin concentrations at first dose attributable to concomitant use of rifampicin, isoniazid and pyrazinamide may be counteracted by a reduction in gatifloxacin concentrations with repeated doses of the four drugs in combination. This suggests that exposure-related toxicity is unlikely to increase with repeated doses of gatifloxacin when it is given with rifampicin, isoniazid, and pyrazinamide.

Two notable points emerge when comparing gatifloxacin exposure reported after single-agent studies with that recorded in the present combination treatment study. Firstly, steady state gatifloxacin AUC achieved in this study was slightly lower than steady state AUC reported in studies where patients were given the drug alone (Johnson et al. 2006; Peloquin et al. 2008). Additionally, differences in AUC could be attributed to different populations and/or dosing regimens. Secondly, despite gatifloxacin pharmacokinetic parameters (including bioavailability) having been reported not to change following multiple doses when the drug was given on its own (Mignot et al. 2002; Johnson et al. 2006), this study found a reduction in drug exposure when combination treatment was employed. This reduction could be explained by the fact that gatifloxacin is a known substrate of the trans-membrane efflux transporter protein P-gp (Kwatra et al. 2010), and rifampicin induces the expression of P-gp (Schuetz et al. 1996). As such, repeated doses of rifampicin may result in reduced gatifloxacin systemic bioavailability due to increased efflux by P-gp expressed on enterocytes and hepatocytes. Gatifloxacin is principally (>80%) cleared unchanged via the kidneys (Johnson et al. 2006). The overall reduction in gatifloxacin concentrations, following multiple doses in combination with rifampicin, isoniazid and pyrazinamide, is thus likely to be the net result of drug-drug interactions observed both following single doses and at steady state. Alternatively reduced concentrations at steady state relative to first dose could be due to overall improvement in health conditions of the patient post treatment initiation. Furthermore, poor

treatment compliance at steady state relative to first dose would equally result in lower drug exposure at steady state relative to that observed at first dose.

Reduced gatifloxacin clearance and recovery in urine was reported following concomitant dosing with probenecid (a drug which inhibits tubular secretion), suggesting that tubular secretion may contribute the elimination of the drug (Nakashima et al. 1995). In our study gatifloxacin clearance increased with creatinine clearance and patient *FFM*. Scaling drug clearance to both *FFM* and creatinine clearance allowed us to estimate that approximately 53% of the dose was cleared via glomerular filtration. Using creatinine clearance as our proxy for renal filtration might, however, overestimate the contribution of this pathway to drug clearance, since approximately 15% of creatinine is actively secreted by the peritubular capillaries of the kidney (Crawford 1948). The remaining 47% of gatifloxacin clearance was scaled to *FFM* and accounted for drug cleared via all pathways other than glomerular filtration. Indeed more than 80% of the gatifloxacin dose is recovered unchanged in the urine with evidence of active tubular secretion reported (Grasela 2000).

Gatifloxacin bioavailability was estimated to be approximately 12% lower at steady state than after a single dose. This, combined with increased patient weight (*FFM*) and creatinine clearance at the second occasion, resulted in a 14.3% reduction of AUC at steady state. The reduction in gatifloxacin exposure following multiple doses is unlikely to be clinically significant, as on an individual level gatifloxacin AUC could increase by as much as 90% or decrease by as much as 62% between the two occasions due to the high IOV in *CL*. Age, sex and HIV status were identified having an effect on the absorption rate constant, but this is unlikely to be clinically relevant, as changes of the absorption rate do not alter the average steady-state concentration of gatifloxacin.

Based on 10 000 Monte Carlo simulations using the final model, 62, 79 and 88% of our study population were predicted to achieve the target ratio of *f*AUC/MIC$\geq$125 following daily 400, 600 and 800 mg respective doses of gatifloxacin. Only when the MIC of gatifloxacin fell below 0.125 µg/mL could 90% of the study population, irrespective of dose, achieve the target ratio. The simulations showed that at 800 mg daily doses of gatifloxacin, approximately 90% of the population would achieve the target ratio when MIC<0.25 µg/mL. These results suggest the current 400 mg daily dosing of gatifloxacin does not achieve optimal drug exposure with

respect to the MIC distribution used. However, using the target ratio of plasma *f*AUC/MIC≥125 to predict the optimal dose of gatifloxacin in this context is a simplification and has its limitations. Notably, bacteriological and clinical outcomes correlated best with the pharmacodynamic index of AUC/MIC≥125 in 74 acutely ill patients treated with ciprofloxacin for lower respiratory tract infections (Forrest et al. 1993). In that study, AUC/MIC≥125 was significantly correlated with a faster bacterial eradication rate, which may decrease the likelihood of antibacterial resistance. Setting the target to a lower value (AUC/MIC<125) could potentially create needless selective pressure increasing the chance of resistance especially with a long duration of therapy (e.g. 4 months). Notably, in a review by Schentag (2000), the pharmacodynamic index target AUC/MIC>125 is recommended for both gram-positive and gram-negative organisms. Although *f*AUC/MIC is widely accepted as a correlate of fluoroquinolone efficacy (Ginsburg et al. 2003), more studies are required to determine whether *f*AUC/MIC≥125 truly correlates with *in vivo* efficacy against MTB. Additionally, the total probability functions, independent of the target, for different gatifloxacin doses are presented (Figure 5.4). The lower boundary in the 80th percentile of the total probability function is equivalent to 90% PTA. The 90% PTA for any new future target can be visualised from this plot. Interestingly, a plasma AUC/MIC ratio of 112-220 was associated with optimal survival amongst patients with tuberculosis meningitis who were treated with a regimen containing gatifloxacin, levofloxacin or ciprofloxacin in addition to standard antituberculosis treatment (Thwaites et al. 2011). Although this ratio is in keeping with the target *f*AUC/MIC≥125, the optimal ratio for the plasma AUC/MIC ratio for pulmonary tuberculosis and tuberculosis meningitis are likely to differ due to differences in tissue penetration and immunity at the site of action. Drug action occurs within pulmonary compartments, including epithelial cells and macrophages, where drug concentrations exceed those found in plasma (Honeybourne et al. 2001). Assuming higher *f*AUC in pulmonary compartments, more patients could achieve the target ratio of *f*AUC/MIC≥125. On the other hand, there are concerns that administering higher doses of gatifloxacin would increase the risk of toxicity such as dysglycemia. Lastly, the optimal dose of gatifloxacin would need to take into account the efficacy and safety profiles of the drug in the context of the contributions from companion drugs in the multidrug regimen and patient immunity.

Further limitations of this study include a failure to measure free gatifloxacin concentrations and lack of study specific information about the MICs. Plasma protein binding of 20%, independent of concentration, was assumed for gatifloxacin (Nakashima et al. 1995) and we used the MIC distribution obtained from 234 clinical isolates of MTB from Spain (Rodriguez et al. 2002). The MTB population reported in the Spanish study were slightly more sensitive to gatifloxacin when compared to moxifloxacin and levofloxacin with reported MIC_{90}'s of 0.25 and 0.5 μg/mL respectively. In agreement with the Spanish study, a similar gatifloxacin MIC_{90} of 0.25 μg/mL was reported against clinical isolates of MTB obtained from numerous sources of broad geographical distribution (Fung-Tomc et al. 2000). Additionally, the aforementioned study reported similar MIC_{50} and distribution range of MIC for MTB reported in the Spanish study. Thus, the assumption that the frequency distribution of gatifloxacin MIC reported in the Spanish study correlates to the MIC distribution found in this study population appears valid. Nonetheless, as demonstrated by (Peloquin et al. 2008), a change in the MIC distribution (e.g. published vs. actual MIC's determined from clinical isolates obtained from study patients) can radically change the ratio of *f*AUC/MIC. Since this study did not measure the MICs of MTB in the study population, it is possible that the true effective MIC could be lower. Moreover, the MICs reflect the activity of gatifloxacin alone and synergism or antagonism in the regimen were not accounted. The relevance of these findings needs to be evaluated alongside the eventual clinical outcomes of the study overall.

5.3. Conclusion

Although increased gatifloxacin exposure was observed in a previous single dose study, gatifloxacin exposure, expressed as AUC, declined following multiple doses of the 4 drugs in the multidrug regimen. Hence exposure-related toxicity is unlikely to increase with repeated doses of gatifloxacin when given concomitantly with rifampicin, isoniazid, and pyrazinamide. Based on predictions of *f*AUC/MIC and the derived proportion of the population achieving optimal bactericidal effect and reduced probability of resistance (CFR), the CFR of the clinically used dose of 400 mg daily was 61%, simulations showed that doubling the dose would result in increasing the CFR to 88%. However, the pharmacokinetics of gatifloxacin needs to be studied in relation to efficacy and safety in pulmonary tuberculosis patients on the multidrug regimen in order to evaluate the optimal gatifloxacin exposures in this context.

6. Population pharmacokinetics of first-line tuberculosis drugs in patients enrolled into the OFLOTUB phase III sub-study

Africa contributed approximately 27% of all new tuberculosis cases in 2012 (World Health Organization 2013). In an attempt to improve patient adherence to treatment and therefore improve disease control, several studies were conducted to shorten the duration of tuberculosis treatment (Gillespie et al. 2014; Jindani et al. 2014; Merle et al. 2014). Results from the randomised phase III OFLOTUB study which attempted to shorten tuberculosis treatment from 6 to 4 months, by substituting ethambutol for gatifloxacin, showed the 4 month test regimen inferior to the standard 6 month control regimen (Merle et al. 2014). The current pharmacokinetic sub-study aimed to investigate concerns regarding appropriate dosing in the test and control regimens. Indeed, a single-dose crossover study in healthy volunteers showed a reduction in the elimination rate of gatifloxacin resulting in a 14% increase in the area under the concentration time curve to infinity ($AUC_{0-\infty}$) when it was given together with rifampicin, isoniazid, and pyrazinamide (McIlleron et al. 2007b). Furthermore, the $AUC_{0-\infty}$ for rifampicin was reduced by 19% when rifampicin, isoniazid and pyrazinamide were given together with gatifloxacin. As sparse pharmacokinetic sampling was employed in the OFLOTUB sub-study, a nonlinear mixed-effects modelling approach, as opposed to the traditional non-compartmental analysis, was utilized to characterise the pharmacokinetics of the five study drugs. Few studies have investigated population pharmacokinetics of anti-tuberculosis drugs in African populations (Wilkins et al. 2006; Peloquin et al. 2008; Wilkins et al. 2008; Wilkins et al. 2011; Jönsson et al. 2011), hence this chapter aims to characterise the population pharmacokinetics of these drugs in African patients and investigate potential drug-drug interactions in rifampicin, isoniazid, and pyrazinamide across treatment regimens.

6.1. Results

Patient demographics and clinical characterises from 343 patients stratified by study site and treatment regimen are presented in Table 3.1 (Chapter 3). Patients had pharmacokinetic observations taken at first dose and approximately one month later. Approximately 92% of patients sampled at first dose were available for follow up pharmacokinetic sampling at

steady state. The majority of patients (58%) were from South Africa. Half of all patients in South African were HIV co-infected while only 12%, 5% and 0% of patients in Benin, Guinea and Senegal were respectively HIV co-infected. The median rifampicin, pyrazinamide, isoniazid and ethambutol dose for all 343 patients was 10.4, 27.8, 5.2 and 19.0 mg/kg respectively.

Rifampicin

In total, 1961 pharmacokinetic observations from 343 patients were available for analysis. A total of 27 occasions (including both occasions for 1 patient profile), comprising 85 (4.3%) observations, were classified as potentially affected by data errors and excluded from the analysis (Chapter 3). Most of the occasions identified were at steady state (occasion 2) and just over half of these included observations approximately 23 to 48 hours post a self-reported dose (pre-dose observations). Patient non-adherence to their dosing schedule (e.g. taking their previous dose just prior to their clinic visit), sample swop or incorrectly labelled samples were likely explanations for their exclusion. A further 89 (4.7%) samples fell below the quantification level (0.1 mg/L) and were substituted with half the quantification level (0.05 mg/L). Rifampicin pharmacokinetic was best described using a one-compartment model with first-order absorption preceded by a series of transit compartments and first-order elimination. The model fit the data well, as shown in the VPC (Figure 6.1), and the values of the final parameter estimates can be found in Table 6.1. Allometric scaling was applied to clearance and volume and normalised to the typical *FFM* of 45 kg in the data set. Rifampicin clearance approximately doubled from 8.29 L/h at first dose to 16.53 L/h (95% CI: 15.77-16.97) roughly 28 days later (Table 6.1). Compared to Benin, Senegal and South Africa, clearance was increased in Guinean patients by 25.4%, while bioavailability was 52.8% higher in patients in Senegal compared to patients in the other three countries. The apparent volume of distribution was approximately 14% higher in patients with HIV co-infection compared to those without HIV. Female patients had slower absorption rates and longer mean transit absorption times compared to male patients as estimated by the 20.3% decrease in the ratio of k_a/MTT. Although no significant differences in rifampicin clearance or bioavailability was detected across treatment regimen, the drugs absorption rate was 35.6% significantly slower in the gatifloxacin containing test regimen when compared the control regimen. Large

random variability in rifampicin k_a and *MTT* was observed between occasions (IOV), while a negative correlation between *MTT* and *F* was detected in each PK occasion, such that patients with longer absorptions times had lower bioavailability. For a reference male patient weighing 70 kg and measuring 1.76 m in height, first dose clearance was estimated at 9.77 L/h while steady state clearance was estimated at 19.46 L/h.

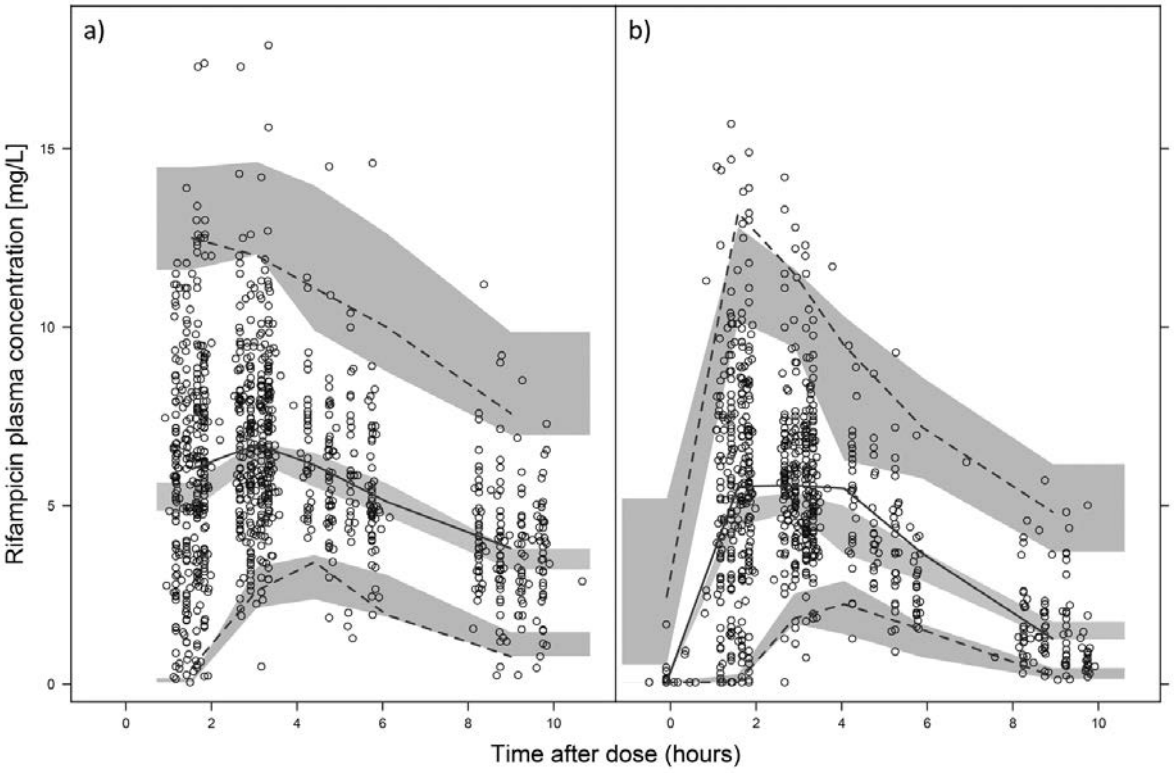

Figure 6.1 *Visual predictive check (VPC) for rifampicin concentration versus time stratified by occasion a) first dose and b) steady-state (Day 28). The solid and dashed lines are the median, 5th and 95th percentiles of the observed rifampicin plasma concentrations, respectively. Shaded areas are the 95% prediction intervals for the median, 5th and 95th percentiles of simulated data. The open circles are observed original data.*

Table 6. 1 *Rifampicin parameter estimates in 343 newly diagnosed pulmonary tuberculosis patients. Precision estimates were obtained from NONMEM (% RSE, reported on approximate standard deviation scale) and the 95% confidence intervals (95% CI) from a nonparametric bootstrap (BS) employing 50 iterations stratified by site.*

Parameter	**Estimate**	**% RSE NONMEM**	**95% CI BS (N=50)**
$CL_{first\ dose}$ (L/h) scaled to TV_*FFM*=45 kg	8.29	3.3	7.9 to 8.8
$CL_{induced}$ (% change from $CL_{first\ dose}$)	99.3	6.4	90.2 to 104.7
Guinea-CL (%)	25.4	31.8	6.3 to 46.1
V (L) scaled to TV_*FFM*=45 kg	63.9	1.9	61.8 to 65.7
HIV-*V* (%)	14.4	21.0	7.5 to 19.9
k_a (1/h)	1.93	7.0	1.67 to 2.31
Regimen-k_a (%)	-35.6	12.5	-27.0 to -46.6
MTT (h)	0.590	6.3	0.540 to 0.648
SEX_{FEMALE}-(k_a/MTT) (%)	-20.3	19.2	-12.6 to -27.4
N	32.7	10.5	23.5 to 42.2
F	1 FIX		
Senegal -F (%)	52.8	11.6	42.8 to 60.3
Inter-individual variability (IIV)			
IIV_*CL* (%CV)	35.2	5.8	25.8 to 41.3
IIV_$CL_{induced}$ (%CV)	30.4	10.8	24.0 to 38.6
Correlation IIV_ *CL*~$CL_{induced}$ (%)	-52.0	12.8	-25.5 to -71.9
IIV_*F* (%CV)	13.4	13.1	8.3 to 17.0
Inter-occasional variability (IOV)			
IOV_k_a (%CV)	70.9	4.9	64.9 to 79.8
IOV_*MTT* (%CV)	59.8	7.9	55.3 to 65.3
IOV_*F* (%CV)	17.2	7.7	12.8 to 21.6

Correlation IOV_*MTT~F* (%)	-30.6	17.1	-8.4 to -70.7
Residual variability			
Additive error (mg/L)	0.0420	34.0	0.0377 to 0.0453
Proportional error (%)	12.8	2.6	11.3 to 14.0

Inter-individual variability (IIV) and inter-occasion variability (IOV), were assumed log normally distributed and expressed as approximate percentage coefficient of variation (%CV); % RSE NONMEM, relative standard error from NONMEM covariance step reported on the approximate standard deviation scale; 95% CI BS (N=50), 95% confidence interval of parameter estimate obtained from nonparametric bootstrap of 50 iterations stratified by site; $CL_{first\ dose}$, estimated clearance at first dose scaled to median FFM of 45 kg (TV_FFM); $CL_{induced}$, induced clearance at steady state estimated as the fractional change from first dose clearance; CL~$CL_{induced}$, correlation between clearance and induced clearance; F, relative bioavailability fixed to 1 (1 FIX); V, apparent volume of distribution scaled to median FFM of 45 kg (TV_FFM); k_a, absorption rate constant; MTT, absorption mean transit time; MTT~F, correlation between MTT and F; N, number of transit compartments; Senegal-F (%), percentage change in F for the Senegal site relative to other sites; SEX_{FEMALE}-(k_a/MTT) (%), percentage change in k_a and MTT (in the opposite direction) for females relative to males; Guinea-CL (%), percentage change in CL for the Guinea site relative to other sites; Regimen-k_a (%), percentage change in k_a between Test regimen and to control regimen (reference); HIV-V (%), percentage change in V for patients with HIV co-infection relative to patients without HIV co-infection; Additive error (mg/L), additive residual error estimated in mg/L; Proportional error (%), proportional residual error reported as a percentage.

<u>*Pyrazinamide*</u>

In total, 1967 pharmacokinetic observations from 342 patients were available for analysis. A total of 29 occasions (including both occasions for 3 patient profiles), comprising 88 (4.4%) observations, were classified as potentially affected by data errors and excluded from the analysis (Chapter 3). Most of the occasions identified were at steady state (occasion 2) and the majority of these included observations approximately 23 to 48 hours post a self-reported dose (pre-dose observations). Patient non-adherence to their dosing schedule (e.g. taking their previous dose just prior to their clinic visit), sample swop or incorrectly labelled samples were likely explanations for their exclusion. A further 8 (0.4%) samples fell below the quantification level (0.2 mg/L) and were substituted with half the quantification level (0.1 mg/L). Pyrazinamide pharmacokinetic was best described using a one-compartment model with first-order absorption preceded by a series of transit compartments and first-order

elimination. The model fit the data well, as shown in the VPC (Figure 6.2), and the values of the final parameter estimates can be found in Table 6.2. Allometric scaling was applied to clearance and volume and normalised to the typical *FFM* of 45 kg in the data set. Pyrazinamide clearance increased by approximately 30% from 2.8 L/h at first dose to 3.6 L/h (95% CI: 3.5-3.8) approximately 28 days later. Patients in Benin had an estimated reduction in bioavailability of 10% compared to patients from Guinea and Senegal. Patients from Benin had faster absorption rates and shorter mean transit absorption times compared to those in South Africa as estimated by the approximate 100% increase in the ratio of k_a/MTT. Patients from Guinea and Senegal similarly had faster absorption rates and shorter abruption transit times compared to those in South Africa. For a reference male patient weighing 70 kg and measuring 1.76 m in height, first dose clearance was estimated at 3.29 L/h while steady state clearance was estimated at 4.29 L/h.

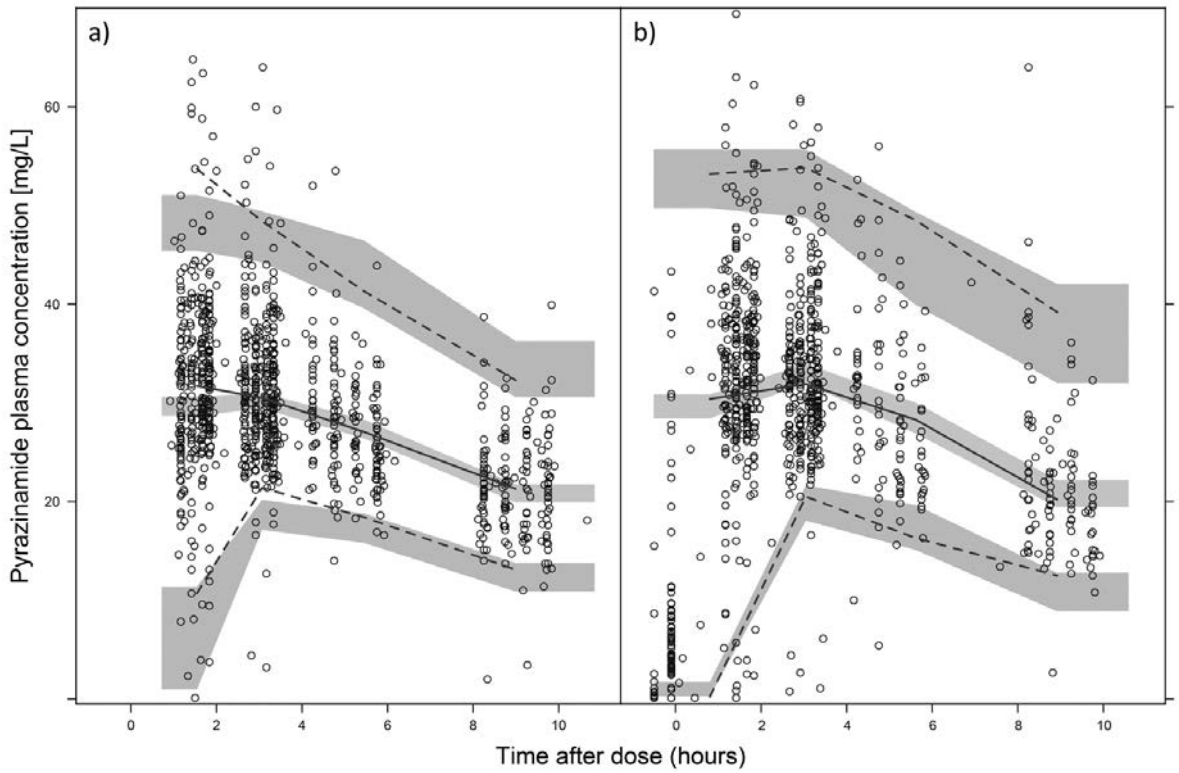

Figure 6.2 *Visual predictive check (VPC) for pyrazinamide concentration versus time stratified by occasion a) first dose and b) steady-state (Day 28). The solid and dashed lines are the median, 5th and 95th percentiles of the observed rifampicin plasma concentrations, respectively. Shaded areas are the*

95% prediction intervals for the median, 5th and 95th percentiles of simulated data. The open circles are observed original data.

Table 6. 2 *Pyrazinamide parameter estimates in 343 newly diagnosed pulmonary tuberculosis patients. Precision estimates were obtained from NONMEM (% RSE, reported on approximate standard deviation scale) and the 95% confidence intervals (95% CI) from a nonparametric bootstrap (BS) employing 50 iterations stratified by site.*

Parameter	**Estimate**	**% RSE NONMEM**	**90% CI BS (N=50)**
$CL_{first\ dose}$ (L/h) scaled to TV_*FFM*=45 kg	2.8	2.4	2.7 to 3.0
$CL_{steady\ state}$ (% change from $CL_{first\ dose}$)	30.3	9.0	23.2 to 36.9
V (L) scaled to TV_*FFM*=45 kg	42.1	0.8	41.3 to 42.9
k_a (1/h)	2.02	5.9	1.75 to 2.17
MTT (h)	0.391	7.5	0.243 to 0.477
N	178	38.8	24 to 641
F	1 FIX		
Benin-*F* (%)	-9.95	17.6	-6.86 to -13.14
Benin-(k_a/*MTT*) (%)	106	27.1	79.6 to 123.8
Guinea-(k_a/*MTT*) (%)	79.8	19.5	54.3 to 169.9
Senegal-(k_a/*MTT*) (%)	67.6	21.0	51.2 to 109.8
Inter-individual variability (IIV)			
IIV_{CL} (%CV)	22.4	4.5	18.5 to 25.8
Inter-occasional variability (IOV)			
IOV_{ka} (%CV)	74.9	4.3	61.1 to 83.0
IOV_{MTT} (%CV)	71.1	5.9	61.8 to 105.2
IOV_F (%CV)	12.9	3.4	11.3 to 14.2
Residual variability			

Additive error (mg/L)	1.2	8.0	0.7 to 1.6
Proportional error (%)	6.69	4.4	5.20 to 7.66

Inter-individual variability (IIV) and inter-occasion variability (IOV), were assumed log normally distributed and expressed as approximate percentage coefficient of variation (%CV); % RSE NONMEM, relative standard error from NONMEM covariance step reported on the approximate standard deviation scale; 95% CI BS (N=50), 95% confidence interval of parameter estimate obtained from nonparametric bootstrap of 50 iterations stratified by site; $CL_{first\ dose}$*, estimated clearance at first dose scaled to median FFM of 45 kg (TV_FFM);* $CL_{steady\ state}$*, steady state clearance estimated as the fractional change in clearance from first dose; V, apparent volume of distribution scaled to median FFM of 45 kg (TV_FFM);* k_a*, absorption rate constant; MTT, absorption mean transit time; N, number of transit compartments; F, relative bioavailability fixed to 1 ; Benin-F (%), % change in F for the Benin relative to other sites; Benin-(*k_a*/MTT) (%), % change in* k_a*/MTT in Benin relative to other sites; Guinea-(*k_a*/MTT) (%), % change in* k_a*/MTT in Guinea relative to other sites; Senegal -(*k_a*/MTT) (%), % change in* k_a*/MTT in Senegal relative to other sites; Additive residual error (mg/L), estimated additive residual error; Proportional error (%), proportional residual error reported as a percentage.*

Isoniazid

In total, 1928 pharmacokinetic observations from 343 patients were available for analysis. A total of 45 occasions (including both occasions for 9 patient profiles), comprising 137 (7.1%) observations, were classified as potentially affected by data errors and excluded from the analysis (Chapter 3). Approximately half the occasions identified were at steady state (occasion 2) and around half of these included a pre-dose sample, approximately 23 to 48 hours post a self-reported dose. Patient non-adherence to their dosing schedule (e.g. taking their previous dose just prior to their clinic visit), sample swop or incorrectly labelled samples were likely explanations for their exclusion. A further 120 (6.6%) samples fell below the limit of quantification (0.1 mg/L) and imputed as half the lower quantification limit (0.05 mg/L). Isoniazid pharmacokinetics was best described using a two-compartment model with first-order absorption preceded by a series of transit compartments. The model fit the data well, as shown in the VPC (Figure 6.3), and the values of the final parameter estimates can be found in Table 6.3. Allometric scaling was applied to all clearance and volume of distribution terms and normalised to the typical *FFM* of 45 kg in the data set. Clearance was found to have a bimodal distribution, which was described using a mixture model classifying patients into fast or slow acetylators, after scaling all clearance and volume parameters with *FFM*. The

estimated proportion of fast vs. slow acetylators varied across different geographical regions. Amongst South Africans, 65% were fast acetylators vs. only 47% of West Africans (Benin, Guinea & Senegal). Additionally, fast acetylators were estimated to have bioavailability 14.3% lower than slow acetylators. Compared to West African patients, South Africans had slower absorption rates and longer transit absorption times as estimated by the 69.2% decrease in the ratio of k_a/MTT. Patients in Guinea had clearance rates 39% higher than the other study sites, while bioavailability was estimated to be 40.6% lower in Guinea and Senegal compared to patients in South Africa and Benin. For a reference male patient weighing 70 kg and measuring 1.76 m in height, fast acetylator clearance was estimated to 24.5 L/h, while slow acetylator clearance was 11.7 L/h.

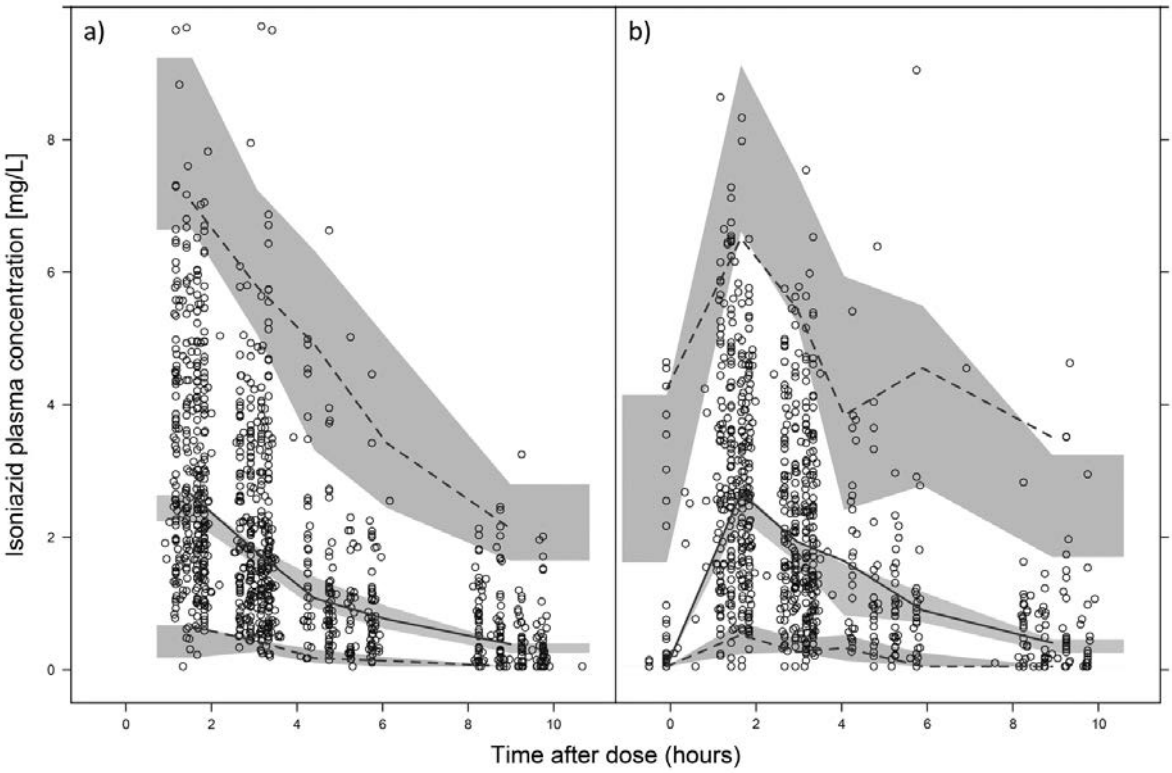

Figure 6.3 *Visual predictive check (VPC) for isoniazid concentration versus time stratified by occasion a) first dose and b) steady-state (Day 28). The solid and dashed lines are the median, 5th and 95th percentiles of the observed rifampicin plasma concentrations, respectively. Shaded areas are the 95% prediction intervals for the median, 5th and 95th percentiles of simulated data. The open circles are observed original data.*

Table 6. 3 *Isoniazid parameter estimates in 343 newly diagnosed pulmonary tuberculosis patients. Precision estimates were obtained from NONMEM (% RSE, reported on approximate standard deviation scale) and the 95% confidence intervals (95% CI) from a nonparametric bootstrap (BS) employing 50 iterations stratified by site.*

Parameter	**Estimate**	**% RSE NONMEM**	**95% CI BS (N=50)**
CL_{slow} (L/h) scaled to TV_*FFM*=45 kg	10.3	3.0	9.9 to 10.5
CL_{fast} (L/h) scaled to TV_*FFM*=45 kg	23.0	3.0	21.8 to 23.0
Guinea-*CL* (%)	39.0	16.9	37.9 to 39.0
Q (L/h) scaled to TV_*FFM*=45 kg	4.14	15.1	4.01 to 4.15
V_c (L) scaled to TV_*FFM*=45 kg	52.6	2.0	51.3 to 53.6
V_p (L) scaled to TV_*FFM*=45 kg	15.6	10.4	15.1 to 15.6
k_a (1/h)	6.35	11.6	6.18 to 6.35
MTT (h)	0.10	11.0	0.09 to 0.10
South Africa-(k_a/*MTT*) (%)	-69.2	3.6	-68.6 to -69.8
N	13.5	9.6	13.3 to 13.7
F_{slow}	1 FIX		
F_{fast} (% change from F_{slow})	-14.2	21.4	-13.9 to -14.6
Guinea & Senegal-*F* (%)	-40.6	9.0	-40.1 to -41.6
Mixture model of Slow:Fast eliminators			
% *Slow*:*Fast* eliminators (South Africa)	35:65	12.0	34 to 35:65 to 66
% *Slow*:*Fast* eliminators (West Africa)	53:47	9.2	52 to 53:47 to 48
Inter-individual variability (IIV)			
IIV_{CL} (%CV)	12.4	11.2	10.0 to 12.4
IIV_F (%CV)	18.9	10.0	18.9 to 19.2
Inter-occasional variability (IOV)			

IOV_{ka} (%CV)	81.0	8.0	76.0 to 81.0
IOV_{MTT} (%CV)	88.5	13.8	86.3 to 90.5
IOV_{F} (%CV)	37.5	3.2	36.2 to 39.7
Residual variability			
Additive error (mg/L)	0.0401	6.1	0.0395 to 0.0413
Proportional error (%)	21.5	2.0	21.3 to 22.1

Inter-individual variability (IIV) and inter-occasion variability (IOV), were assumed log normally distributed and expressed as approximate percentage coefficient of variation (%CV); % RSE NONMEM, relative standard error from NONMEM covariance step reported on the approximate standard deviation scale; 95% CI BS (N=50), 95% confidence interval of parameter estimate obtained from nonparametric bootstrap of 50 iterations stratified by site; Mixture model of Slow:Fast eliminators, estimation of the percentage of slow vs. fast eliminators using a mixture model; % Slow:Fast eliminators (South Africa), estimated percentage of slow vs. fast eliminators in South African study site; % Slow:Fast eliminators (West Africa), estimated percentage of slow vs. fast eliminators in Benin, Guinea & Senegal study sites; CL_{slow}, estimated clearance for slow eliminators scaled to median FFM of 45 kg (TV_FFM); CL_{fast}, estimated clearance for fast eliminators scaled to median FFM of 45 kg (TV_FFM); F_{slow}, reference bioavailability fixed to 1 for slow eliminators (1 FIX); F_{fast}, bioavailability for fast eliminators estimated as the fractional change from F_{slow}; Q, inter-compartmental clearance scaled to median FFM of 45 kg (TV_FFM); V_c, apparent volume of distribution for central compartment scaled to median FFM of 45 kg (TV_FFM); V_p, apparent volume of distribution for peripheral compartment scaled to median FFM of 45 kg (TV_FFM); k_a, absorption rate constant; MTT, absorption mean transit time; N, number of transit compartments; Guinea & Senegal-F (%), percentage change in F in Guinea & Senegal relative to other sites; Guinea-CL (%), percentage change in CL in Guinea relative to other sites; South Africa-(k_a/MTT) (%), percentage change in (k_a/MTT) in South Africa relative to other sites; Additive residual error (mg/L), additive error; Proportional error (%), proportional residual error reported as a percentage.

Ethambutol

In total, 882 pharmacokinetic observations from 171 patients were available for analysis. A total of 13 occasions (including both occasions for 1 patient profile), comprising 39 (4.4%) observations, were classified as potentially affected by data errors and excluded from the analysis (Chapter 3). Approximately half the occasions identified were at steady state (occasion 2) and just over half of these included observations approximately 23 to 48 hours post a self-reported dose (pre-dose observations). Patient non-adherence to their dosing

schedule (e.g. taking their previous dose just prior to their clinic visit), sample swop or incorrectly labelled samples were likely explanations for their exclusion. A further 5 samples (0.5%) fell below the quantification level (0.1 mg/L) and were substituted with half the quantification level (0.05 mg/L). Ethambutol pharmacokinetics was best described using a two-compartment model with first order absorption preceded by a series of transit compartments and first order elimination describing first dose and steady state kinetics. The model fit the data well, as shown in the VPC (Figure 6.4), and the values of the final parameter estimates can be found in Table 6.4. Ethambutol bioavailability increased by 11.4% from first dose to approximately 28 days later. Additionally, patients with HIV co-infection had approximately 15% lower bioavailability compared to patients without HIV. Clearance was estimated at 46.7 L/h and scaled with inter-compartmental clearance (Q) using *FFM* normalised to the typical *FFM* of 45 kg in the data set. V parameters were scaled with WT and normalised to the typical WT of 55 kg in the data set. Scaling clearance parameters with *FFM* and normalising to a *FFM* of a reference patient weighing 70 kg and measuring 1.76 m in height, clearance was estimated at 53 L/h. Scaling volume parameters with total weight and normalising to a WT of a reference patient weighing 70 kg, volume of the central compartment (V_c) was estimated at 199 L while peripheral compartment volume (V_p) was estimated at 566 L.

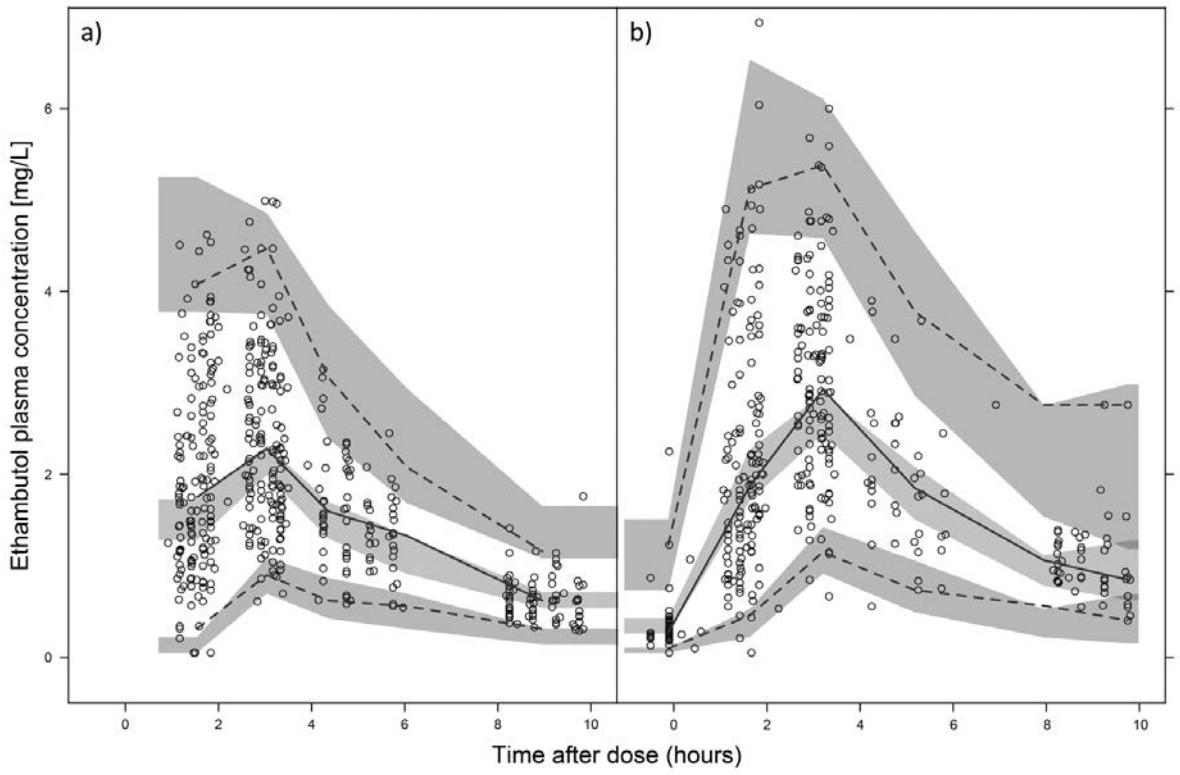

Figure 6.4 *Visual predictive check (VPC) for ethambutol concentration versus time stratified by occasion a) first dose and b) steady-state (Day 28). The solid and dashed lines are the median, 5th and 95th percentiles of the observed rifampicin plasma concentrations, respectively. Shaded areas are the 95% prediction intervals for the median, 5th and 95th percentiles of simulated data. The open circles are observed original data.*

Table 6. 4 *Ethambutol parameter estimates in 171 newly diagnosed pulmonary tuberculosis patients. Precision estimates were obtained from NONMEM (% RSE, reported on approximate standard deviation scale) and the 95% confidence intervals (95% CI) from a nonparametric bootstrap (BS) employing 50 iterations stratified by site.*

Parameter	**Estimate**	**% RSE NONMEM**	**95% CI BS (N=50)**
CL (L/h) scaled to TV_*FFM*=45 kg	46.7	5.1	43.6 to 49.7
Q (L/h) scaled to TV_*FFM*=45 kg	66.6	9.0	53.9 to 84.0
V_c (L) scaled to TV_WT=55 kg	157	15.3	2 to 181
V_p (L) scaled to TV_WT=55 kg	445	9.3	392 to 577
k_a (1/h)	0.957	18.1	0.431 to 1.187
MTT (h)	1.04	4.5	0.92 to 1.81
N	8.53	21.3	3.65 to 12.69
$F_{first\ dose}$	1 FIX		
$F_{steady\ state}$ (% change from $F_{first\ dose}$)	11.4	41.6	3.8 to 16.5
HIV-*F* (% change from Non-HIV)	-14.7	21.9	-6.6 to -21.6
Inter-individual variability (IIV)			
IIV_{CL} (%CV)	29.6	11.0	21.7 to 35.4
Inter-occasional variability (IOV)			
IOV_{ka} (%CV)	63.0	14.0	0.6 to 76.9
IOV_{MTT} (%CV)	37.3	12.1	28.9 to 45.5
IOV_F (%CV)	21.0	11.9	14.4 to 25.0
Residual variability			
Additive error (mg/L)	0.0692	35.5	0.0387 to 0.0920
Proportional error (%)	21.3	6.1	19.1 to 28.0

Inter-individual variability (IIV) and inter-occasion variability (IOV), were assumed log normally distributed and expressed as approximate percentage coefficient of variation (%CV); % RSE NONMEM, relative standard error from NONMEM covariance step reported on the approximate standard deviation scale; 95% CI BS (N=50), 95%

confidence interval of parameter estimate obtained from nonparametric bootstrap of 50 iterations stratified by site; CL, estimated clearance scaled to median FFM of 45 kg (TV_FFM)); $F_{first\ dose}$, reference bioavailability fixed to 1 at first dose (1 FIX); F $F_{steady\ state}$, steady state bioavailability estimated as the fractional change from first dose; Q, inter-compartmental clearance scaled to median FFM of 45 kg; V_c, apparent volume of distribution for central compartment scaled to median WT of 55 kg; V_p, apparent volume of distribution for peripheral compartment scaled to median WT of 55 kg; k_a, absorption rate constant; MTT, absorption mean transit time; N, number of transit compartments; HIV-F (%), % change in F in HIV infected patients relative to non HIV infected patients; Additive residual error (mg/L), additive error reported as mg/L; Proportional error (%), proportional residual error reported as a percentage.

Gatifloxacin

Model results are presented in Chapter 5.

Model-based estimates of AUC and C_{MAX}

Drug exposures expressed as AUC and C_{MAX} were derived from final pharmacokinetic models and reported in Table 6.5. Box plots of C_{MAX} for each drug are illustrated in reference to target concentration thresholds for rifampicin, isoniazid, pyrazinamide and ethambutol reported by (Alsultan and Peloquin 2014) (Figure 6.5). Reference concentration ranges for gatifloxacin were sourced from Grasela (2000). Notably, 73% (n=252) patients failed to achieve the rifampicin C_{MAX} threshold while 43% (n=147) failed to achieve the isoniazid threshold concentration. Approximately 85% of patients with HIV co-infection had rifampicin C_{MAX} below the 8 mg/L compared to 68% of patients without HIV co-infection (χ^2=11.10, p<0.05). Similarly, 69% and 78% of patients randomized into the control and test regimens respectively had rifampicin C_{MAX} <8 mg/L. The proportion of patients with rifampicin C_{MAX} below the lower limit of recommended reference range was only significantly different across treatment regimen (1-sided Fishers exact p=0.0361). Although 76% of male patients *vs*. 68% of female patients achieved rifampicin C_{MAX} below the 8 mg/L threshold, the trend did not reach statistical significance. Only 26% of patients from Senegal had rifampicin C_{MAX} <8 mg/L compared to 82% of patients outside of Senegal. Furthermore, only 37% of patients from Senegal have isoniazid C_{MAX} <3 mg/L compared to 77% of patients outside Senegal having C_{MAX} below the 3 mg/L threshold. Approximately 34% of South African patients, compared to 56%

of patients outside South Africa, failed to achieve an isoniazid C_{MAX} of 3 mg/L. Similarly, 56% of fast isoniazid metabolisers, compared to 31% of slow isoniazid metabolisers, had isoniazid C_{MAX} <3 mg/L. Comparisons between drug exposures (AUC and C_{MAX}) in our study are contrast with other African studies for which data are provided in comparable format and summarized in Table 6.6. Similarly, a summary of steady state rifampicin, pyrazinamide, isoniazid and ethambutol exposure, expressed as AUC and C_{MAX}, is reported across each study site in Table 6.7.

Table 6. 5 *Drug plasma peak concentrations (C_{MAX}) and area under the concentration-time profile from 0 to 24 hours (AUC_{0-24}) at steady state and from 0 to infinity hours ($AUC_{0-\infty}$) at first dose of 343 patients within the OFLOTUB phase III pharmacokinetic sub-study stratified by study drug and treatment regimen. Exposure variables are reported as median (interquartile range) and [range] at first dose (FD) and steady state (SS).*

	Isoniazid		**Rifampicin**		**Pyrazinamide**		**Ethambutol**	**Gatifloxacin**
	Test (n=169)	**Control (n=174)**	**Test (n=169)**	**Control (n=174)**	**Test (n=169)**	**Control (n=174)**	**Control (n=174)**	**Test (n=169)**
SS AUC_{0-24} [mg·h/L]	**14.3**	**14.1**	**36.3**	**34.9**	**411**	**391**	**23**	**35.4**
median (IQR)	(9.2 – 23.5)	(8.3 – 22.2)	(28.2 – 47.1)	(29.0 – 48.5)	(359 – 468)	(333 – 458)	(20 – 29)	(31.0 – 40.1)
[range]	[3.1 – 40.8]	[1.4 – 60.2]	[11.9 – 91.1]	[10.6 – 98.9]	[203 – 759]	[218 – 1257]	[7 – 53]	[21.0 – 60.1]
SS C_{MAX} [mg/L]	**3.3**	**3.4**	**6.2**	**6.8**	**36.2**	**35.4**	**3.2**	**3.8**
median (IQR)	(2.4 – 4.5)	(2.4 – 4.5)	(5.1 – 7.9)	(5.6 – 8.5)	(32.2 – 40.1)	(31.5 – 39.3)	(2.7 – 3.7)	(3.5 – 4.3)
[range]	[0.7 – 8.0]	[0.5 – 7.2]	[1.4 – 13.2]	[2.0 – 15.6]	[9.2 – 60.4]	[21.9 – 62.1]	[1.5 – 5.5]`	[2.5 – 5.8]
FD $AUC_{0-\infty}$ [mg·h/L]	**15.0**	**13.8**	**71.8**	**68.7**	**542**	**532**	**22**	**41.2**
median (IQR)	(9.2 – 21.4)	(8.2 – 20.6)	(57.0 – 93.8)	(54.7 – 94.9)	(470 – 626)	(455 – 627)	(18 – 27)	(36.2 – 46.6)
[range]	[3.3 – 57.1]	[2.5 – 54.0]	[10.6 – 190.7]	[17.9 – 219.2]	[261 – 1163]	[282 – 1189]	[9 – 47]	[22.9 – 74.8]
FD C_{MAX} [mg/L]	**3.3**	**3.2**	**7.0**	**7.7**	**32.5**	**33.4**	**2.7**	**3.9**
median (IQR)	(2.4 – 4.3)	(2.3 – 4.4)	(5.7 – 8.3)	(6.1 – 9.4)	(28.8 – 37.2)	(29.5 – 37.6)	(2.2 – 3.2)	(3.6 – 4.4)
[range]	[1.1 – 7.1]	[1.0 – 8.5]	[2.3 – 15.7]	[3.3 – 17.7]	[18.6 – 60.6]	[21.8 – 56.9]	[1.1 – 4.5]	[2.6 – 6.1]

SS, steady state; FD, first dose; IQR, interquartile range; Test, test regimen; isoniazid, rifampicin, pyrazinamide; gatifloxacin, Control, control regimen; isoniazid, rifampicin, pyrazinamide, ethambutol.

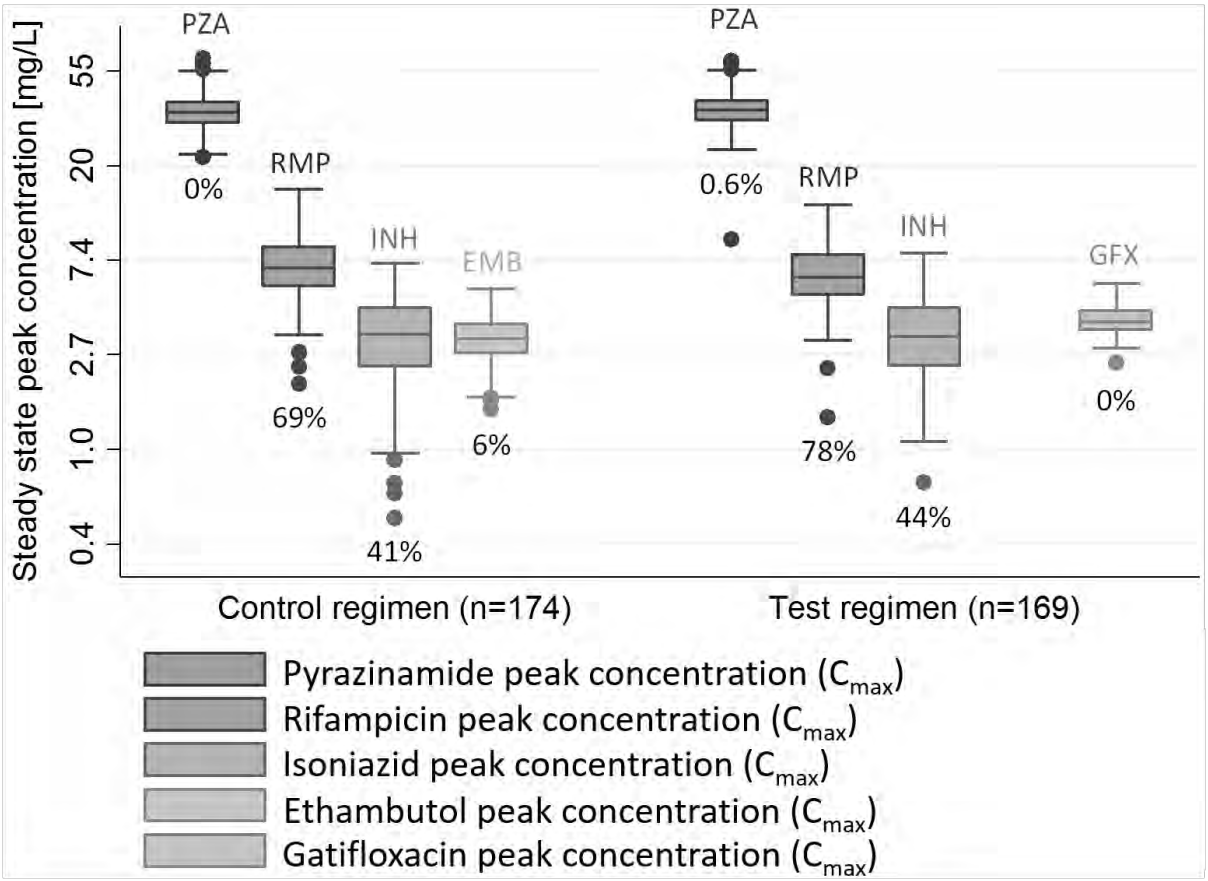

Figure 6.5 *Box plots representing steady state plasma peak concentrations (C_{MAX}) for each drug within the OFLOTUB phase III sub-study stratified by treatment regimen. The % of patients with C_{MAX} below the lower limit of the published reference range is plotted below each respective boxplot. Peak concentration reference ranges recommended (C_{MAX} [mg/L]) for ethambutol (EMB) (2-6), isoniazid (INH) (3-5), rifampicin (RMP) (8-24) and pyrazinamide (PZA) (20-50) by Alsultan and Peloquin (Alsultan and Peloquin 2014). The published gatifloxacin (GFX) C_{MAX} range (2.3-6.1mg/L) extracted from Grasela (Grasela 2000). The proportion of patients with C_{MAX} below the lower limit of recommended reference range was significantly different across treatment regimen only for rifampicin ($p<0.05$).*

Table 6. 6 *Steady state (SS) plasma peak concentration (C_{MAX}) and area under the concentration-time profile from 0 to 24 hours (AUC) for rifampicin (RMP), isoniazid (INH), pyrazinamide (PZA), and ethambutol (EMB) within 343 patients randomised into the OFLOTUB phase III pharmacokinetic sub-study. Results of the present study are contrast with other African studies for which data are provided in comparable format. Exposure variables are reported as median, (interquartile range) and [range] stratified by clinical study*.*

Drug exposure	**Current study Median (IQR) [range]**	**Chigutsa Median [range]**	**Tostmann Median [range]**	**McIlleron Median (IQR)**
SS RMP C_{MAX} (mg/L)	6.5 (5.3-8.2) [1.4-15.6]	7.3 [3.7-11.0]	8.9 [5.9-14.8]	7.2 (5.9-8.8)
SS RMP AUC (mg·hr/L)	36 (28-48) [11-99]	48 [18-126]	40 [27-68]	36 (28-48)
SS INH C_{MAX} (mg/L)	3.3 (2.4-4.5) [0.5-8.0]	2.5 [0.7-7.7]	2.8 [1.0-4.6]	1.7 (1.2-2.2)
SS INH AUC (mg·hr/L)	14 (9-23) [1-60]	14 [6-63]	11 [3.7-22.7]	6 (4-9)
SS PZA C_{MAX} (mg/L)	36 (32-40) [9-62]	34 [11-90]	38 [29-51]	35 (28-42)
SS PZA AUC (mg·hr/L)	402 (344-463) [203-1257]	420 [153-798]	344 [209-610]	260 (213-337)
SS EMB C_{MAX} (mg/L)	3.2 (2.7-3.7) [1.5-5.5]	3.1 [1.6-5.1]	3.3 [2.2-5.8]	3.0 (2.3-3.8)
SS EMB AUC (mg·hr/L)	23 (20-29) [7-53]	32 [16-73]	20 [13-32]	17 (13-21)

*******Chigutsa, the median dose per kg body weight for rifampicin, isoniazid and pyrazinamide and ethambutol was respectively 10.6, 5.0, 26.5 and 18.2 mg/kg (Chigutsa et al. 2015); Tostmann, the median dose per kg body weight for rifampicin, isoniazid and pyrazinamide and ethambutol was respectively 10.4, 5.2, 27.8 and 19.1 mg/kg (Tostmann et al. 2013) and McIlleron, the median dose per kg body weight for rifampicin, isoniazid and pyrazinamide and ethambutol was respectively 9.2, 4.6, 24.6 and 16.9 mg/kg (McIlleron et al. 2012). Within our study the median mg/kg body weight dose for rifampicin, isoniazid and pyrazinamide and ethambutol dose for all 343 patients was respectively 10.4, 5.2, 27.8 and 19 mg/kg.*

Table 6. 7 *Steady state (SS) plasma peak concentration (C_{MAX}) and area under the concentration-time profile from 0 to 24 hours (AUC) for rifampicin (RMP), isoniazid (INH), pyrazinamide (PZA) and ethambutol (EMB) within patients randomised into the OFLOTUB phase III pharmacokinetic sub-study at the four study sites. Exposure variables are reported as median, (interquartile range) and [range] stratified by study site.**

Drug exposure	**Benin Median (IQR) [range]**	**Guinea Median (IQR) [range]**	**Senegal Median (IQR) [range]**	**South Africa Median (IQR) [range]**
SS RMP C_{MAX} (mg/L)	6.3 (5.5-7.8) [3.2-13.5]	6.3 (5.2-8.5) [3.7-13.2]	9.3 (8.0-11.1) [5.2-15.6]	5.9 (4.9-7.1) [1.4-13.6]
SS RMP AUC (mg·hr/L)	36 (30-44) [18-99]	34 (24-42) [13-83]	52 (43-61) [27-89]	33 (27-43) [11-91]
SS INH C_{MAX} (mg/L)	4.0 (3.0-4.6) [2.3-6.1]	2.4 (2.1-3.3) [1.1-5.5]	2.5 (2.2-3.0) [1.3-4.6]	3.6 (2.5-4.6) [0.5-8.0]
SS INH AUC (mg·hr/L)	16 (10-25) [6-35]	8 (5-14) [2-24]	14 (7-17) [4-28]	15 (10-27) [1-60]
SS PZA C_{MAX} (mg/L)	32 (30-35) [26-43]	37 (35-41) [27-53]	36 (34-38) [27-49]	37 (32-42) [9-62]
SS PZA AUC (mg·hr/L)	348 (312-411) [260-583]	404 (365-459) [218-651]	391 (355-422) [280-565]	419 (353-505) [203-1257]
SS EMB C_{MAX} (mg/L)	3.0 (2.6-3.6) [1.7-5.5]	3.5(3.0-3.9) [1.9-5.3]	3.4 (3.1-3.9) [2.9-4.9]	3.1 (2.6-3.6) (1.5-5.3]
SS EMB AUC (mg·hr/L)	24 (20-29) [15-38]	26 (21-31) [16-39]	25 (22-28) [18-42]	22 (19-28) [7-53]

****** Benin (n=52); Guinea (n=38); Senegal (n=53); South Africa (n=200). Within the EMB containing 6-month control regimen of the study, the numbers of patients within each study site are as follows: Benin, n=27; Guinea, n=19; Senegal, n=27; South Africa, n=101.*

6.2. Discussion

Population pharmacokinetics for rifampicin, isoniazid, pyrazinamide and ethambutol are characterized in sub-group of 343 African patients randomized into control and test regimens of the OFLOTUB study. Drug exposures in our study were comparable to several other clinical studies investigating first line anti-tuberculosis drug pharmacokinetics in African populations (Tappero et al. 2005; McIlleron et al. 2006; Chideya et al. 2009; Tostmann et al. 2013; Chigutsa

et al. 2015). Additionally, drug exposure, expressed as AUC, was comparable across treatment regimen. Considering AUC is predictive of outcome in tuberculosis patients (Pasipanodya et al. 2013; Chigutsa et al. 2015), treatment regimens were likely clinically equivalent.

Although no significant difference in rifampicin bioavailability or clearance was observed across treatment regimen, there was a significant effect on the absorption rate which could explain significantly lower rifampicin peak concentrations observed in test arm patients. Subsequently, patients in the test regimen of the study were 3.7 (95% CI: 1.0-2.6, 1-sided Fishers exact p=0.0361) times more likely to have rifampicin peak concentrations below 8 mg/L when compared to those in the control regimen. Similar findings in a single dose interaction study was reported with significant 20% reductions in rifampicin C_{MAX} when dosed together with gatifloxacin, isoniazid and pyrazinamide (McIlleron et al. 2007b). Remarkably, nearly 80% of patients randomized into the gatifloxacin containing test regimen and 70% in the control regimen, failed to achieve the recommended rifampicin C_{MAX} of 8 mg/L. Similarly, low rifampicin concentrations have been reported in South African patients on standard therapy, with 61% - 69% failing to achieve the 8 mg/L threshold (McIlleron et al. 2006; McIlleron et al. 2012), while approximately 78% - 84% of patients from Botswana (Tappero et al. 2005; Chideya et al. 2009), 90% from Kenya (Choudhri et al. 1997), and 100% from Burkino Faso (Saleri et al. 2012) had concentrations below the 8 mg/L rifampicin threshold. Furthermore, low isoniazid C_{MAX} was observed in our study population with 41% and 44% of patients in the control and test regimens respectively failing to achieve the isoniazid steady state C_{MAX} threshold of 3 mg/L (Alsultan and Peloquin 2014). Similarly, McIlleron et al (McIlleron et al. 2012) reported low isoniazid concentrations in South African patients with somewhat higher proportions of approximately 88% failing to achieve the lower limit of the reported reference range (Alsultan and Peloquin 2014), while 89% of patients from Kenya (Choudhri et al. 1997), 53% of patients from Tanzania (Tostmann et al. 2013), 30% - 36% of patients from Botswana (Tappero et al. 2005; Chideya et al. 2009), and 19% - 29.4% of patients from Mozambique (Bhatt et al. 2014) failed to achieve isoniazid C_{MAX} >3 mg/L. Discrepancies in isoniazid concentration may be explained by NAT2 gene polymorphisms which vary widely between populations (Sabbagh et al. 2008). In the present study, 47% of patients classified as fast metabolisers achieved isoniazid C_{MAX} >3 mg/L compared to 69% of slow metabolisers achieving peak concentrations above this threshold. Similarly, Denti et al

reported approximately 50% of fast metabolisers failing to achieve a C_{MAX} above 3 mg/L while approximately 75% of slow metabolisers achieved this target concentration (Denti et al. 2015). Additionally, variable isoniazid concentrations observed in relatively hot African countries may partially be explained by the drugs temperature liable properties detected even at -20 degrees Celsius (Hutchings et al. 1983). In the current study, more than 90% of patients achieved pyrazinamide and ethambutol C_{MAX} above the recommended concentration thresholds of 20 mg/L and 2 mg/L respectively (Alsultan and Peloquin 2014). Similarly, more than 90% of patients in other African studies achieved pyrazinamide C_{MAX} >20 mg/L (Choudhri et al. 1997; Tappero et al. 2005; Chideya et al. 2009; McIlleron et al. 2012; Tostmann et al. 2013). Wide-ranging proportions of patients with ethambutol concentrations below 2 mg/L were reported in 0% of patients from Tanzania (Tostmann et al. 2013), 39% - 41% of patients from Botswana (Tappero et al. 2005; Chideya et al. 2009), and in 2% (McIlleron et al. 2006), 12% (McIlleron et al. 2012), and 25% of patients from South Africa (Denti et al. 2015). Variability in patient characteristics, treatment regimens, and pharmacokinetic laboratory assay may account for some of the observed discrepancies in ethambutol exposures across studies. The prevalence of low rifampicin and isoniazid C_{MAX} in our study population is of concern, hence the need to characterise exposure-response relationships to confirm clinical significance in future studies.

Autoinduction of rifampicin metabolism occurs following multiple repeated doses resulting in lower exposures (Acocella 1978). Rifampicin systemic and pre-systemic clearance increases via induction of intestinal and hepatic enzymes and transporters (Loos et al. 1987; Schuetz et al. 1996). Our current rifampicin model estimates autoinduction as the fractional change in clearance (which includes systemic and pre-systemic clearance) from first dose to steady state approximately 28 days later. Model estimates predict an approximate 2-fold increase in clearance from baseline, whereby clearance at first dose increased by 99.3% (95% CI: 90.2-104.7) yielding a steady state clearance of 16.5 L/h (95% CI: 15.8-17.0). Consequently, AUC's observed at first dose were halved in patients approximately 28 days later. Denti and colleagues (Denti et al. 2010) found a similar 2.18 fold increase in clearance over a 28 day period following multiple repeated doses in 61 South African patients. Loos and colleagues (Loos et al. 1985) reported a 59% increase in systemic clearance and a 25% decrease in bioavailability (pre-systemic). The combined systemic and pre-systemic clearance

(autoinduction) accounts for an approximate 84% increase in rifampicin elimination which was somewhat lower compared to our estimate of 99.3%. This difference is likely due to low patient numbers in their study (n=12), genetic differences between German and African patients and the shorter follow up time observed between first and last dose (21 days) likely underestimating the extent of autoinduction expected to take between 30 and 40 days (Denti et al. 2010; Smythe et al. 2012). In a previous study (Smythe et al. 2012), using a semi-mechanistic enzyme turn over model, we predicted a 1.82 fold increase in clearance from first dose following multiple doses in patients randomized into the control regimen of the study (n=174). The current rifampicin model did not find a significant difference in autoinduction across treatment regimen, hence the difference in autoinduction estimates between the previous study and the current study is likely the result of increased power and accuracy with the addition of 169 patients used during the estimation of this parameter. Furthermore, there was large inter-individual variability in the autoinduction parameter estimated at 30.4% (95% CI: 24-38.6). Clinically, autoinduction of rifampicin metabolism results in the proportion of patients achieving peak concentrations above the 8 mg/L threshold decreasing from 37% to 27% following multiple repeated doses. Interestingly, rifampicin model predictions (VPC's) were observed to underestimate steady state C_{MAX}. A saturable absorption pathway, demonstrated by (Chirehwa et al. 2015), is likely to explain the under prediction of peak concentrations. Supporting the saturable absorption hypothesis, VPC's stratified by dose (450 vs. 600 mg), confirmed only the 600 mg dose to underestimate peak concentrations at steady state (data not shown). Furthermore, model estimates better predict peak concentrations at first dose compared to steady state. Multiple repeated daily dosing similarly influenced pyrazinamide and ethambutol steady state kinetics in our study population. Pyrazinamide clearance increased by approximately 30% (95% CI: 23.2-36.9) from first dose to steady state. In support of our findings, Chirehwa and colleagues equally found pyrazinamide steady state clearance to increase by approximately 25% from first dose (Chirehwa et al. 2015). However, the increase in pyrazinamide clearance following multiple repeated doses is likely not important as equal proportions of study patients achieved peak concentrations above the 20 mg/L threshold at first dose and steady state. Ethambutol bioavailability was estimated to increase by approximately 11% (95% CI: 3.8-16.5) following multiple repeated doses. Consequently, the proportion of patients achieving peak concentrations above the 2 mg/L threshold more than doubled from 6% to 15% from first dose to steady state.

The aetiology of site effects on rifampicin, isoniazid and pyrazinamide pharmacokinetics is unclear. We speculate that unique dietary factors influencing pre-systemic transporters, such as P-glycoprotein, might cause the increased bioavailability observed in patients from Senegal (Bhardwaj et al. 2002). Patients with tuberculosis and HIV co-infection are reported having decreased plasma concentrations of anti-tuberculosis drugs (Zhu et al. 2004; McIlleron et al. 2006; Chideya et al. 2009; Jönsson et al. 2011; McIlleron et al. 2012), with malabsorption, due to diarrhoea, suggested as a reason for reduced drug exposures in antiretroviral naive patients (Gurumurthy et al. 2004). In our study, HIV co-infection was found to affect rifampicin and ethambutol pharmacokinetics. HIV co-infected patients had approximately 15% lower ethambutol bioavailability relative to patients without HIV infection**.** Jönsson and colleagues similarly reported HIV co-infected patients having 15.4% lower ethambutol bioavailability compared to patients without HIV infection (Jönsson et al. 2011). The effect of HIV co-infection on ethambutol exposure is unlikely to be important as 6% of patients either with or without HIV co-infection had ethambutol C_{MAX} below the 2 mg/L threshold. In our previous study, patients with HIV co-infection were estimated to have a 29.6% increase in the apparent volume of distribution of rifampicin compared to those without HIV infection. Similarly, our current model, incorporating patients randomized into both test and control regimens, predict HIV co-infection to increase the apparent volume of distribution of rifampicin by approximately 14%. Consequently, patients with HIV co-infection were approximately 3 times more likely to have rifampicin peak concentrations below 8 mg/L compared to those without HIV coinfection (OR=2.7, 95% CI: 1.5-4.9). Notably, no significant difference in rifampicin bioavailability nor clearance was estimated between patients with or without HIV co-infection resulting in comparable median steady AUC's of 34 and 36 mg·h/L respectively.

In the absence of genotype or isoniazid metabolite data, a mixture model was employed to classify the study participant as fast or slow acetylator phenotypes. Fast eliminators were predicted to have a median clearance of 23 L/h, approximately double the 10.3 L/h estimated for slow metabolisers. In agreement with our findings, Wilkins and colleagues (Wilkins et al. 2011) reported fast acetylators having a clearance of 21.6 L/h while slow acetylators had a median clearance of 9.7 L/h. Fast metabolisers additionally were estimated having 14.2% lower bioavailability compared to slow metabolisers in our study population. An estimated

60-65% of South Africans are classified as fast metabolisers (Bach et al. 1976; Loktionov et al. 2002), compared to approximately 50% of West Africans (Patin et al. 2006; Touré et al. 2012).

Limitations and strengths

Extensive characterisation of the pharmacokinetic curve, especially peak concentration, was restricted by sparse sampling with patients having only three pharmacokinetic samples taken at first dose and/or at steady state. Mixed effects modelling was employed to interpret the data as this technique suitably handles study designs incorporating limited sampling strategies. Additionally, multiple study sites enabled the current study to better investigate between site differences in pharmacokinetic exposure without the usual confounders of study drug, study design and laboratory assay masking regional differences.

6.3. Conclusion

In summary, rifampicin, isoniazid, pyrazinamide and ethambutol pharmacokinetics are characterised in a large cohort of 343 African patients randomized into the OFLOTUB pharmacokinetic sub-study. The study identified a single drug-drug interaction where the rifampicin absorption rate was significantly reduced when dosed together with gatifloxacin, isoniazid, and pyrazinamide. Consequently, patients in the gatifloxacin containing test regimen had reduced peak concentrations when compared to those in the standard 6-month control regimen although the AUC remained comparable across treatment regimen. Despite 78% and 43% of patients having low rifampicin and isoniazid peak concentrations respectively, similar drug exposures in terms of AUC and C_{MAX} were reported in other African studies. HIV co-infected patients in the test regimen of the study were 3 times more likely to have rifampicin peak concentrations below the 8 mg/L threshold compared to all other patients. Classification and regression tree analyses incorporating drug exposures along with patient and mycobacterial characteristics will help identify predictors for patient outcome and their interactions in future studies.

7. Predictors of culture conversion and long term outcome in African patients treated for drug sensitive pulmonary tuberculosis

The pharmacokinetic-pharmacodynamic (PK/PD) study reported in this chapter was nested within the phase III OFLOTUB trial investigating a 4-month gatifloxacin containing regimen for treating tuberculosis (Merle et al. 2014). Experiments in the tuberculosis hollow fiber system model have demonstrated the role of drug concentration in killing MTB and preventing relapse in tuberculosis patients (Pasipanodya et al. 2013). Clinical trials have demonstrated that low pyrazinamide peak concentrations associated with poor outcome (defined as a composite of treatment failure and death) (Chideya et al. 2009). Similarly, elevated rifampicin exposure, expressed as peak concentration (C_{MAX}) and area under the steady state concentration–time curve (AUC), has been demonstrated to significantly reduce bacterial load and increase culture conversion rates (Boeree et al. 2015; Chigutsa et al. 2015).

Isoniazid has a rapid bactericidal action, eliminating the majority of drug susceptible organisms within the first few days of tuberculosis treatment (Mitchison 2000). Thereafter rifampicin and pyrazinamide take over the bactericidal role during the intensive phase of treatment while ethambutol, having a bacteriostatic action, protects against rifampicin resistance in the event of initial isoniazid resistance (Blumberg et al. 2003). During the 4-month continuation phase of isoniazid and rifampicin treatment, persisting organism are eliminated via the sterilizing action of rifampicin (Mitchison 2000). Gatifloxacin has demonstrated rapid bactericidal action on log phase cultures (Paramasivan et al. 2005) and has been suggested to improve the sterilizing activity of the standard treatment regimen when it replaced ethambutol (Rustomjee et al. 2008).

The aim of this chapter was to identify predictors of both culture conversion at 2 months and long term outcome by 24 months through the utilizing classification and regression tree analysis (CART) (Breiman et al. 1984; Pasipanodya et al. 2013).

7.1. Results

Clinical and bacteriological measures

Patient clinical and bacteriological characteristics stratified by study outcome and treatment regimen are summarized in Table 7.1 for 2-month outcome and Table 7.2 for 24-month outcome. Patients who could not be assessed for efficacy outcomes were excluded from the analysis, and their clinical and bacteriological characteristics are summarized in the tables below. Patient drug exposures in terms of the pharmacokinetic measures AUC and C_{MAX} are summarized in Table 7.3 and Table 7.4 for 2-month and 24-month composite outcome respectively. The proportion of patients that achieved peak concentrations below the lower limit of the reference ranges for each study drug are provided in Table 7.5.

Table 7.1 *(a) 2-month composite outcome stratified by treatment regimen and (b) patient clinical characteristics and baseline bacterial burden stratified by treatment regimen and availability.*

(a) Stratified characteristics:	**Control regimen: 135 (52)**	**Test regimen: 126 (48)**
Culture conversion at 2 months: n (%)	89 (66)	94 (75)
No Culture conversion: n (%)	38 (28)	24 (19)
Culture conversion at 2-month which could not be assessed: n (%)	8 (6)	8 (6)

(b) Stratified characteristics:	**Control regimen: 127 (49)**	**Test regimen: 118 (45)**	**Not available: 16 (6)**
Baseline lung cavitation (CAV): n (%)	85 (67)[a]	86 (73)	12 (75)
Baseline lung zone scores of 4-6 (ZONE)[b]: n (%)	58 (46)[c]	55 (47)	6 (38)
Baseline smear status (SMR)[d]:	21 (17)	12 (10)	3 (19)
1+ n (%)			
2+ n (%)	42 (33)	33 (28)	4 (25)
3+ n (%)	64 (50)	73 (62)	9 (56)
HIV positive: n (%)	38 (30)	32 (27)	5 (25)
SEX (female): n (%)	43 (34)	36 (31)	4 (25)
AGE in years:	28	29	27
median (range)	(18-57)	(18-57)	(18-55)
Body Mass Index (BMI)[e]:	19	20	18
median (range)	(14-32)	(14-29)	(15-27)

[a] *3 missing CAV outcomes for both outcomes in control regimen.*

[b] *ZONE score ranges from 0 to 6, with 0 indicating that no lung regions are affected and 6 indicating that all lung regions are affected.*

[c] *3 missing ZONE scores for culture conversion in control regimen.*

[d] *SMR findings were scored 1+ to 3+, with higher numbers indicating more severe disease.*

[e] *BMI is the weight in kilograms divided by the square of the height in meters.*

Table 7.2 *(a) Long term 24-month composite outcome stratified by treatment regimen and (b) patient clinical characteristics and baseline bacterial burden stratified by treatment regimen and availability. *Patients who could not be assessed for the efficacy outcomes were excluded from the analysis*

(a) Stratified characteristics:	**Control regimen: 135 (52)**	**Test regimen: 126 (48)**
24 month favourable composite outcome (FAV): n (%)	103 (76)	95 (75)
24 month unfavourable composite outcome (Not FAV): n (%)	16 (12)	21 (17)
Lost to follow-up on treatment: n	6	3
Consent withdrawn on treatment: n	1	1
Died on treatment: n	1	1
Treatment failure: n	3	1
Culture recurrence after end of treatment: n	5	15
24 month outcome which could not be assessed*: n (%)	16 (12)	10 (8)
Died after treatment*: n	2	2
Loss to follow-up after treatment*: n	12	8
Consent withdrawn after treatment*: n	1	0
Withdrawn after treatment*: n	1	0

(b) Stratified characteristics:	**Control regimen: 119 (46)**	**Test regimen: 116 (44)**	**Not available: 26 (10)**
Baseline lung cavitation (CAV): n (%)	81 (68)[a]	87 (75)	15 (58)
Baseline lung zone scores of 4-6 (ZONE)[b]: n (%)	54 (45)[c]	57 (49)	8 (31)
Baseline smear status (SMR)[d]:	20 (17)	13 (11)	3 (12)
1+ n (%)			
2+ n (%)	36 (30)	32 (28)	11 (42)
3+ n (%)	63 (53)	71 (61)	12 (46)
HIV positive: n (%)	37 (31)	32 (28)	6 (23)
SEX (female): n (%)	40 (34)	36 (31)	7 (27)
AGE in years:	28	29	37
median (range)	(18-57)	(18-57)	(20-53)

Body Mass Index (BMI)[e]: median (range)	19 (14-32)	20 (14-29)	18 (14-29)

[a]3 missing CAV outcomes for both outcomes in control regimen.

[b]ZONE score ranges from 0 to 6, with 0 indicating that no lung regions are affected and 6 indicating that all lung regions are affected.

[c]4 missing ZONE scores for 24 month outcome in control regimen.

[d]SMR findings were scored 1+ to 3+, with higher numbers indicating more severe disease.

[e]BMI is the weight in kilograms divided by the square of the height in meters.

Table 7.3 *Patient pharmacokinetic parameters at 2 months stratified by study outcome and treatment regimen.*

Parameters: Median {IQR} (range)	**Control regimen (n=127)**	**Test regimen (n=118)**	**Statistics***
EMB AUC [mg·hr/L]	23 {20-29} (7-53)	n/a	n/a
EMB C_{MAX} [mg/L]	3.2 {2.7-3.8} (1.7-5.5)	n/a	n/a
GFX AUC [mg·hr/L]	n/a	35 {30-40} (23-60)	n/a
GFX C_{MAX} [mg/L]	n/a	3.8 {3.5-4.3} (2.5-5.8)	n/a
INH AUC [mg·hr/L]	13 {7-21} (1-50)	13 {8-22} (3-39)	ns
INH C_{MAX} [mg/L]	3.1 {2.3-4.3} (0.5-6.0)	3.1 {2.3-4.1} (1.1-8.0)	ns
RMP AUC [mg·hr/L]	34 {27-46} (12-89)	36 {28-50} (13-91)	ns
RMP C_{MAX} [mg/L]	6.8 {5.5-8.4} (2.0-15.6)	6.2 {5.1-8.0} (1.4-13.2)	T= -1.82, p=0.035
PZA AUC [mg·hr/L]	377 {321-452} (218-797)	411 {349-500} (203-759)	T= -1.98, p=0.024
PZA C_{MAX} [mg/L]	34.6 {31.1-39.2} (21.9-62.1)	35.9 {32.0-40.7} (23.8-60.4)	ns

*AUC, 24-hour area under the steady state concentration–time curve; C_{MAX}, steady state peak concentration; IQR, interquartile range; range, minimum to maximum; Control regimen, 6-month regimen consisting of ethambutol (EMB), isoniazid, (INH), rifampicin, (RMP) and pyrazinamide (PZA); Test regimen, 4-month regimen where EMB was replaced with gatifloxacin (GFX); Culture conversion, smear and culture negative at 2 months. *Test statistics reported from T-Tests comparing log_{10} transformed drug concentrations between control and test regimens. ns = non-significant*

Table 7.4 *Patient pharmacokinetic parameters at 24 months stratified by study outcome and treatment regimen.*

Parameters: Median {IQR} (range)	**Control regimen (n=119)**	**Test regimen (n=116)**	**Statistics***
EMB AUC [mg·hr/L]	23 {20-29} (7-53)	n/a	n/a
EMB C_{MAX} [mg/L]	3.2 {2.8-3.8} (1.7-5.3)	n/a	n/a
GFX AUC [mg·hr/L]	n/a	34 {30-40} (23-60)	n/a
GFX C_{MAX} [mg/L]	n/a	3.8 {3.4-4.2} (2.5-5.8)	n/a
INH AUC [mg·hr/L]	13 {7-21} (1-50)	13 {8-22} (3-39)	ns
INH C_{MAX} [mg/L]	3.2 {2.2-4.2} (0.5-6.0)	3.1 {2.2-4.2} (0.7-8.0)	ns
RMP AUC [mg·hr/L]	34 {28-47} (12-89)	36 {28-51} (13-91)	ns
RMP C_{MAX} [mg/L]	6.8 {5.5-8.5} (2.0-15.6)	6.3 {5.1-8.1} (1.4-13.2)	T= 1.85, p=0.033
PZA AUC [mg·hr/L]	388 {326-457} (218-932)	410 {352-502} (203-759)	T= -1.78, p=0.038
PZA C_{MAX} [mg/L]	35.0 {31.2-39.1} (21.9-59.0)	35.9 {32.2-40.4} (23.8-60.4)	ns

*AUC, 24-hour area under the steady state concentration–time curve; C_{MAX}, steady state peak concentration; IQR, interquartile range; range, minimum to maximum; Control regimen, 6-month regimen consisting of ethambutol (EMB), isoniazid (INH), rifampicin (RMP) and pyrazinamide (PZA); Test regimen, 4-month regimen where EMB was replaced with gatifloxacin (GFX); Culture conversion, smear and culture negative at 2 months. *Test statistics reported from T-Tests comparing log_{10} transformed drug concentrations between control and test regimens. ns = non-significant*

Table 7.5 *The number and (%) of patients with C_{MAX} below the reference range.* [a]

	Culture conversion at 2 months (n=245)		24-month composite outcome (n=235)	
Pharmacokinetic parameters: [mg/L]	**Control regimen (n=127)**	**Test regimen (n=118)**	**Control regimen (n=119)**	**Test regimen (n=116)**
EMB C_{MAX}	9 (7%)	n/a	8 (7%)	n/a
GFX C_{MAX}	n/a	0 (0)%	n/a	0 (0%)
INH C_{MAX}	58 (46%)	53 (45%)	52 (44%)	54 (47%)
RMP C_{MAX}	90 (71%)	90 (76%)	84 (71%)	87 (75%)
PZA C_{MAX}	0 (0%)	0 (0%)	0 (0%)	0 (0%)

[a] *Reference range (C_{MAX} [mg/L]) for ethambutol (EMB) (2-6), isoniazid (INH) (3-5), rifampicin (RMP) (8-24) and pyrazinamide (PZA) (20-50) from (Alsultan and Peloquin 2014) and for gatifloxacin (GFX) (2.3-6.1) from (Grasela 2000). No significant differences in the proportion of patients achieving peak concentrations below the lower limit of the recommended reference range were observed across treatment regimen at 2- and/or 24-month outcome.*

2-month outcome

CART identified treatment regimen as the primary predictor for culture conversion at 2 months, followed by isoniazid in the test regimen and rifampicin in the control arm (Figure 7.1). Patients in the test regimen achieved 80% favourable outcome while patients in the control regimen achieved 70% favourable outcome after 2 months of treatment (Figures 7.2).

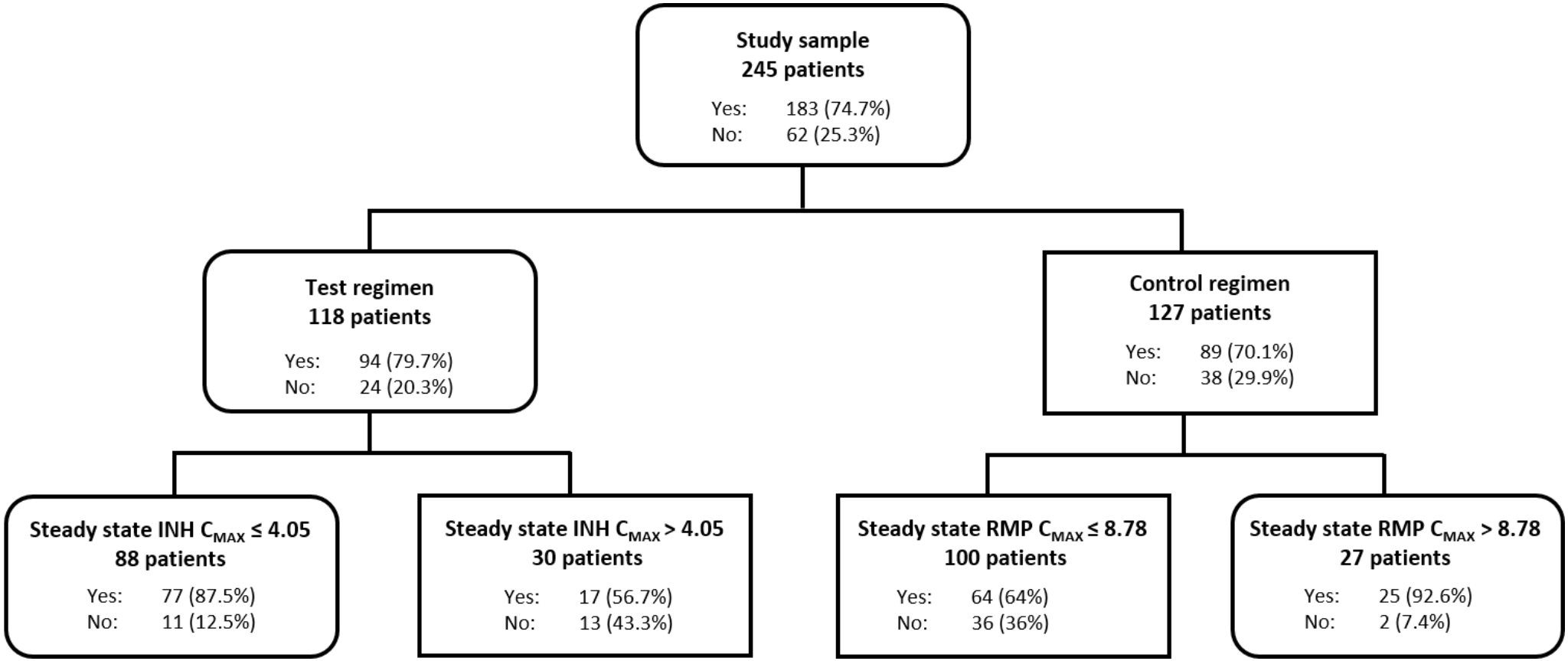

Figure 7.1 Variables predictive of 2-month sputum conversion in 245 patients randomized into the OFLOTUB phase III pharmacokinetic sub-study. Pharmacokinetic parameters, patient demographics and bacterial burden were examined in the initial models and decision trees. The 4-month, gatifloxacin containing test regimen, as well as rifampicin and isoniazid peak concentrations (mg/L) were best predictors of 2-month sputum conversion. Only 7% of patients within the control regimen with rifampicin peak concentrations above 8.78 mg/L were still sputum positive at 2 months.

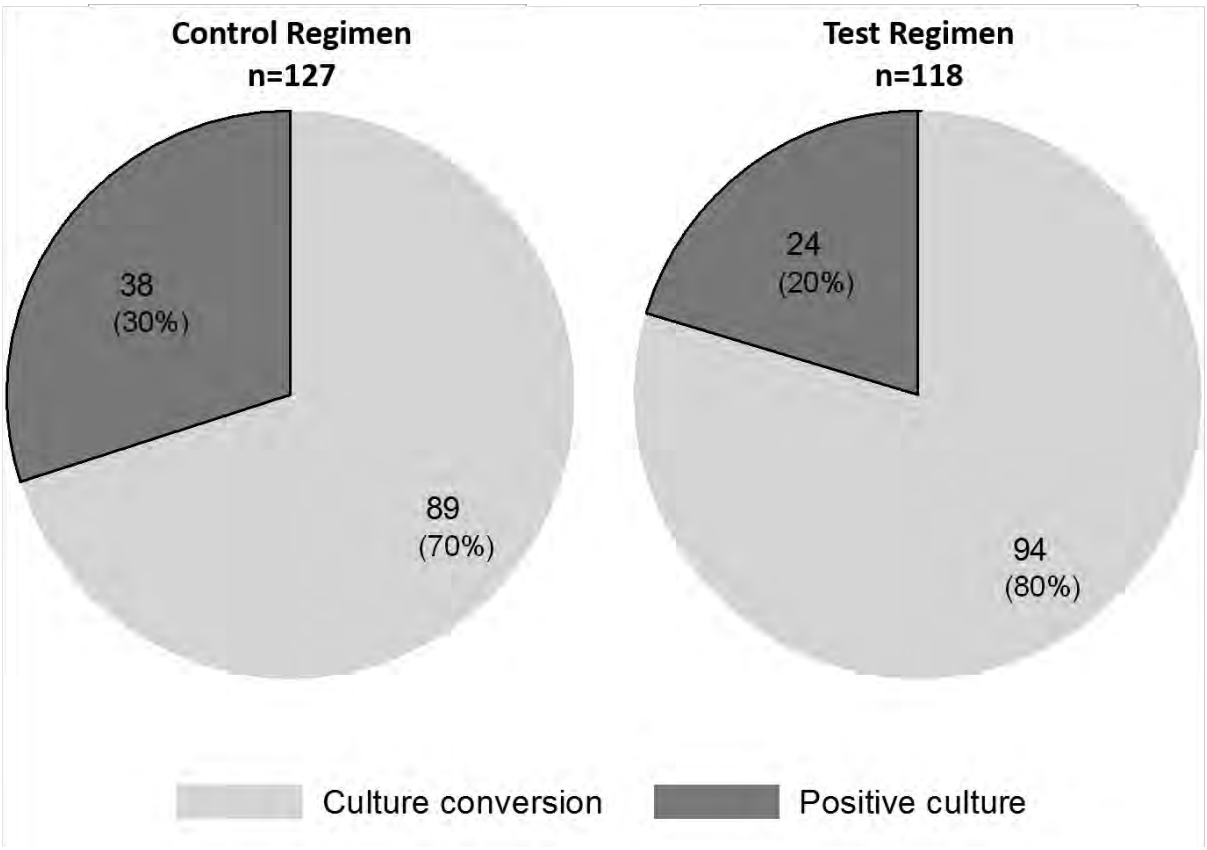

Figure 7.2 *Culture conversion rates at 2 months post treatment initiation for 245 patients randomized into the OFLOTUB pharmacokinetic sub-study. Culture conversion rates (n, (%)) are stratified by treatment regimen. Left hand plot represents culture conversion rates within the standard 6-month control regimen (n=127) receiving rifampicin, isoniazid, pyrazinamide and ethambutol (n=8 outcomes not available for culture assessment within the control regimen were excluded). The right hand plot represents culture conversion rates from 118 patients randomized to the 4-month test regimen where ethambutol was replaced with gatifloxacin (n=8 outcomes not available for culture assessment within the test regimen were excluded). Patients within the test regimen of the study achieved greater culture conversion rates (80%) compared to patients within the control regimen of the study (70%). Reasons for non-availability are summarized within Table 7.1.*

Patients in the control regimen, with rifampicin C_{MAX} >8.78 mg/L were 7.3 (95% CI: 1.6-32.6) times more likely to culture convert by 2 months when compared to patients failing to achieve this target. Patients in the control arm showed a significant exposure-response relationship with patients achieving the highest quartile of rifampicin AUC being 4.2 (95% CI: 1.4-12.9, Fisher's exact p=0.017) times more likely to culture convert than patients with rifampicin AUC in the lowest quartile (Figure 7.3). This relationship was not evident in the test arm. In the control regimen, rifampicin AUC and C_{MAX} were significantly greater (T-test, $p<0.05$ in both

cases) in patients who culture converted compared to those who did not achieve conversion at this time point.

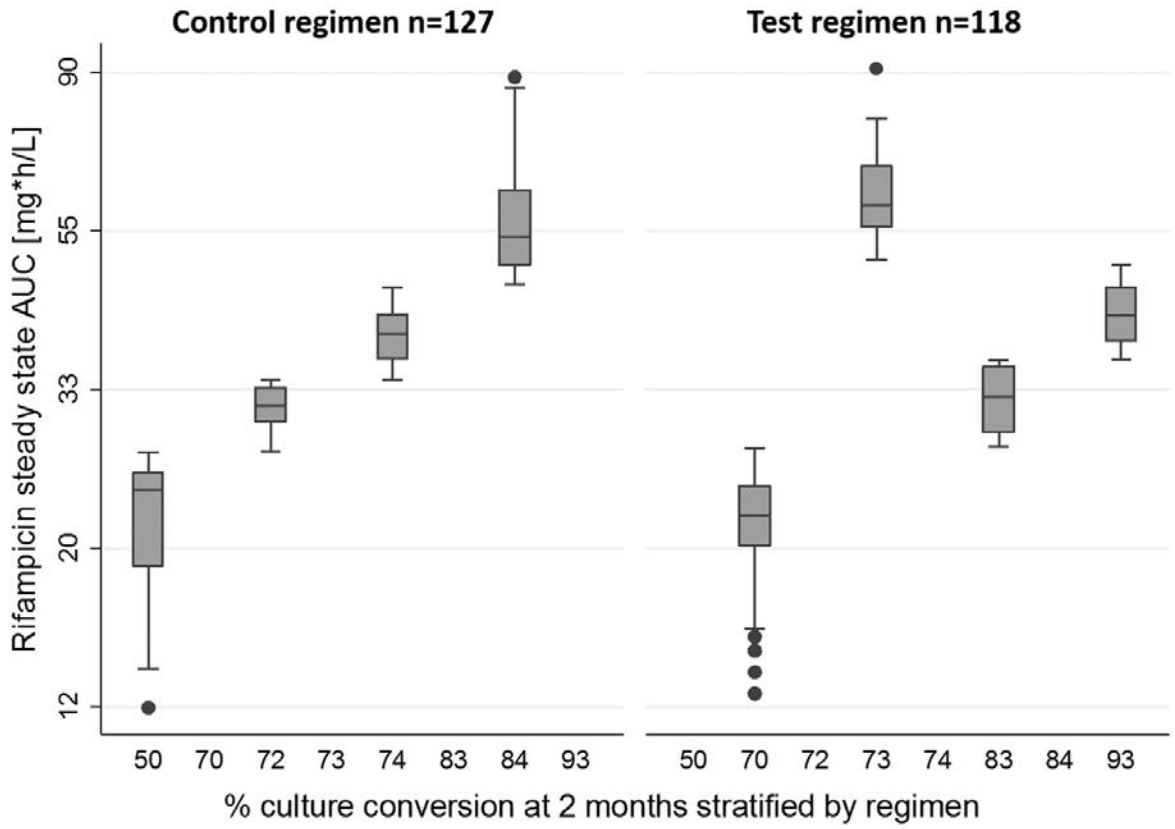

Figure 7.3 *Quartile plots, representing rifampicin 24-hour area under the steady state concentration–time curve (AUC) and their corresponding rates of culture conversion at 2 months for 245 patients stratified by treatment regimen. Only in the control regimen of the study (left hand panel), was a significant association observed between rifampicin concentration and outcome. This was reflected in patients with rifampicin AUC in the top quartile being 5.4 (95% CI: 1.7-17.6) times more likely to culture convert than those with rifampicin AUC in the lowest quartile.*

Patients in the favourable test regimen, however, were at greater risk of remaining culture positive at 2 months if they had high isoniazid exposures. Correspondingly, patients in this regimen were 5.2 (95% CI: 2.0-13.4) times more likely to culture convert if their isoniazid C_{MAX} $\leq$4.05 mg/L compared to patients with isoniazid C_{MAX} >4.05 mg/L. Patients in the test regimen with isoniazid AUC in the lowest quartile were 17 times more likely to culture convert compared to patients with isoniazid exposure in the top quartile (OR=17, 95% CI: 2-146,

Fishers exact p=0.011) (Figure 7.4). Patients with culture conversion at 2 months had significantly lower isoniazid AUC and C_{MAX} compared to patients having positive culture at 2 months in the test regimen (T-Test, $p<0.05$ in both cases). No significant correlation was observed between isoniazid exposure and 2-month outcome in the control regimen. No additional significant differences in AUC or C_{MAX} of the drugs were observed by 2-month outcome.

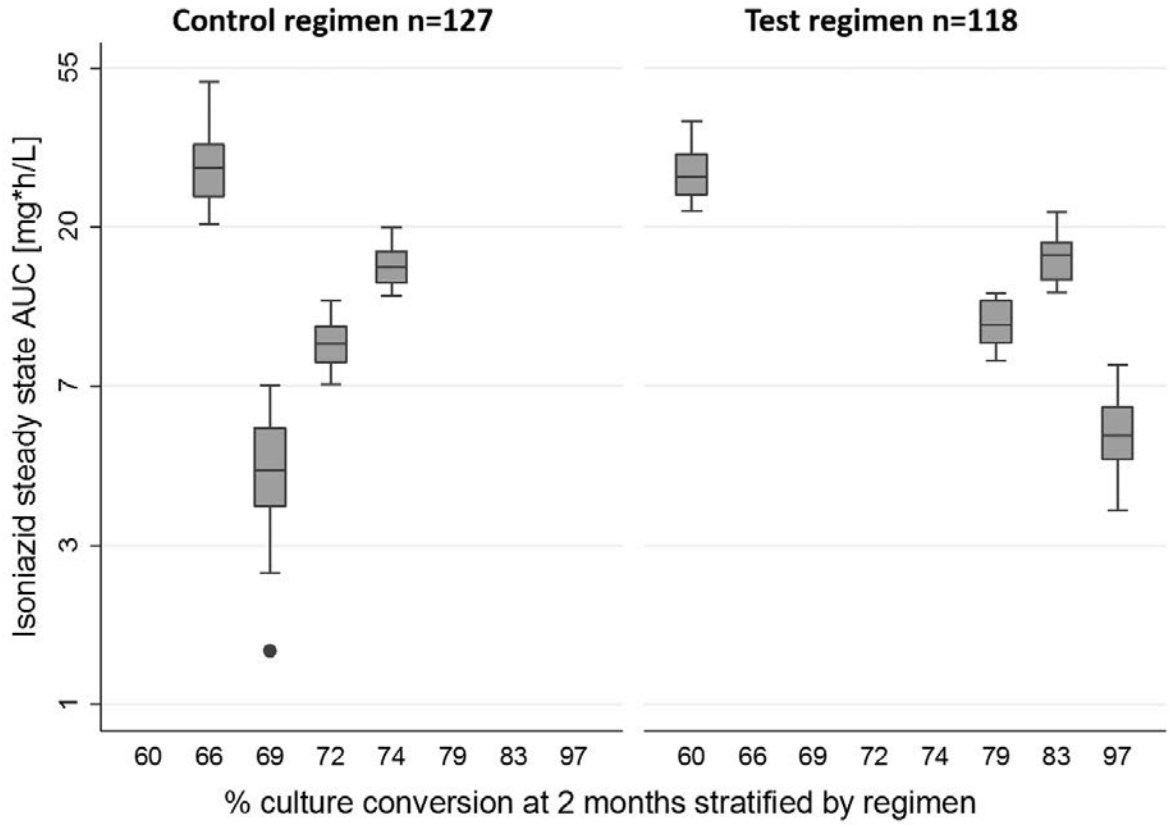

Figure 7.4 *Quartile plots, representing isoniazid 24-hour area under the steady state concentration–time curve (AUC) and their corresponding rates of culture conversion at 2 months for 245 patients stratified by treatment regimen. Only in the test regimen of the study (right hand panel), was a significant association observed between isoniazid concentration and outcome. This was reflected in patients with isoniazid AUC in the lowest quartile being 19.3 (95% CI: 2.3-161.6) times more likely to culture convert than those with isoniazid AUC in the top quartile.*

To examine the split driven by isoniazid C_{MAX} >4.05 mg/L in the test regimen, surrogates for this divide were investigated. isoniazid AUC, gatifloxacin $C_{MAX,}$ pyrazinamide C_{MAX} and AGE were identified by CART as the top four surrogates for the isoniazid C_{MAX} threshold of 4.05

mg/L. Applying this isoniazid C_{MAX} threshold, along with the top four surrogates (i.e. isoniazid AUC (24 mg·h/L), gatifloxacin C_{MAX} (4.6 mg/L), pyrazinamide C_{MAX} (51.1 mg/L) and AGE (42 years)), it was found that while patients achieving isoniazid C_{MAX} >4.05 mg/L were 5 times more likely to have positive culture at 2 months, the only surrogate for the isoniazid C_{MAX} threshold to predict the 2-month outcome was isoniazid AUC. This reflects the strong correlation between isoniazid C_{MAX} and AUC (r^2=0.81) and suggests that isoniazid exposure and not any of the other predictors are responsible for the observed split. When adjusting for surrogates in the final model, CART identified isoniazid and rifampicin C_{MAX} as predictors having relative variable importance scores above 80%, reaffirming the importance of rifampicin and isoniazid exposure (C_{MAX}) highlighted by the CART tree (Figure 7.1). In contrast, all remaining predictors had variable importance scores below 50%. As such, neither gatifloxacin AUC nor C_{MAX} were associated with outcome while AGE, BMI, HIV status, SEX, baseline sputum smear, lung zone and cavitation scored <5% indicating their lack of ability to predict culture conversion at 2 months.

24-month outcome

CART identified treatment regimen as the primary predictor for long term outcome followed by rifampicin and ethambutol in the control regimen and pyrazinamide and rifampicin in the test regimen (Figure 7.5). Patients randomized into the 6-month control regimen were classified as having favourable long term outcome compared to patients randomized to the 4-month gatifloxacin containing test regimen. Patients in the control regimen achieved 87% favourable outcome while patients in the test regimen achieved 82% favourable outcome 24 months post treatment completion (Figure 7.6).

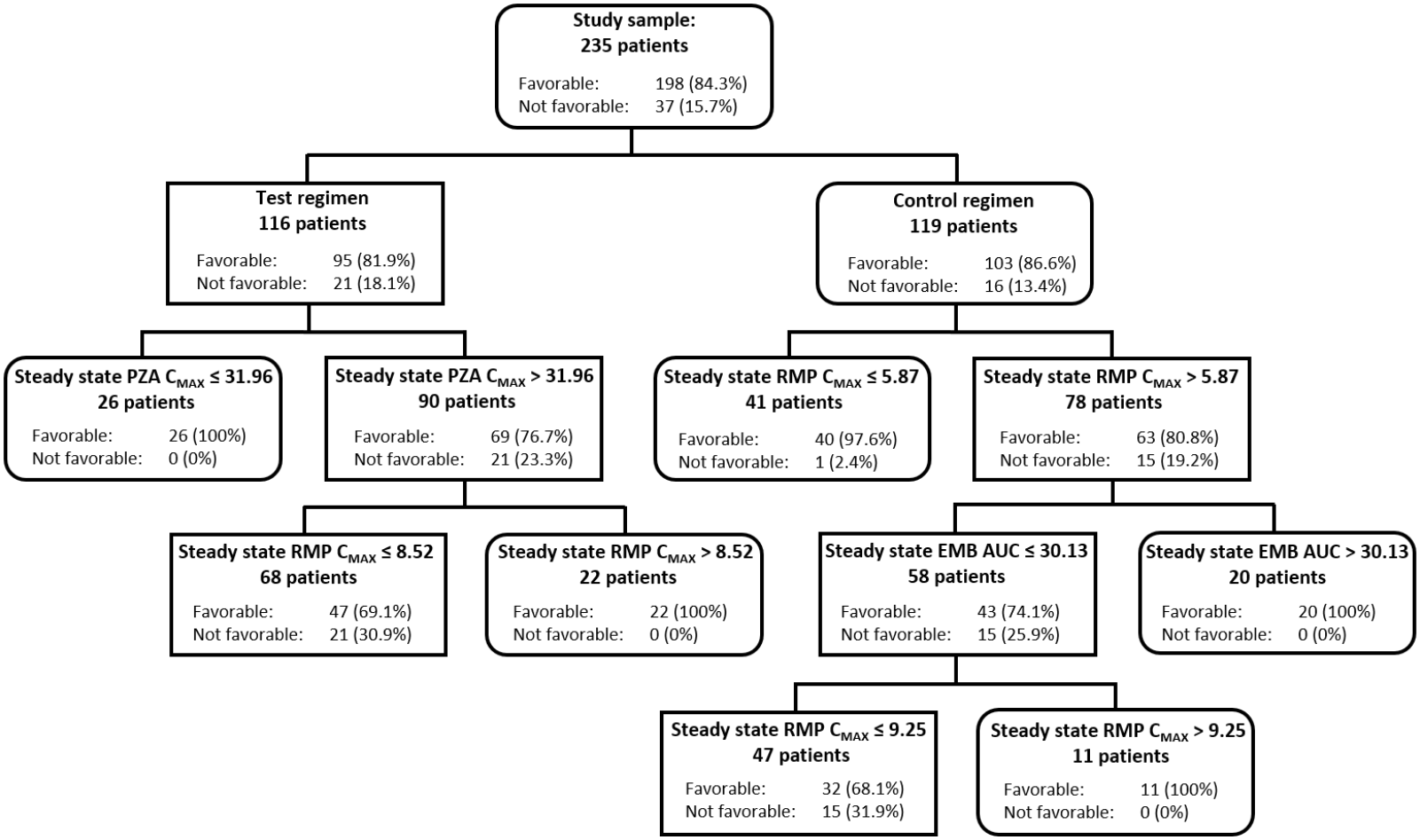

Figure 7. 5 *Variables predictive of long-term (24-month) outcome in 235 patients randomized into the OFLOTUB pharmacokinetic sub-study. Pharmacokinetic parameters, patient demographics and bacterial burden were examined in the initial models and decision trees. Treatment regimen was the primary predictor for long term outcome followed by pyrazinamide and rifampicin peak concentrations (C_{MAX}) within the 4-month gatifloxacin containing test regimen. Rifampicin C_{MAX} and ethambutol 24-hour area under the concentration–time curve (AUC) were most predictive of outcome in the 6-month control regimen. C_{MAX} and AUC cut-off concentrations were included within each node. The final decision tree correctly classified 63% & 73% of favourable and unfavourable outcomes respectively within the study population.*

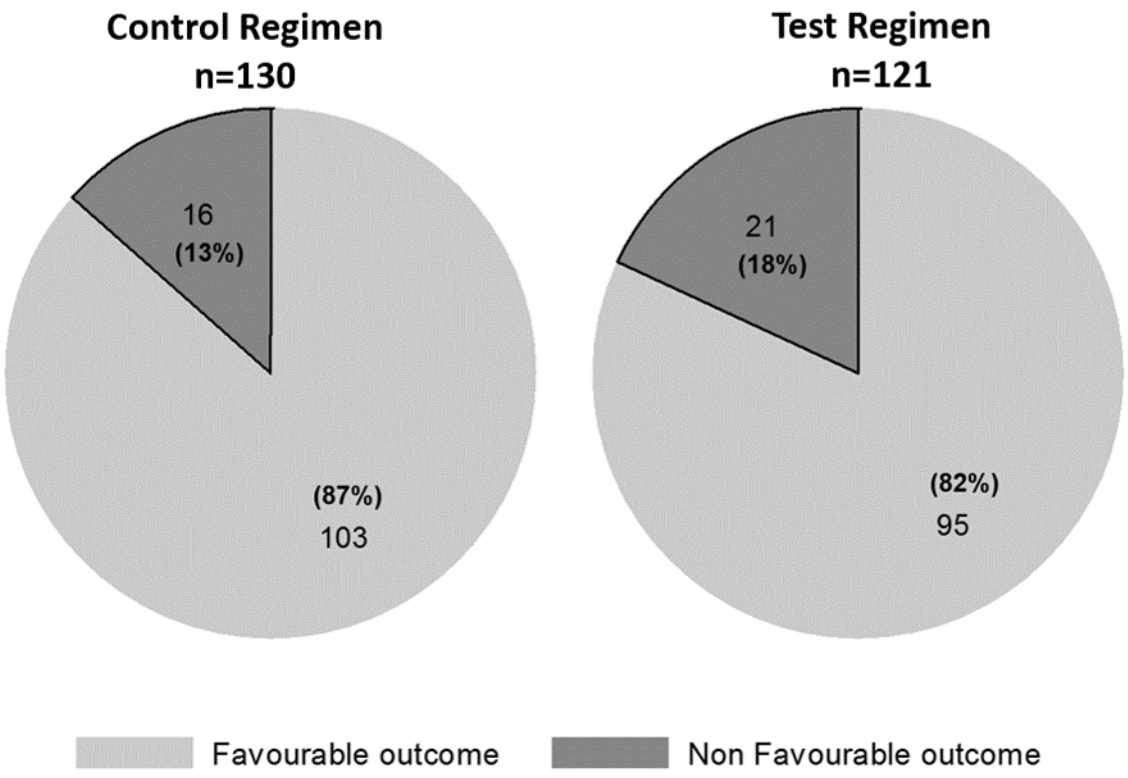

Figure 7.6 *Long term composite outcome rates for 235 patients randomized into the OFLOTUB pharmacokinetic sub-study. Outcome is defined at 24 months post treatment completion and stratified by treatment regimen. Left hand pie chart represents favourable and unfavourable rates in the standard 6-month control regimen representing 119 patients receiving 2 months of rifampicin, isoniazid, pyrazinamide and ethambutol followed by 4 months of rifampicin and isoniazid (n=15 outcomes not available for assessment in the control regimen were excluded). The right hand panel represents 24-month outcome rates from 116 patients randomized to the 4-month test regimen where ethambutol was replaced with gatifloxacin during the first 2 months followed by 2 months of rifampicin, isoniazid and gatifloxacin (n=10 outcomes not available for assessment in the test regimen were excluded). Reasons for non-availability are summarized in Table 6.2.*

CART identified that in the control regimen, rifampicin C_{MAX} $\leq$5.87 mg/L was the primary selector for favourable outcome. However, patients with C_{MAX} >5.87 mg/L, still achieved favourable outcome under two conditions, firstly if ethambutol AUC>30.13 mg·h/L or alternatively if ethambutol was $\leq$30.13 mg·h/L but rifampicin C_{MAX} >9.25 mg/L. This suggests that patients with high ethambutol AUC (i.e. $\leq$30.13 mg·h/L) or high rifampicin C_{MAX} (i.e. >9.25 mg/L) are able to overcome the risk of poor outcome associated with rifampicin C_{MAX} between 5.87 and 9.25 mg/L. Patients in the control regimen were 9.5 (95% CI: 1.2-74.9) times more likely to achieve favourable 24-month outcome if rifampicin C_{MAX} was $\leq$5.87 mg/L compared

to those with rifampicin exposure above this threshold. Notably, patients with rifampicin C_{MAX} exceeding this threshold, were equally likely to achieve good outcome if ethambutol AUC >30.13 mg·h/L (95% CI: 0.03-16.89, z=0.252, p>0.05) or if ethambutol AUC $\leq$30.13 mg·h/L but rifampicin C_{MAX} >9.25 (95% CI: 0.04-30.79, z=0.0.96, p>0.05). Notably, no clinical patient characteristics (age, sex and BMI) nor baseline bacterial burden (baseline lung zone, sputum smear & cavitation) were found to explain the poor outcome of patients with intermediate rifampicin C_{MAX} (>5.87 and <9.25 mg/L), although this group included a lower proportion of HIV co-infected patients in comparison to those with rifampicin C_{MAX} <5.87 mg/L (χ^2=4.16, p<0.05).

Within the test regimen, CART identified pyrazinamide C_{MAX} as the primary driver for favourable outcome. Patients with pyrazinamide C_{MAX} $\leq$31.96 mg/L were 16.4 times more likely to have a favourable outcome than those with higher pyrazinamide C_{MAX} (CI: 1.0-280.4, Fisher's exact p=0.035). Patients with pyrazinamide C_{MAX} >31.96 mg/L were, however, equally likely to achieve favourable outcome if rifampicin C_{MAX} >8.52 m/L (CI: 0.02-61.79, z=0.081, p>0.05). Correspondingly, patients in the test regimen were 5.1 (95% CI: 1.0-26.8, 1-sided Fisher's exact p=0.0393) times more likely to have favourable outcome given their pyrazinamide AUC or C_{MAX} was in the lowest quantile vs. patients with pyrazinamide AUC or C_{MAX} in the top quantile (Figure 6.7). Consistently, patients in the test regimen with favourable long term outcome at 24 months had significantly lower pyrazinamide AUC and C_{MAX} compared to those with poor outcome at this time point (p<0.05, in both cases).

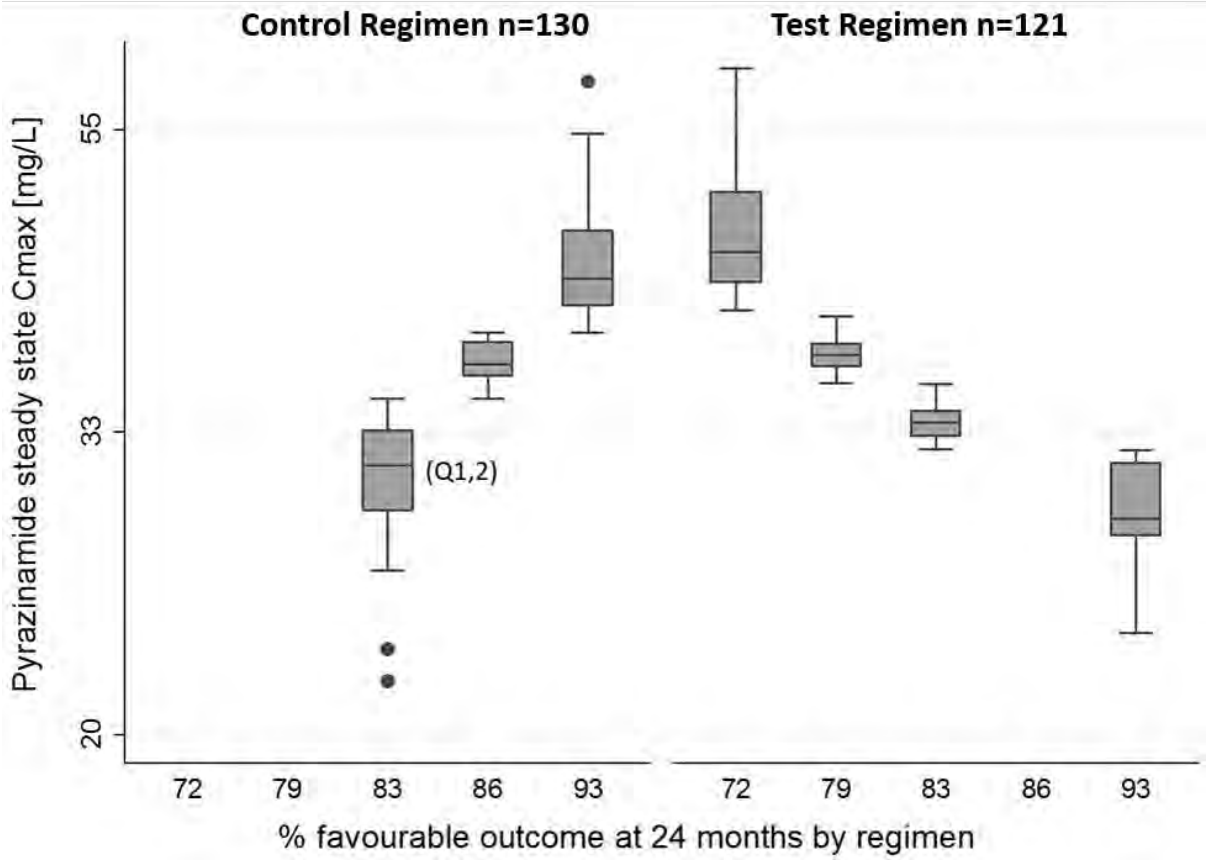

Figure 7.7 *Quartile plots of pyrazinamide steady state peak concentration (C_{MAX}) and their corresponding rates of long term outcome in 235 patients randomized into the OFLOTUB pharmacokinetic sub-study. Quartiles of pyrazinamide C_{MAX} and their corresponding 24-month outcome rates are stratified by treatment regimen. Although higher pyrazinamide exposure appeared to correlate with more favourable long-term outcome in the control regimen of the study, higher pyrazinamide exposures were significantly associated with poorer outcome in the test regimen. Patients in the test regimen were 5.1 times (95% CI: 1.0-26.8, Fisher's exact p=0.039) more likely to have favourable outcome given their pyrazinamide C_{MAX} was in the 1st quartile vs. patients with pyrazinamide C_{MAX} in the top quartile. 'Q1,2' represents the 1st and 2nd quartiles of pyrazinamide C_{MAX} in the control regimen.*

To examine the unexpected split driven by pyrazinamide C_{MAX} >31.96 mg/L in the test regimen, surrogates for this split were investigated. Pyrazinamide AUC, rifampicin C_{MAX} and gatifloxacin C_{MAX} were identified by CART as the top three surrogates for the pyrazinamide C_{MAX} cut-off of 31.96 mg/L. Applying this pyrazinamide C_{MAX} threshold, along with the top three surrogates (i.e. pyrazinamide AUC (286 mg·h/L), rifampicin C_{MAX} (4.2 mg/L) and gatifloxacin C_{MAX} (2.7 mg/L)), it was found that while patients achieving pyrazinamide C_{MAX} >31.96 mg/L were 16 times more likely to have poor long term outcome at 24 months, none of the three surrogates for the pyrazinamide C_{MAX} threshold predicted the 24-month

outcome. This indicates that the split is unlikely driven by predictors other than pyrazinamide exposure (C_{MAX}) in the data set.

Adjusting for surrogates in the final CART model, clinical patient characteristics (e.g. age, BMI, HIV status and sex) along with baseline bacterial burden (baseline lung zone, sputum smear & cavitation) contributed little to the prediction of long term outcome, scoring a relative variable importance of <1%. Notably, gatifloxacin exposure at the 24-month outcome contributed less than 5% towards the relative variable importance score with a corresponding lack of association between gatifloxacin AUC or C_{MAX} and the 24-month outcome.

When replacing the composite 24-month long term outcome with microbiological failure (MBF) (defined as the composite of treatment failure and relapse), CART produced a very similar predictive tree (Figure 7.8). While predictors in the test regimen illustrated the same pattern, with pyrazinamide $C_{MAX} \leq 32.07$ mg/L and rifampicin $C_{MAX} > 8.52$ mg/L selecting for favourable outcome, no further predictors of favourable outcome were identified in the control regimen.

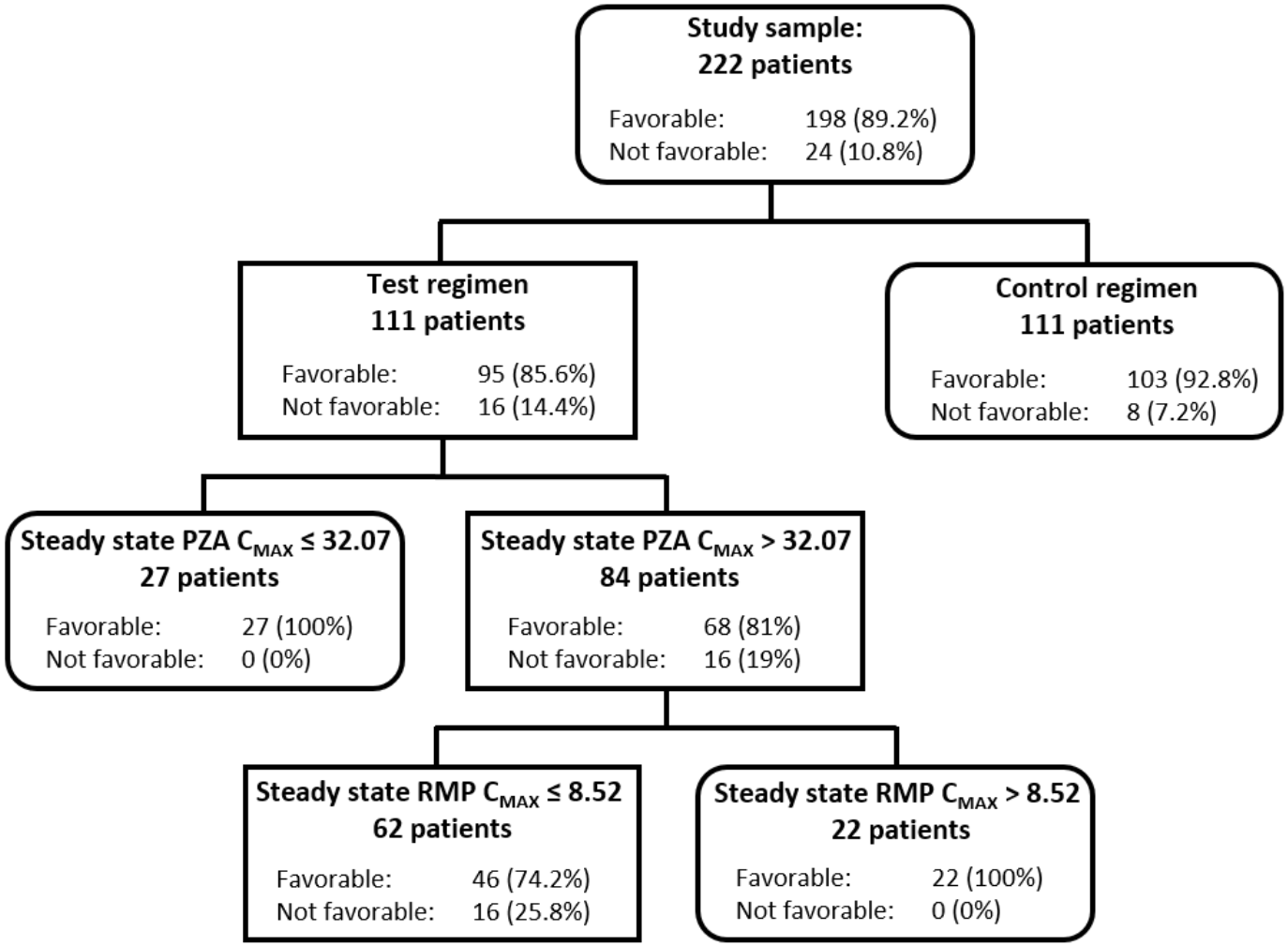

Figure 7.8 *Variables predictive of microbiological failure (MBF) in 222 patients randomized into the OFLOTUB pharmacokinetic sub-study. Pharmacokinetic parameters, patient demographics and bacterial burden were examined in the initial models and decision trees. Treatment regimen was the primary predictor for MBF followed by pyrazinamide and rifampicin peak concentrations (C_{MAX}) within the 4-month gatifloxacin containing test regimen. The 6-month control regimen was not further split by any predictors.*

Culture conversion rates at 2 months did not predict favourable outcome at 24 months (OR=1.8, 95% CI: 0.8-4.1). However, 2-month culture conversion rates significantly predicted MBF at 24 months. Patients failing to culture convert at 2 months were 2.9 (95% CI: 1.2-7.0) times more likely to have MBF when compared to patients who culture converted by this time point.

7.2. Discussion

2-month outcome

CART identified treatment regimen as the top predictor for 2-month culture conversion. Culture conversion rates of 80% were observed in patients randomized into the 4-month gatifloxacin containing test regimen. Similar conversion rates of 77% and 84% were observed in the gatifloxacin containing regimens of the OFLOTUB phase II and phase III studies respectively (Rustomjee et al. 2008; Merle et al. 2014). Indeed, *in vitro* and murine studies demonstrated that gatifloxacin has potent bactericidal activity against *M. tuberculosis* hence its inclusion within pulmonary tuberculosis treatment regimens (Paramasivan et al. 2005; Cynamon et al. 2007). Accordingly, patients randomized into the 4-month gatifloxacin containing test regimen were approximately twice as likely to culture convert at 2 months as patients receiving the standard 6-month control regimen. Unexpectedly, patients with elevated isoniazid exposure (in the top quartile) achieved significantly lower culture conversion rates compared to patients with isoniazid exposures in the 1st quartile. Antagonism between moxifloxacin and rifampicin, demonstrated in a murine study (Balasubramanian et al. 2012) and within hollow-fiber system model experiments (Drusano et al. 2010) might to explain the lack of an exposure-response relationship for rifampicin in the gatifloxacin containing test regimen. Similarly, isoniazid antagonism on the activity of the combination of pyrazinamide and rifampicin observed in murine studies (Grosset et al. 1992; Almeida et al. 2009b) may explain the isoniazid exposure-response observed in the gatifloxacin containing test regimen. Conceivably, we only observe the antagonistic activity of isoniazid in patients randomised into the gatifloxacin containing test regimen due to rifampicin's activity being compromised by combination with a fluoroquinolone in this regimen. The exact mechanism responsible for the unanticipated exposure-response profiles

is uncertain and requires further investigation of the bactericidal effect of drug regimens including a combinations of the drugs. Interestingly, Drusano and colleagues using their hollow fiber infection model, demonstrated the combination of moxifloxacin and rifampicin synergistic for resistance suppression but antagonistic for cell kill (Drusano et al. 2010). In our study, exposure-response profiles of rifampicin, pyrazinamide and isoniazid in patients receiving the test regimen, suggest synergism for culture conversion at low drug exposures while antagonism was observed at higher exposures.

Elevated rifampicin exposure predicted culture conversion in the control regimen of our study, where patients were approximately 7 times more likely to culture convert given their rifampicin C_{MAX} $\geq$8.78 mg/L. *In vitro* studies have indeed demonstrated rifampicin concentration dependent killing of *M. tuberculosis* (Gumbo et al. 2007a) along with clinical studies demonstrating greater microbial killing following exposure to higher rifampicin concentrations (Boeree et al. 2015). A similar rifampicin C_{MAX} threshold of 8.2 mg/L predicted culture conversion at 2 months in patients receiving the standard 6-month regimen (Chigutsa et al. 2015). Equally, the suggested 8 mg/mL cut-off suggested by Peloquin (2002) was in agreement with our suggested threshold. However, the proposed cut-off of 6.6 mg/mL by Pasipanodya and colleagues appeared low (Pasipanodya et al. 2013). A likely explanation for the relatively low rifampicin C_{MAX} threshold identified in their study could be due to several factors including the high pyrazinamide exposure in their study population relative to ours. The median (range) pyrazinamide C_{MAX} in our study, in relation to the 2-month outcome, was approximately 35 (22-62) mg/L while the median (range) in the Pasipanodya et al. study was approximately 50 (1-90) mg/mL. Additionally, the median (range) rifampicin AUC in our study was approximately 33 (13-87) mg·h/L while the median (range) in their study was approximately 15 (0-45) mg·h/L. This discrepancy in drug exposure is also likely the reason why pyrazinamide and not rifampicin exposure was the primary predictor for culture conversion in their study. Notably, only 4 of 130 subjects in the control regimen of our study achieved pyrazinamide C_{MAX} above the threshold of 58.3 mg/L suggested by (Pasipanodya et al. 2013). As a result of bactericidal synergism between rifampicin and pyrazinamide (Mitchison and Davies 2012), elevated pyrazinamide exposure likely compensates for the identification of the relatively low rifampicin C_{MAX} threshold of 6.6 mg/L predicting culture conversion. Bactericidal synergism between rifampicin and pyrazinamide was similarly

demonstrated by (Chigutsa et al. 2015) whereby the odds of culture conversion increased significantly from 3.8 to 6.0 when comparing patients that attained the rifampicin threshold with those that achieved this threshold in addition to elevated pyrazinamide exposure. In the present study, patients in the control regimen were 5 times more likely to achieve culture conversion given their rifampicin exposure was in the top quartile relative to patients having exposure below the 25th percentile. Although bactericidal synergism between rifampicin and pyrazinamide has been reported by others (Zhang and Mitchison 2002; Ahmad et al. 2011; Chigutsa et al. 2015) this study failed to detect it.

24-month outcome

CART identified treatment regimen as the primary predictor for the 24-month outcome with 87% of patients achieving favourable outcome in the 6-month control regimen vs. 82% in the 4-month gatifloxacin containing test regimen. Overall, extreme ranges of rifampicin exposure (i.e. C_{MAX} $\leq$5.87 mg/L and. >9.25 mg/L) and raised ethambutol exposure predicted favourable long term outcome in the control regimen, while low pyrazinamide and raised rifampicin exposure predicted favourable outcome in the test regimen. Indeed, results from the PanACEA study demonstrate the ability of elevated rifampicin exposures to increase the sterilizing ability of a regimen including standard doses of ethambutol, pyrazinamide and isoniazid (Boeree et al. 2015). Applying a peak concentration reference range (Alsultan and Peloquin 2014), an abysmal 70% of patients in the control regimen of our study achieve rifampicin peak concentration below 8 mg/L (Chapter 6). These findings strongly suggest the need to increase rifampicin exposure for improved long term outcome. Against this background, the favourable long-term outcome observed in patients in the control regimen with rifampicin exposure $\leq$5.87 mg/L was unexpected and the driver of this pattern remains unclear. This finding could however be due to unmeasured confounders incorporated within the composite outcome, as there were fewer MBF in this arm compared to the test regimen. Raised ethambutol exposure improved long term outcome in this study. Indeed the ability of increased ethambutol exposure to improve the sterilizing activity of the standard regimen has been noted before (Chigutsa et al. 2015). However, in contrast to the present study, this ability was only observed in patients with low rifampicin exposure. Differences in outcome

could, however, be due to the contrasting use of liquid and solid culture medium between the two studies (Boeree et al. 2015; Moreira et al. 2015) but highlights that much is still unclear about the interactions between these drugs. Interestingly, while ethambutol has bactericidal activity when dosed as monotherapy (Jindani et al. 2003) it has been shown to antagonise the sterilising ability of rifampicin and the combination of rifampicin and isoniazid (Dickinson et al. 1977; Jindani et al. 2003). Indeed, higher relapse rates have been observed in patients receiving drug regimens containing ethambutol *vs* those without this drug (Hong Kong Chest Service / British Medical Research Council 1982). Nonetheless, antagonism was not observed in the current study.

CART classified patients randomized into the 4-month gatifloxacin containing test regimen having unfavourable long term composite outcome. Our results were in agreement with the parent phase III study (Merle et al. 2014) demonstrating higher proportions of relapse in the test regimen compared to the control regimen. Indeed, patients randomized into the test regimen of our sub-study were three times more likely to relapse (culture positive post treatment cure) compared to patients in the control regimen (OR=3.4, 95% CI: 1.2-9.6, Fisher's exact p=0.019). The sterilizing role which rifampicin and pyrazinamide possess in the standard tuberculosis treatment regimen is well known (Mitchison 2000). Compromise to either drugs sterilizing ability would likely result in patients having poor outcome as demonstrated by Chideya et al. (2009) where patients with low pyrazinamide C_{MAX} were three times more likely than patients with normal pyrazinamide C_{MAX} to have poor treatment outcome. Unexpectedly, in the test regimen of this study, patients with raised pyrazinamide exposure (C_{MAX} >31.96 mg/L), were 16 times more likely to have unfavourable outcome when compared to patients with pyrazinamide exposure below this threshold. Indeed, pyrazinamide exposure was significantly higher in patients having unfavourable long term outcome compared to patients having favourable outcome. Respectively, patients achieving pyrazinamide exposure (AUC or C_{MAX}) in the 1st quartile were 5 times more likely to have favourable outcome compared to patients with drug exposure above the 75th percentile. Clearly this significant exposure-response relationship was unusual and requires investigation for potential surrogate effects. Pyrazinamide AUC, rifampicin C_{MAX} and gatifloxacin C_{MAX} were identified by CART as the top three surrogates for the pyrazinamide C_{MAX} threshold. All three surrogates failed to predict the 24-month outcome suggesting elevated pyrazinamide C_{MAX}

predictive for poor 24-month outcome in the test regimen. No additional significant exposure-response relationship was identified between rifampicin, isoniazid, ethambutol nor gatifloxacin and the 24-month outcome. Notably, *in vitro* studies have demonstrated gatifloxacin's limited ability to add to the sterilizing activity of rifampicin and isoniazid and consequently suggested its possible failure to shorten the duration of present treatment regimens (Paramasivan et al. 2005). Similarly, a murine study demonstrated moxifloxacin to add minimal sterilizing effect to the standard regimen (Nuermberger et al. 2004). Furthermore, moxifloxacin was demonstrated having poor penetration into necrotic lung lesions where persisting bacilli reside (Prideaux et al. 2015) potentially explaining its inability to shorten the duration of tuberculosis treatment in recent clinical trials (Gillespie et al. 2014; Jindani et al. 2014). In our study, it appears as though pyrazinamide's sterilizing ability in the gatifloxacin containing test regimen was antagonized, resulting in higher proportions of patients having unfavourable long term outcome compared to patients in the control regimen.

Although culture conversion at 2 months fails to predict the composite 24-month long term outcome, it does predict MBF at this time point. The fact that the CART models predicting outcome were similar in the test regimen for the 24-month and MBF outcomes but not in the control regimen, suggests that the influence of MBF in the composite outcome predominates in the test regimen but not in the control arm. This is mirrored in the test arm having three times the relapse rate and suggests that 2-month culture conversion rates could reflect the sterilising ability of treatment. This higher rate of relapse in the test regimen enabled better statistical resolution of drug effects when compared to the control regimen where CART was unable to identify further predictors of MBF. Although applied as the gold standard for assessing sterilising activity of tuberculosis treatment (Mitchison 1993), the value of 2-month culture conversion as a surrogate marker for relapse rate is controversial (Burman 2003; Perrin et al. 2007).

Study limitations

CART is a data dependent modelling tool and relies on the integrity of the data used in the analysis. PK data incorporated in this analysis was collected approximately 1 month into

therapy while outcome measures were defined either 2 months following the start of treatment or 24 months post treatment completion. Additionally, PK data was collected during the intensive phase of treatment, hence the PK effect of the continuation phase of treatment could not be directly related onto the long term outcome. MIC data was not available in our sub-study, hence the typical PK/PD index of AUC/MIC was not applied as it was for other studies investigating exposure-response profiles for rifampicin, pyrazinamide, isoniazid, ethambutol and gatifloxacin and tuberculosis treatment outcome (Thwaites et al. 2011; Chigutsa et al. 2015).

7.3. Conclusion

In tuberculosis patients on a standard regimen, measures of rifampicin exposure better predict culture conversion and long term outcome than patient clinical characteristics (AGE, BMI, SEX and HIV status) and baseline indicators of bacterial burden (cavitation, sputum smear, and lung zone). Increased rifampicin exposure predicts culture conversion in the control regimen, where patients are approximately 7 times more likely to culture convert given their rifampicin peak concentrations exceed 8.78 mg/L. Consistent with OFLOTUB phase II and III study findings, our study demonstrated improved 2-month culture conversion rates in the 4-month test regimen when compared to the standard 6-month control regimen. Although replacement of ethambutol with gatifloxacin improved 2-month culture conversion rates, the sterilizing ability of the gatifloxacin containing test regimen was diminished such that patients experienced three times more relapse by 24 months when compared with patients on the standard regimen. CART identified the usual sterilizing ability of pyrazinamide to be antagonised in patients receiving the gatifloxacin containing test regimen, such that patients were 16 times more likely to have favourable long-term outcome given their pyrazinamide peak concentration was equal to or below 31.96 mg/L. Patients with pyrazinamide peak concentrations above 31.96 mg/L were, however, equally likely to achieve favourable outcome given their rifampicin peak concentrations exceeded 8.52 mg/L. Notably, gatifloxacin exposure (AUC or C_{MAX}) was not significantly associated with either short- or long-term outcome in our study. Overall the role of rifampicin exposure in culture conversion (a proxy for bacterial kill) is consistent with HFS experiments and clinical studies. Thus, for

shortening therapy, the background regimen needs to be dose optimized prior to the addition of companion drugs.

8. Synthesis

Tuberculosis remains one of the most pressing health challenges worldwide with Africa reported having the highest burden of the disease in 2014. Improving patient adherence to treatment remains a primary challenge to managing the disease as nonadherence to treatment likely results in treatment failure, relapse and increased emergence of drug-resistant tuberculosis. The OFLOTUB phase III study investigated the safety and efficacy of a shortened 4-month gatifloxacin containing regimen compared to the standard 6-month control regimen. A total of 343 adults that were enrolled in Benin, Guinea, Senegal, and South Africa were randomized to receive rifampicin, isoniazid, pyrazinamide, and ethambutol in the standard 6-month control regimen or the 4-month test regimen where gatifloxacin replaced ethambutol. The shortened 4-month regimen was expected to improve patient adherence to treatment and reduce emergence of resistance. Drug–drug interactions affecting both gatifloxacin and rifampicin concentration were, however, identified when gatifloxacin was dosed with rifampicin, isoniazid, and pyrazinamide in a single dose study highlighting the requirement to investigate the regimens pharmacokinetics at steady state. Furthermore, several authors have demonstrated drug concentration to be an important predictor for clinical outcome. Despite the high burden of disease, pharmacokinetic characterisation of antituberculosis drugs remains limited in the African population. As such, this thesis aimed to characterise population pharmacokinetic / pharmacodynamic relationships in pulmonary tuberculosis infected African adult patients participating in the phase III OFLOTUB study. All these objectives were achieved by (1) developing a semi-mechanistic pharmacokinetic-enzyme turn-over model to describe autoinduction of rifampicin's metabolism (2) evaluating the population pharmacokinetics and dose of gatifloxacin at first dose and steady state when dosed with rifampicin, isoniazid, and pyrazinamide using Monte Carlo simulations (3) characterising the population pharmacokinetics of rifampicin, isoniazid, pyrazinamide, and ethambutol and investigate potential drug-drug interactions and lastly (4) identify factors predictive of 2-month culture conversion or 24-month long-term composite outcome. Key findings of each chapter are discussed below, as are the recommendations that emanate from this body of work.

8.1. A semimechanistic pharmacokinetic-enzyme turnover model to explain rifampicin autoinduction in adults with tuberculosis

The currently recommended doses of rifampicin are believed to be at the lower end of the dose-response curve. Rifampicin induces its own metabolism, although the effect of dose on the extent of autoinduction was not known at the start of this study. Accordingly, this chapter aimed to investigate rifampicin autoinduction in 174 patients receiving the standard 6-month regimen using a semimechanistic pharmacokinetic-enzyme turnover model. Additionally, the influence of different scaling methods on a covariate selection procedure was assessed using four basic structural models. The final model included allometric scaling with *NFM* applied to clearance and apparent volume of distribution, although the low estimates of fat mass (*Ffat*) suggest *FFM* as a better descriptor of size than total weight. Although HIV infection was associated with a 30% increase in the apparent volume of distribution, simulations demonstrated the effect of HIV on rifampicin exposure (AUC) to be clinically negligible. Model-based simulations showed close-to-maximum induction achieved after 450 mg daily dosing, since negligible increases in clearance were observed following the 600 mg/day regimen. Thus, this model predicts that dosing above 600 mg/day is unlikely to result in higher magnitudes of autoinduction. In a typical 55 kg male without HIV infection, clearance, which was 7.76 L/h at the first dose, increased 1.82- and 1.85-fold at steady state after daily dosing with 450 and 600 mg, respectively. Corresponding reductions of 41% and 42%, respectively, in the area under the concentration-versus-time curve from 0 to 24 h were estimated. The turnover of the inducible process was estimated to have a half-life of approximately 8 days in a typical patient. Assuming 4 to 5 half-lives to steady state, this corresponds to a duration of approximately 32 to 40 days to reach the fully induced state for rifampicin autoinduction.

8.2. Assessment of first dose and steady-state gatifloxacin pharmacokinetics and dose in patients with pulmonary tuberculosis through the use of Monte Carlo simulations

A prior single-dose study found that gatifloxacin exposure increased by 14% when dosed together with rifampicin, isoniazid, and pyrazinamide. Thus, this chapter evaluated the first dose and steady-state pharmacokinetics of gatifloxacin when daily doses were given to patients with newly diagnosed drug-sensitive pulmonary tuberculosis as part of a

combination regimen including rifampicin, isoniazid, and pyrazinamide. Furthermore, gatifloxacin dose was evaluated with respect to the probability of attaining a suggested PK/PD target (free fraction of gatifloxacin AUC over MIC (*f*AUC/MIC)) using Monte Carlo simulations. Population pharmacokinetics of gatifloxacin was described from first dose to a median of 28 days in 169 adults randomized into the test regimen of the OFLOTUB pharmacokinetic sub-study. Simulations revealed that 400 mg/day achieves effective exposure in more than 90% of patients only for MTB strains with MIC<0.125 mg/L, suggesting higher gatifloxacin doses for optimal outcome. The median AUC of 41.2 mg·h/L at first dose decreased on average by 14.3% following multiple 400 mg daily doses. However, this difference was modest when compared to the large inter-occasion variability in clearance and bioavailability suggesting the reduction in exposure is unlikely to be of clinical significance. It was concluded that systemic exposure to gatifloxacin declines with repeated daily 400 mg doses when used together with rifampicin, isoniazid and pyrazinamide, possibly compensating for any initial elevation in gatifloxacin levels due to a drug interaction observed in a prior single dose interaction study.

8.3. Population pharmacokinetics of first-line tuberculosis drugs in patients enrolled into the OFLOTUB phase III sub-study

Applying nonlinear mixed effects modelling, this chapter characterized rifampicin, isoniazid, pyrazinamide, and ethambutol pharmacokinetics in a large cohort of 343 African patients randomized into the OFLOTUB pharmacokinetic sub-study. Chapter 4 characterized the pharmacokinetics of gatifloxacin in test arm patients. The effect of body size was described using allometric scaling, and, among other covariates, the effect of HIV status and treatment regimen were investigated. First-order elimination and transit absorption compartments characterised the kinetics of all four drugs. Isoniazid and ethambutol were described by two-compartment disposition models, while pyrazinamide and rifampicin by one-compartment models. The median steady state peak concentration for rifampicin, isoniazid, pyrazinamide, ethambutol and gatifloxacin was respectively estimated at 6.5, 3.3, 35.8, 3.2 and 3.8 mg/L. Consistent with literature findings, approximately 73.0, 43.0, 0.3, 6.0 and 0.0% of patients failed to achieve previously reported target concentrations for rifampicin, isoniazid, pyrazinamide, ethambutol, and gatifloxacin, respectively. Despite 73% and 43% of patients

having low rifampicin and isoniazid peak concentrations respectively, similar drug exposures in terms of AUC and C_{MAX} were reported in other African studies. The study identified a single drug-drug interaction where the rifampicin absorption rate was significantly reduced when dosed together with gatifloxacin, isoniazid, and pyrazinamide. Consequently, patients in the gatifloxacin containing test regimen had significantly reduced rifampicin C_{MAX}'s when compared to those in the standard 6-month control regimen although the AUC remained comparable across treatment regimen. Similarly, HIV co-infected patients were more likely to have rifampicin C_{MAX} <8 mg/L when compared to those without HIV coinfection, despite having comparable AUC. Accordingly, HIV co-infected patients in the test regimen of the study were identified having low rifampicin exposure with only 11% achieving rifampicin C_{MAX} >8 mg/L threshold compared to 29% in the remainder of patients. The prevalence of low rifampicin and isoniazid C_{MAX} in our study population was of concern and hence required characterisation of the exposure-response relationships to confirm clinical significance.

8.4. Predictors of culture conversion and long term outcome in African patients treated for drug sensitive pulmonary tuberculosis

This chapter identified predictors for 2-month culture conversion rates and 24-month long term outcome in newly diagnosed African adult patients randomized into the OFLOTUB pharmacokinetic sub-study through the use of classification and regression tree analysis. Potential predictors of outcome included steady state AUC and C_{MAX} for rifampicin, isoniazid, pyrazinamide, ethambutol, and gatifloxacin, patient demographics (age, sex, BMI and HIV status) and baseline indicators of bacterial burden (cavitation, sputum smear, and lung zone). In tuberculosis patients on a standard regimen, measures of rifampicin exposure better predict culture conversion and long term outcome than patient clinical characteristics and baseline indicators of bacterial burden. Increased rifampicin exposure predicts culture conversion in the control regimen, where patients are approximately 7 times more likely to culture convert given their rifampicin C_{MAX} >8.78 mg/L. Our study confirmed improved 2-month culture conversion rates in the 4-month gatifloxacin containing test regimen when compared to the standard 6-month control regimen. Although replacement of ethambutol with gatifloxacin improved 2-month culture conversion rates, the sterilizing ability of the

gatifloxacin containing test regimen was diminished such that patients experienced three times more relapse by 24 months when compared with patients on standard regimen. Subsequently, CART identified patients receiving the gatifloxacin containing test regimen being 16 times more likely to have favourable long-term outcome given their pyrazinamide C_{MAX} was $\leq$31.96 mg/L suggesting the sterilizing ability of pyrazinamide may be compromised. Patients with pyrazinamide C_{MAX} >31.96 mg/L were, however, equally likely to achieve favourable outcome given their rifampicin C_{MAX} >8.52 mg/L highlighting the requirement for elevated rifampicin exposure to improve the sterilising ability of the test regimen. Notably, gatifloxacin exposure (AUC or C_{MAX}) was not significantly associated with either short- or long-term outcome in our study. Overall the role of rifampicin exposure in culture conversion (a proxy for bacterial kill) is consistent with HFS experiments and clinical studies. Thus, for shortening therapy, the background regimen needs to be dose optimized prior to the addition of companion drugs.

8.5. Overarching conclusions

This thesis contributed to a better understanding of the pharmacokinetic and pharmacodynamic characteristics of drugs commonly used to treat tuberculosis infected patients. As is typical of doctoral theses it has generated numerous hypotheses that when pursued will provide even greater insight in the field. It was found that gatifloxacin concentrations did not accumulate following multiple dosing together with rifampicin, isoniazid, and pyrazinamide as much as it was the initial concern following observations from a single dose interaction study. The current pharmacokinetic study, however, identified a drug-drug interaction resulting in significantly reduced rifampicin peak concentrations in patients receiving the gatifloxacin containing test regimen compared to those on standard regimen although the AUC remained comparable across regimen. Similarly, HIV co-infected patients had significantly reduced rifampicin peak concentrations resulting in HIV co-infected patients in the test regimen of the study being 3 times more likely to have concentrations below the 8 mg/L threshold compared to all other patients. In tuberculosis patients on a standard regimen, increased rifampicin exposure better predicted culture conversion and long-term outcome than patient clinical characteristics and baseline indicators of bacterial

burden. Furthermore, the rifampicin enzyme turn-over model suggested increased rifampicin doses unlikely to result in higher magnitudes of autoinduction. In the gatifloxacin-containing test regimen of the study, negative effects of increased isoniazid and pyrazinamide concentrations at 2- and 24-months emphasised that much is still unclear regarding the pharmacodynamic interactions between these drugs and the various outcome measures. Gatifloxacin exposure (AUC or C_{MAX}) was not significantly associated with either short- or long-term outcome in the CART analysis although simulations suggested higher doses were required for optimal outcome. This discrepancy is likely the result of the current pharmacokinetic study not including gatifloxacin MIC data as was the case for the simulation study which included MIC data within the PK/PD target (i.e. *f*AUC/MIC). Overall, drug exposure was a stronger predictor for 2-month culture conversion and 24-month long-term outcomes compared to non-pharmacokinetic factors including baseline parasite burden, cavity, and HIV status.

9. References

Acocella G (1978) Clinical pharmacokinetics of rifampicin. Clin Pharmacokinet 3:108–127. doi: 10.2165/00003088-197803020-00002

Acocella G (1983) Pharmacokinetics and metabolism of rifampin in humans. Rev Infect Dis 5:S428.

Ahmad Z, Fraig MM, Bisson GP, et al (2011) Dose-dependent activity of pyrazinamide in animal models of intracellular and extracellular tuberculosis infections. Antimicrob Agents Chemother 55:1527–32. doi: 10.1128/AAC.01524-10

Almeida D, Nuermberger E, Tasneen R, et al (2009a) Paradoxical effect of isoniazid on the activity of rifampin-pyrazinamide combination in a mouse model of tuberculosis. Antimicrob Agents Chemother 53:4178–84. doi: 10.1128/AAC.00830-09

Almeida D, Nuermberger E, Tasneen R, et al (2009b) Paradoxical effect of isoniazid on the activity of rifampin-pyrazinamide combination in a mouse model of tuberculosis. Antimicrob Agents Chemother 53:4178–4184. doi: 10.1128/AAC.00830-09

Alsultan A, Peloquin CA (2014) Therapeutic drug monitoring in the treatment of tuberculosis: an update. Drugs 74:839–54. doi: 10.1007/s40265-014-0222-8

Alvirez-Freites E, Carter J, Cynamon M (2002) In vitro and in vivo activities of gatifloxacin against *Mycobacterium tuberculosis*. Antimicrob Agents Chemother 46:1022–1025. doi: 10.1128/AAC.46.4.1022-1025.2002

Ambrose PG, Bhavnani SM, Cirincione BB, et al (2003) Gatifloxacin and the elderly: pharmacokinetic-pharmacodynamic rationale for a potential age-related dose reduction. J Antimicrob Chemother 52:435–440. doi: 10.1093/jac/dkg370

Anderson BJ, Holford NHG (2008) Mechanism-based concepts of size and maturity in pharmacokinetics. Annu Rev Pharmacol Toxicol 48:303–332. doi: 10.1146/annurev.pharmtox.48.113006.094708

Anderson BJ, Holford NHG (2009) Mechanistic basis of using body size and maturation to predict clearance in humans. Drug Metab Pharmacokinet 24:25–36. doi:

10.2133/dmpk.24.25

Awaness AM, Mitchison DA (1973) Cumulative effects of pulsed exposures of *Mycobacterium tuberculosis* to isoniazid. Tubercle 54:153–158. doi: 10.1016/0041-3879(73)90035-4

Babalik A, Kilicaslan Z, Caner SS, et al (2013) A registry-based cohort study of pulmonary tuberculosis treatment outcomes in Istanbul, Turkey. Jpn J Infect Dis 66:115–120. doi: 10.7883/yoken.66.115

Bach PH, Susan B, Bima B, Leary WP (1976) Isoniazid acetylator status of black South African tuberculosis patients. South African Med J 50:1132–1134.

Balasubramanian V, Solapure S, Gaonkar S, et al (2012) Effect of coadministration of moxifloxacin and rifampin on *Mycobacterium tuberculosis* in a murine aerosol infection model. Antimicrob Agents Chemother 56:3054–7. doi: 10.1128/AAC.06383-11

Bateman C (2013) Drug stock-outs: inept supply-chain management and corruption. South African Med. J. 103:600–602.

Beal S, Sheiner L, Boeckmann A, Bauer R (2009) NONMEM User's Guides 1989-2009.

Beal SL (2001) Ways to fit a PK model with some data below the quantification limit. J Pharmacokinet Pharmacodyn 28:481–504.

Benedetti MS, Dostert P (1994) Induction and autoinduction properties of rifamycin derivatives: a review of animal and human studies. Environ Health Perspect 102:101–105. doi: 10.1289/ehp.94102s9101

Bergstrand M, Hooker AC, Wallin JE, Karlsson MO (2011) Prediction- corrected visual predictive checks for diagnosing nonlinear mixed-effects models. AAPS J 13:134–151.

Bhardwaj RK, Glaeser H, Becquemont L, et al (2002) Piperine, a major constituent of black pepper, inhibits human P-glycoprotein and CYP3A4. J Pharmacol Exp Ther 302:645–50. doi: 10.1124/jpet.102.034728

Bhatt NB, Barau C, Amin A, et al (2014) Pharmacokinetics of rifampin and isoniazid in tuberculosis-HIV-coinfected patients receiving nevirapine- or efavirenz-based

antiretroviral treatment. Antimicrob Agents Chemother 58:3182–90. doi: 10.1128/AAC.02379-13

Blumberg HM, Burman WJ, Chaisson RE, et al (2003) American Thoracic Society/Centers for Disease Control and Prevention/Infectious Diseases Society of America: treatment of tuberculosis. Am J Respir Crit Care Med 167:603–662. doi: 10.1164/rccm.167.4.603

Boeree MJ, Diacon AH, Dawson R, et al (2015) A dose ranging trial to optimize the dose of rifampin in the treatment of tuberculosis. Am J Respir Crit Care Med 191:150205122801009. doi: 10.1164/rccm.201407-1264OC

Breiman L, Friedman J, Stone C, Olshen R (1984) Classification and regression trees. Boca Raton: Chapman and Hall/CRC

Burman WJ (2003) The hunt for the elusive surrogate marker of sterilizing activity in tuberculosis treatment. Am J Respir Crit Care Med 167:1299–1300. doi: 10.1164/rccm.2302005

Burman WJ, Goldberg S, Johnson JL, et al (2006) Moxifloxacin versus ethambutol in the first 2 months of treatment for pulmonary tuberculosis. Am J Respir Crit Care Med 174:331–8. doi: 10.1164/rccm.200603-360OC

Cambau E, Drancourt M (2014) Steps towards the discovery of *Mycobacterium tuberculosis* by Robert Koch, 1882. Clin Microbiol Infect 20:196–201. doi: 10.1111/1469-0691.12555

Campbell EA, Korzheva N, Mustaev A, et al (2001) Structural mechanism for rifampicin inhibition of bacterial RNA polymerase. Cell 104:901–912. doi: 10.1016/S0092-8674(01)00286-0

Chen J, Raymond K (2006) Roles of rifampicin in drug-drug interactions: underlying molecular mechanisms involving the nuclear pregnane X receptor. Ann Clin Microbiol Antimicrob 5:3. doi: 10.1186/1476-0711-5-3

Chideya S, Winston CA, Peloquin CA, et al (2009) Isoniazid, rifampin, ethambutol, and pyrazinamide pharmacokinetics and treatment outcomes among a predominantly HIV-infected cohort of adults with tuberculosis from Botswana. Clin Infect Dis 48:1685–94.

doi: 10.1086/599040

Chigutsa E, Pasipanodya JG, Visser ME, et al (2015) Impact of nonlinear interactions of pharmacokinetics and MICs on sputum bacillary kill rates as a marker of sterilizing effect in tuberculosis. Antimicrob Agents Chemother 59:38–45. doi: 10.1128/AAC.03931-14

Chigutsa E, Visser ME, Swart EC, et al (2011) The SLCO1B1 rs4149032 polymorphism is highly prevalent in South Africans and is associated with reduced rifampin concentrations: dosing implications. Antimicrob Agents Chemother 55:4122–7. doi: 10.1128/AAC.01833-10

Chirehwa M, Rustomjee R, Mthiyane T, et al (2014) Population pharmacokinetics of pyrazinamide among HIV/TB co-infected patients at different levels of immunosuppression in South Africa. In: 17th World Congress of Basic and Clinical Pharmacology.

Chirehwa MT, Rustomjee R, Mthiyane T, et al (2015) Model-based evaluation of higher doses of rifampicin using a semi-mechanistic model incorporating auto-induction and saturation of hepatic extraction. Antimicrob Agents Chemother 60:487–494. doi: 10.1128/AAC.01830-15

Choudhri SH, Hawken M, Gathua S, et al (1997) Pharmacokinetics of antimycobacterial drugs in patients with tuberculosis, AIDS, and diarrhea. Clin Infect Dis 25:104–111. doi: 10.1086/514513

Clayden P, Collins S, Damiels C, et al (2014) 2014 Pipeline Report HIV, Hepatitis (HCV), and Tuberculosis (TB) drugs, diagnosis, vaccines, prevention technologies, research toward a cure, and immune-based and gene therapies in development.

Cockcroft DW, Gault MH (1976) Prediction of creatinine clearance from serum creatinine. Nephron 16:31–41. doi: 10.1159/000180580

Conde MB, Efron A, Loredo C, et al (2009) Moxifloxacin versus ethambutol in the initial treatment of tuberculosis: a double-blind, randomised, controlled phase II trial. Lancet 373:1183–9. doi: 10.1016/S0140-6736(09)60333-0

Cosivi O, Grange JM, Daborn CJ, et al (1998) Zoonotic tuberculosis due to *Mycobacterium bovis* in developing countries. Emerg Infect Dis 4:59–70. doi: 10.3201/eid0401.980108

Crawford B (1948) Depression of the exogenous creatinine/inulin or thiosulphate clearance ratios in man by diodrast and p-aminohippuric acid. J Clin Invest 27:172–175.

Cynamon M, Sklaney MR, Shoen C (2007) Gatifloxacin in combination with rifampicin in a murine tuberculosis model. J Antimicrob Chemother 60:429–32. doi: 10.1093/jac/dkm200

da Silva PEA, Palomino JC (2011) Molecular basis and mechanisms of drug resistance in *Mycobacterium tuberculosis*: Classical and new drugs. J Antimicrob Chemother 66:1417–1430. doi: 10.1093/jac/dkr173

Davies G, Nuermberger E (2008) Pharmacokinetics and pharmacodynamics in the development of anti-tuberculosis drugs. Tuberculosis (Edinb) 88 Suppl 1:S65–74. doi: 10.1016/S1472-9792(08)70037-4

Denti P, Jeremiah K, Chigutsa E, et al (2015) Pharmacokinetics of isoniazid, pyrazinamide, and ethambutol in newly diagnosed pulmonary TB patients in Tanzania. PLoS One 10:e0141002. doi: 10.1371/journal.pone.0141002

Denti P, Smythe W, Simonsson US, et al (2010) A population pharmacokinetic model for rifampicin auto-induction. In: Proceedings of the 3rd Intl. Workshop on Clinical Pharmacology of TB Drugs.

Diacon AH, Patientia RF, Venter A, et al (2007) Early bactericidal activity of high-dose rifampin in patients with pulmonary tuberculosis evidenced by positive sputum smears. Antimicrob Agents Chemother 51:2994–6. doi: 10.1128/AAC.01474-06

Dickinson JM, Aber VR, Mitchison DA (1977) Bactericidal activity of streptomycin, isoniazid, rifampin, ethambutol, and pyrazinamide alone and in combination against Mycobacterium Tuberculosis. Am Rev Respir Dis 116:627–35.

Dickinson JM, Mitchison DA (1981) Experimental models to explain the high sterilizing activity of rifampin in the chemotherapy of tuberculosis. Am Rev Respir Dis 123:367–

71. doi: 10.1164/arrd.1981.123.4.367

Donald PR, Parkin DP, Seifart HI, et al (2007) The influence of dose and N-acetyltransferase-2 (NAT2) genotype and phenotype on the pharmacokinetics and pharmacodynamics of isoniazid. Eur J Clin Pharmacol 63:633–639. doi: 10.1007/s00228-007-0305-5

Donald PR, Sirgel FA, Botha FJ, et al (1997) The early bactericidal activity of isoniazid related to its dose size in pulmonary tuberculosis. Am J Respir Crit Care Med 156:895–900.

Dorman SE, Johnson JL, Goldberg S, et al (2009) Substitution of moxifloxacin for isoniazid during intensive phase treatment of pulmonary tuberculosis. Am J Respir Crit Care Med 180:273–80. doi: 10.1164/rccm.200901-0078OC

Drusano GL, Sgambati N, Eichas A, et al (2010) The combination of rifampin plus moxifloxacin is synergistic for suppression of resistance but antagonistic for cell kill of *Mycobacterium tuberculosis* as determined in a hollow-fiber infection model. MBio. doi: 10.1128/mBio.00139-10

Dubois A, Gsteiger S, Balser S, et al (2012) Pharmacokinetic similarity of biologics: analysis using nonlinear mixed-effects modeling. Clin Pharmacol Ther 91:234–42. doi: 10.1038/clpt.2011.216

Dutta NK, Karakousis PC (2015) Can the duration of tuberculosis treatment be shortened with higher dosages of rifampicin? Front Microbiol 6:1117. doi: 10.3389/fmicb.2015.01117

Faber K, Muller M, Jansen P (2003) Drug transport proteins in the liver. Adv Drug Deliv Rev 55:107–124.

Fahimi F, Tabarsi P, Kobarfard F, et al (2013) Isoniazid, rifampicin and pyrazinamide plasma concentrations 2 and 6 h post dose in patients with pulmonary tuberculosis. Int J Tuberc Lung Dis 17:1602–1606. doi: 10.5588/ijtld.13.0019

Forrest A, Nix DE, Ballow CH, et al (1993) Pharmacodynamics of intravenous ciprofloxacin in seriously ill patients. Antimicrob Agents Chemother 37:1073–1081. doi: 10.1128/AAC.37.5.1073.Updated

Fung-Tomc J, Minassian B, Kolek B, et al (2000) In vitro antibacterial spectrum of a new broad-spectrum 8-methoxy fluoroquinolone, gatifloxacin. J Antimicrob Chemother 45:437–446.

Gabrielsson JL, Weiner DL (1999) Methodology for pharmacokinetic/pharmacodynamic data analysis. Pharm. Sci. Technol. Today 2:244–252.

Gajjar DA, LaCreta FP, Uderman HD, et al (2000) A dose-escalation study of the safety, tolerability, and pharmacokinetics of intravenous gatifloxacin in healthy adult men. Pharmacotherapy 20:49S–58S.

Geick A, Eichelbaum M, Burk O (2001) Nuclear receptor response elements mediate induction of intestinal MDR1 by rifampin. J Biol Chem 276:14581–14587. doi: 10.1074/jbc.M010173200

Getahun H, Matteelli A, Abubakar I, et al (2015) Management of latent *Mycobacterium tuberculosis* infection: WHO guidelines for low tuberculosis burden countries. Eur Respir J 46:1563. doi: 10.1183/13993003.01245-2015

Gillespie SH, Crook AM, McHugh TD, et al (2014) Four-month moxifloxacin-based regimens for drug-sensitive tuberculosis. N Engl J Med 140907080012008. doi: 10.1056/NEJMoa1407426

Ginsburg AS, Grosset JH, Bishai WR (2003) Fluoroquinolones, tuberculosis, and resistance. Lancet Infect Dis 3:432–442. doi: 10.1016/S1473-3099(03)00671-6

Goldberg S (2016) TBTC study 31: rifapentine-containing tuberculosis treatment shortening regimens (S31/A5349). In: ClinicalTrials.org. https://clinicaltrials.gov/ct2/show/NCT02410772. Accessed 4 Jan 2016

Grasela DM (2000) Clinical pharmacology of gatifloxacin, a new fluoroquinolone. Clin Infect Dis 31 Suppl 2:S51–S58. doi: 10.1086/314061

Grosset J, Truffot-Pernot C, Lacroix C, Ji B (1992) Antagonism between isoniazid and the combination pyrazinamide-rifampin against tuberculosis infection in mice. Antimicrob Agents Chemother 36:548–51.

Gumbo T, Angulo-Barturen I, Ferrer-Bazaga S (2015) Pharmacokinetic-pharmacodynamic and dose-response relationships of antituberculosis drugs: recommendations and standards for industry and academia. J Infect Dis 211 Suppl:S96–S106. doi: 10.1093/infdis/jiu610

Gumbo T, Dona CSWS, Meek C, Leff R (2009) Pharmacokinetics-pharmacodynamics of pyrazinamide in a novel in vitro model of tuberculosis for sterilizing effect: a paradigm for faster assessment of new antituberculosis drugs. Antimicrob Agents Chemother 53:3197–204. doi: 10.1128/AAC.01681-08

Gumbo T, Louie A, Deziel MR, et al (2007a) Concentration-dependent *Mycobacterium tuberculosis* killing and prevention of resistance by rifampin. Antimicrob Agents Chemother 51:3781–8. doi: 10.1128/AAC.01533-06

Gumbo T, Louie A, Liu W, et al (2007b) Isoniazid's bactericidal activity ceases because of the emergence of resistance, not depletion of *Mycobacterium tuberculosis* in the log phase of growth. Antimicrob Agents Chemother 9113:194–201. doi: 10.1128/AAC.00185-07

Gumbo T, Louie A, Liu W, et al (2007c) Isoniazid bactericidal activity and resistance emergence: integrating pharmacodynamics and pharmacogenomics to predict efficacy in different ethnic populations. Antimicrob Agents Chemother 51:2329–36. doi: 10.1128/AAC.00185-07

Gurumurthy P, Ramachandran G, Hemanth Kumar AK, et al (2004) Decreased bioavailability of rifampin and other antituberculosis drugs in patients with advanced human immunodeficiency virus disease. Antimicrob Agents Chemother 48:4473–4475. doi: 10.1128/AAC.48.11.4473-4475.2004

Hall RG, Leff RD, Gumbo T (2009) Treatment of active pulmonary tuberculosis in adults: current standards and recent advances. Insights from the Society of Infectious Diseases Pharmacists. Pharmacotherapy 29:1468–1481. doi: 10.1592/phco.29.12.1468

Harling K, Ueckert S, Hooker AC, et al (2010) Abstract 1842. In: PAGE 19.

Hassan M, Svensson USH, Ljungman P, et al (1999) A mechanism-based pharmacokinetic-enzyme model for cyclophosphamide autoinduction in breast cancer patients. Br J Clin

Pharmacol 48:669–677. doi: 10.1046/j.1365-2125.1999.00090.x

Heep M, Rieger U, Beck D, Lehn N (2000) Mutations in the beginning of the rpoB gene can induce resistance to rifamycins in both *Helicobacter pylori* and *Mycobacterium tuberculosis*. Antimicrob Agents Chemother 44:1075–1077.

Holford NHG (2005) Abstract 738. In: PAGE 14.

Holford NHG (1996) A size standard for pharmacokinetics. Clin Pharmacokinet 30:329–332.

Holford NHG, Karlsson MO (2008) Abstract 1434. In: PAGE 17.

Honeybourne D, Banerjee D, Andrews J, Wise R (2001) JAC Concentrations of gatifloxacin in plasma and pulmonary compartments following a single 400 mg oral dose in patients undergoing fibre-optic bronchoscopy. J Antimicrob Chemother 48:63–66.

Hong Kong Chest Service / British Medical Research Council (1982) Controlled trial of 4 three-times-weekly regimens and a daily regimen all given for 6 months for pulmonary tuberculosis. Second report: the results up to 24 months. Tubercle 63:89–98. doi: 10.1016/S0041-3879(82)80044-5

Hu Y, Liu A, Ortega-Muro F, et al (2015) High-dose rifampicin kills persisters, shortens treatment duration, and reduces relapse rate in vitro and in vivo. Front Microbiol 6:641. doi: 10.3389/fmicb.2015.00641

Hutchings A, Monie RD, Spragg B, Routledge PA (1983) A method to prevent the loss of isoniazid and acetylisoniazid in human plasma. Br J Clin Pharmacol 15:263–6.

Jamis-Dow C a, Katki a G, Collins JM, Klecker RW (1997) Rifampin and rifabutin and their metabolism by human liver esterases. Xenobiotica 27:1015–1024. doi: 10.1080/004982597239994

Jayaram R, Gaonkar S, Kaur P, et al (2003) Pharmacokinetics-pharmacodynamics of rifampin in an aerosol infection model of tuberculosis. Antimicrob Agents Chemother 47:2118–2124. doi: 10.1128/AAC.47.7.2118-2124.2003

Jayaram R, Shandil RK, Gaonkar S, et al (2004) Isoniazid pharmacokinetics-pharmacodynamics in an aerosol infection model of tuberculosis. Antimicrob Agents

Chemother 48:2951–7. doi: 10.1128/AAC.48.8.2951-2957.2004

Jindani A, Doré CJ, Mitchison DA (2003) Bactericidal and sterilizing activities of antituberculosis drugs during the first 14 days. Am J Respir Crit Care Med 167:1348–1354. doi: 10.1164/rccm.200210-1125OC

Jindani A, Harrison TS, Nunn AJ, et al (2014) High-dose rifapentine with moxifloxacin for pulmonary tuberculosis. N Engl J Med 371:1599–1608. doi: 10.1056/NEJMoa1314210

Johnson JL, Hadad DJ, Boom WH, et al (2006) Early and extended early bactericidal activity of levofloxacin , gatifloxacin and moxifloxacin in pulmonary tuberculosis. Int J Tuberc Lung Dis 10:605–612.

Jonsson EN, Karlsson MO (1998) Xpose - An S-PLUS based population pharmacokinetic/pharmacodynamic model building aid for NONMEM. Comput Methods Programs Biomed 58:51–64. doi: 10.1016/S0169-2607(98)00067-4

Jönsson S, Davidse A, Wilkins J, et al (2011) Population pharmacokinetics of ethambutol in South African tuberculosis patients. Antimicrob Agents Chemother 55:4230–4237. doi: 10.1128/AAC.00274-11

Kanabus A (2016) TBFacts.org. http://www.tbfacts.org/. Accessed 4 Jan 2016

Karumbi J, Garner P (2015) Directly observed therapy for treating tuberculosis. Cochrane database Syst Rev 5:CD003343. doi: 10.1002/14651858.CD003343.pub4

Khandelwal A, Harling K, Jonsson EN, et al (2011) A fast method for testing covariates in population PK/PD Models. AAPS J 13:464–72. doi: 10.1208/s12248-011-9289-2

Kwatra D, Vadlapatla RK, Vadlapudi AD, et al (2010) Interaction of gatifloxacin with efflux transporters: a possible mechanism for drug resistance. Int J Pharm 395:114–21. doi: 10.1016/j.ijpharm.2010.05.027

LaPlante K, Mersfelder T, Ward K, Quilliam B (2008) Prevalence of and risk factors for dysglycemia in patients receiving gatifloxacin and levofloxacin in an outpatient setting . Pharmacotherapy 28:82–89.

Lee CN, Heifets LB (1987) Determination of minimal inhibitory concentrations of

antituberculosis drugs by radiometric and conventional methods. Am Rev Respir Dis 136:349–52. doi: 10.1164/ajrccm/136.2.349

Lee CS, Brater DC, Garnbertoglio G, et al (1980) Kinetics of oral ethambutol in the normal subject. J Pharmacokinet Biopharm 22:615–621.

Lin J (2003) Drug-drug interaction mediated by inhibition and induction of P-glycoprotein. Adv Drug Deliv Rev 55:53 – 81.

Lindbom L, Pihlgren P, Jonsson EN (2005) PsN-Toolkit - a collection of computer intensive statistical methods for non-linear mixed effect modeling using NONMEM. Comput Methods Programs Biomed 79:241–257.

Loktionov A, Moore W, Spencer SP, et al (2002) Differences in N -acetylation genotypes between Caucasians and Black South Africans : implications for cancer prevention. Cancer Detect Prev 26:15–22.

Loos U, Musch E, Jensen JC, et al (1985) Pharmacokinetics of oral and intravenous rifampicin during chronic administration. Klin Wochenschr 63:1205–1211.

Loos U, Musch E, Jensen JC, et al (1987) Influence of the enzyme induction by rifampicin on its presystemic metabolism. Pharmacol Ther Ther 33:201–204. doi: 10.1016/0163-7258(87)90052-0

McIlleron H, Meintjes G, Burman WJ, Maartens G (2007a) Complications of antiretroviral therapy in patients with tuberculosis: drug interactions, toxicity, and immune reconstitution inflammatory syndrome. J Infect Dis 196:S63–S75. doi: 10.1086/518655

McIlleron H, Norman J, Kanyok TP, et al (2007b) Elevated gatifloxacin and reduced rifampicin concentrations in a single-dose interaction study amongst healthy volunteers. J Antimicrob Chemother 60:1398–401. doi: 10.1093/jac/dkm393

McIlleron H, Rustomjee R, Vahedi M, et al (2012) Reduced antituberculosis drug concentrations in HIV-infected patients who are men or have low weight: implications for international dosing guidelines. Antimicrob Agents Chemother 56:3232–3238. doi: 10.1128/AAC.05526-11

McIlleron H, Wash P, Burger A, et al (2006) Determinants of rifampin, isoniazid, pyrazinamide, and ethambutol pharmacokinetics in a cohort of tuberculosis patients. Antimicrob Agents Chemother 50:1170–1177. doi: 10.1128/AAC.50.4.1170-1177.2006

Mehlhorn AJ, Brown DA (2007) Safety concerns with fluoroquinolones. Ann Pharmacother 41:1859–66. doi: 10.1345/aph.1K347

Merle CS, Fielding K, Sow OB, et al (2014) A four-month gatifloxacin-containing regimen for treating tuberculosis. N Engl J Med 371:1588–1598. doi: 10.1056/NEJMoa1315817

Mignot A, Brault M, Millérioux L, Stahlberg H (2002) Multiple-dose pharmacokinetics and excretion balance of Gatifloxacin , a new fluoroquinolone antibiotic , following oral administration to healthy caucasian volunteers. Chemotherapy 48:116–121.

Mitchison D, Coates A (2004) Predictive in vitro models of the sterilizing activity of anti-tuberculosis drugs. Curr Pharm Des 10:3285–3295. doi: 10.2174/1381612043383269

Mitchison D, Davies G (2012) The chemotherapy of tuberculosis: past, present and future. Int J Tuberc Lung Dis 16:724–32. doi: 10.5588/ijtld.12.0083

Mitchison DA (2000) Role of individual drugs in the chemotherapy of tuberculosis. Int. J. Tuberc. Lung Dis. 4:796–806.

Mitchison DA (1993) Assessment of new sterilizing drugs for treating pulmonary tuberculosis by culture at 2 months. Am Rev Respir Dis 147:1062–3. doi: 10.1164/ajrccm/147.4.1062

Mitchison DA, Jindani A, Davies GR, Sirgel F (2007) Isoniazid activity is terminated by bacterial persistence. J Infect Dis 195:1871–1872. doi: 10.1086/518046

Mitnick CD, McGee B, Peloquin CA (2009) Tuberculosis pharmacotherapy: strategies to optimize patient care. Expert Opin Pharmacother 10:381–401. doi: 10.1517/14656560802694564

Moreira A da SR, Huf G, Vieira MAM da S, et al (2015) Liquid vs solid culture medium to evaluate proportion and time to change in management of suspects of tuberculosis - a pragmatic randomized trial in secondary and tertiary health care units in Brazil. PLoS

One 10:e0127588. doi: 10.1371/journal.pone.0127588

Mouton JW, Dudley MN, Cars O, et al (2005a) Standardization of pharmacokinetic/pharmacodynamic (PK/PD) terminology for anti-infective drugs: an update. J Antimicrob Chemother 55:601–7. doi: 10.1093/jac/dki079

Mouton JW, Punt N, Vinks AA (2005b) A retrospective analysis using Monte Carlo simulation to evaluate recommended ceftazidime dosing regimens in healthy volunteers, patients with cystic fibrosis, and patients in the intensive care unit. Clin Ther 27:762–72. doi: 10.1016/j.clinthera.2005.06.013

Müller B, Dürr S, Alonso S, et al (2013) Zoonotic *Mycobacterium bovis* – induced tuberculosis in humans. Emerg Infect Dis 19:899–908.

Nakajima A, Fukami T, Kobayashi Y, et al (2011) Human arylacetamide deacetylase is responsible for deacetylation of rifamycins: rifampicin, rifabutin, and rifapentine. Biochem Pharmacol 82:1747–56. doi: 10.1016/j.bcp.2011.08.003

Nakashima M, Uematsu T, Kosuge K, et al (1995) Single- and multiple-dose pharmacokinetics of AM-1155, a new 6-fluoro-8-methoxy quinolone, in humans. Antimicrob Agents Chemother 39:2635–2640. doi: 10.1128/AAC.39.12.2635.Updated

Niemi M, Backman JT, Fromm MF, et al (2003) Pharmacokinetic interactions with Rifampicin. Clin Pharmacokinet 42:819–850. doi: 10.2165/00003088-200342090-00003

Nuermberger E, Grosset J (2004) Pharmacokinetic and pharmacodynamic issues in the treatment of mycobacterial infections. Eur J Clin Microbiol Infect Dis 23:243–55. doi: 10.1007/s10096-004-1109-5

Nuermberger EL, Yoshimatsu T, Tyagi S, et al (2004) Moxifloxacin-containing regimen greatly reduces time to culture conversion in murine tuberculosis. Am J Respir Crit Care Med 169:421–6. doi: 10.1164/rccm.200310-1380OC

Pantel A, Petrella S, Matrat S, et al (2011) DNA gyrase inhibition assays are necessary to demonstrate fluoroquinolone resistance secondary to gyrB mutations in *Mycobacterium tuberculosis*. Antimicrob Agents Chemother 55:4524–9. doi:

10.1128/AAC.00707-11

Paramasivan CN, Sulochana S, Kubendiran G, et al (2005) Bactericidal action of gatifloxacin, rifampin, and isoniazid on logarithmic- and stationary-phase cultures of *Mycobacterium tuberculosis*. Antimicrob Agents Chemother 49:627–31. doi: 10.1128/AAC.49.2.627-631.2005

Parkin DP, Vandenplas S, Botha FJ, et al (1997) Trimodality of isoniazid elimination: phenotype and genotype in patients with tuberculosis. Am J Respir Crit Care Med 155:1717–22. doi: 10.1164/ajrccm.155.5.9154882

Park-Wyllie LY, Juurlink DN, Kopp A, et al (2006) Outpatient gatifloxacin therapy and dysglycemia in older adults. N Engl J Med 354:1352–1361.

Pasipanodya J, Gumbo T (2011) An oracle: antituberculosis pharmacokinetics-pharmacodynamics, clinical correlation, and clinical trial simulations to predict the future. Antimicrob Agents Chemother 55:24–34. doi: 10.1128/AAC.00749-10

Pasipanodya J, Srivastava S, Gumbo T (2012) Meta-analysis of clinical studies supports the pharmacokinetic variability hypothesis for acquired drug resistance and failure of antituberculosis therapy. Clin Infect Dis 55:169–177. doi: 10.1093/cid/cis353

Pasipanodya JG, McIlleron H, Burger A, et al (2013) Serum drug concentrations predictive of pulmonary tuberculosis outcomes. J Infect Dis 208:1464–73. doi: 10.1093/infdis/jit352

Patin E, Harmant C, Kidd KK, et al (2006) Sub-Saharan African coding sequence variation and haplotype diversity at the NAT2 gene. Hum Mutat 27:720. doi: 10.1002/humu.9438

Peloquin C (2003) What is the “right” dose of rifampin? Int. J. Tuberc. Lung Dis. 7:3–5.

Peloquin CA (2002) Therapeutic drug monitoring in the treatment of tuberculosis. Drugs 62:2169–2183. doi: 10.2165/00003495-200262150-00001

Peloquin CA (1999) Pharmacokinetics of rifampin under fasting conditions, with food, and with antacids. Chest 115:12. doi: 10.1378/chest.115.1.12

Peloquin CA, Bulpitt AE, Jaresko GS, et al (1998) Pharmacokinetics of pyrazinamide under fasting conditions, with food, and with antacids. Pharmacother J Hum Pharmacol Drug

Ther 18:1205–1211. doi: 10.1002/j.1875-9114.1998.tb03138.x

Peloquin CA, Bulpitt AMYE, Jaresko GS, et al (1999a) Pharmacokinetics of ethambutol under fasting conditions, with food, and with antacids. Antimicrob Agents Chemother 43:568–572.

Peloquin CA, Hadad DJ, Molino LPD, et al (2008) Population pharmacokinetics of levofloxacin, gatifloxacin, and moxifloxacin in adults with pulmonary tuberculosis. Antimicrob Agents Chemother 52:852–7. doi: 10.1128/AAC.01036-07

Peloquin CA, Jaresko GS, Yong CL, et al (1997) Population pharmacokinetic modeling of isoniazid, rifampin, and pyrazinamide. Antimicrob Agents Chemother 41:2670–9.

Peloquin CA, Namdar R, Dodge AA, Nix DE (1999b) Pharmacokinetics of isoniazid under fasting conditions, with food, and with antacids. Int J Tuberc lung Dis 3:703–10.

Perlman DC, Segal Y, Rosenkranz S, et al (2005) The clinical pharmacokinetics of rifampin and ethambutol in HIV-infected persons with tuberculosis.

Perrin FMR, Lipman MCI, McHugh TD, Gillespie SH (2007) Biomarkers of treatment response in clinical trials of novel antituberculosis agents. Lancet Infect Dis 7:481–90. doi: 10.1016/S1473-3099(07)70112-3

Perry CM, Barman Balfour JA, Lamb HM (1999) Gatifloxacin. Drugs 58:683–696. doi: 10.2165/00003495-199958040-00010

Pillai G, Davies G, Denti P, et al (2013) Pharmacometrics: opportunity for reducing disease burden in the developing world: the case of Africa. CPT pharmacometrics Syst Pharmacol 2:e69. doi: 10.1038/psp.2013.45

Prahl JB, Johansen IS, Cohen AS, et al (2014) Clinical significance of 2 h plasma concentrations of first-line anti-tuberculosis drugs: a prospective observational study. J Antimicrob Chemother 69:2841–7. doi: 10.1093/jac/dku210

Prideaux B, Via LE, Zimmerman MD, et al (2015) The association between sterilizing activity and drug distribution into tuberculosis lesions. Nat Med 21:1223–7. doi: 10.1038/nm.3937

Rangaka MX, Cavalcante SC, Marais BJ, et al (2015) Controlling the seedbeds of tuberculosis: diagnosis and treatment of tuberculosis infection. Lancet 386:2344–2353. doi: 10.1016/S0140-6736(15)00323-2

Rastogi N, Labrousse V, Goh KS (1996) In vitro activities of fourteen antimicrobial agents against drug susceptible and resistant clinical isolates of *Mycobacterium tuberculosis* and comparative intracellular activities against the virulent H37Rv strain in human macrophages. Curr Microbiol 33:167–175. doi: 10.1007/s002849900095

Rodriguez J, Ruiz M, Lo M, Royo G (2002) In vitro activity of moxifloxacin, levofloxacin , gatifloxacin and linezolid against *Mycobacterium tuberculosis*. Int J Antimicrob Agents 20:464–467.

Ruslami R, Nijland H, Aarnoutse R (2006) Evaluation of high- versus standard-dose rifampin in Indonesian patients with pulmonary tuberculosis. Antimicrob Agents Chemother 50:822–823. doi: 10.1128/AAC.50.2.822

Ruslami R, Nijland HMJ, Alisjahbana B, et al (2007) Pharmacokinetics and tolerability of a higher rifampin dose versus the standard dose in pulmonary tuberculosis patients. Antimicrob Agents Chemother 51:2546–51. doi: 10.1128/AAC.01550-06

Rustomjee R, Lienhardt C, Kanyok T, et al (2008) A Phase II study of the sterilising activities of ofloxacin , gatifloxacin and moxifloxacin in pulmonary tuberculosis. Int J Tuberc Lung Dis 12:128–138.

Sabbagh A, Langaney A, Darlu P, et al (2008) Worldwide distribution of NAT2 diversity: implications for NAT2 evolutionary history. BMC Genet 9:21. doi: 10.1186/1471-2156-9-21

Sahai J, Gallicano K, Swick L, et al (1997) Reduced plasma concentrations of antituberculosis drugs in patients with HIV infection. Ann Intern Med 127:289 – 293.

Sahota T, Della Pasqua O (2012) Feasibility of a fixed-dose regimen of pyrazinamide and its impact on systemic drug exposure and liver safety in patients with tuberculosis. Antimicrob Agents Chemother 56:5442–9. doi: 10.1128/AAC.05988-11

Saleri N, Dembélé SM, Villani P, et al (2012) Systemic exposure to rifampicin in patients with tuberculosis and advanced HIV disease during highly active antiretroviral therapy in Burkina Faso. J Antimicrob Chemother 67:469–72. doi: 10.1093/jac/dkr445

Salfinger M, Heifets LB (1988) Determination of pyrazinamide MICs for *Mycobacterium tuberculosis* at different pHs by the radiometric method. Antimicrob Agents Chemother 32:1002–1004.

Sato K, Tomioka H, Sano C, et al (2003) Comparative antimicrobial activities of gatifloxacin, sitafloxacin and levofloxacin against *Mycobacterium tuberculosis* replicating within Mono Mac 6 human macrophage and A-549 type II alveolar cell lines. J Antimicrob Chemother 52:199–203. doi: 10.1093/jac/dkg343

Savic RM, Jonker DM, Kerbusch T, O. KM (2007) Implementation of a transit compartment model for describing drug absorption in pharmacokinetic studies. J Pharmacokinet Pharmacodyn 34:711–726.

Schentag JJ (2000) Clinical pharmacology of the fluoroquinolones: studies in human dynamic/kinetic models. Clin Infect Dis 31 Suppl 2:S40–4. doi: 10.1086/314059

Schentag JJ, Gilliland KK, Paladino JA (2001) What have we learned from pharmacokinetic and pharmacodynamic theories? Pharmacology 14260:39–46.

Schuetz EG, Beck WT, Schuetz JD (1996) Modulators and substrates of P-glycoprotein and cytochrome P4503A coordinately up-regulate these proteins in human colon carcinoma cells. Mol Pharmacol 49:311–318.

Shleeva MO, Bagramyan K, Telkov M V, et al (2002) Formation and resuscitation of “non-culturable” cells of *Rhodococcus rhodochrous* and *Mycobacterium tuberculosis* in prolonged stationary phase. Microbiology 148:1581–91. doi: 10.1099/00221287-148-5-1581

Singh M, Chauhan DS, Gupta P, et al (2009) In vitro effect of fluoroquinolones against *Mycobacterium tuberculosis* isolates from Agra & Kanpur region of north India. Indian J Med Res 129:542–547.

Sirgel FA, Donald PR, Odhiambo J, et al (2000) A multicentre study of the early bactericidal activity of anti-tuberculosis drugs. J Antimicrob Chemother 45:859–870.

Smythe W, Khandelwal A, Merle C, et al (2012) A semimechanistic pharmacokinetic-enzyme turnover model for rifampin autoinduction in adult tuberculosis patients. Antimicrob Agents Chemother 56:2091–8. doi: 10.1128/AAC.05792-11

Srivastava S, Musuka S, Sherman C, et al (2010) Efflux-pump-derived multiple drug resistance to ethambutol monotherapy in *Mycobacterium tuberculosis* and the pharmacokinetics and pharmacodynamics of ethambutol. J Infect Dis 201:1225–31. doi: 10.1086/651377

Staudinger JL, Xu C, Cui YJ, Klaassen CD (2010) Nuclear receptor-mediated regulation of carboxylesterase expression and activity. Expert Opin Drug Metab Toxicol 6:261–271. doi: 10.1517/17425250903483215

Steinberg D, Colla P (1995) CART: tree structured nonparametric data analysis.

Strobl C, Malley J, Tutz G (2009) An introduction to recursive partitioning: rationale, application, and characteristics of classification and regression trees, bagging, and random forests. Psychol Methods 14:323–48. doi: 10.1037/a0016973

Sulochana S, Rahman F, Paramasivan CN (2005) In vitro activity of fluoroquinolones against *Mycobacterium tuberculosis*. J Chemother 17:169–73. doi: 10.1179/joc.2005.17.2.169

Suo J, Chang CE, Lin TP, Heifets LB (1988) Minimal inhibitory concentrations of isoniazid, rifampin, ethambutol, and streptomycin against *Mycobacterium tuberculosis* strains isolated before treatment of patients in Taiwan. Am Rev Respir Dis 138:999–1001. doi: 10.1164/ajrccm/138.4.999

Tappero JW, Bradford WZ, Agerton TB, et al (2005) Serum concentrations of antimycobacterial drugs in patients with pulmonary tuberculosis in Botswana. Clin Infect Dis 41:461–469. doi: 10.1086/431984

Tasso L, Bettoni CC, Oliveira LK, Dalla Costa T (2008) Evaluation of gatifloxacin penetration into skeletal muscle and lung by microdialysis in rats. Int J Pharm 358:96–101. doi:

10.1016/j.ijpharm.2008.02.023

Thwaites GE, Bhavnani SM, Chau TTH, et al (2011) Randomized pharmacokinetic and pharmacodynamic comparison of fluoroquinolones for tuberculous meningitis. Antimicrob Agents Chemother 55:3244–53. doi: 10.1128/AAC.00064-11

Timmins GS, Deretic V (2006) Mechanisms of action of isoniazid. Mol Microbiol 62:1220–1227. doi: 10.1111/j.1365-2958.2006.05467.x

Tomioka H, Sato K, Akaki T, Kajitani H (1999) Comparative in vitro antimicrobial activities of the newly synthesized quinolone HSR-903, sitafloxacin (DU-6859a), gatifloxacin (AM-1155), and levofloxacin against *Mycobacterium tuberculosis* and *Mycobacterium avium* complex. Antimicrob Agents Chemother 43:3001–3004.

Torres-Gonzalez P, Soberanis-Ramos O, Martinez-Gamboa A, et al (2013) Prevalence of latent and active tuberculosis among dairy farm workers exposed to cattle infected by *Mycobacterium bovis*. PLoS Negl Trop Dis 7:e2177. doi: 10.1371/journal.pntd.0002177

Tostmann A, Mtabho CM, Semvua HH, et al (2013) Pharmacokinetics of first-line tuberculosis drugs in Tanzanian patients. Antimicrob Agents Chemother 57:3208–13. doi: 10.1128/AAC.02599-12

Touré A, Diop C, Cabral M, et al (2012) Study of NAT2 genetic polymorphism in West African subjects: example of an healthy non-smoker Senegalese population. Mol Biol Rep 39:10489–96. doi: 10.1007/s11033-012-1931-2

Tuberculosis Research Center (2002) Shortening short course chemotherapy: A randomized clinical trial for treatment of smear positive pulmonary tuberculosis with regimens using ofloxacin in. Indian J Tuberc 49:27–38.

Um S, Lee SW, Kwon SY, et al (2007) Low serum concentrations of anti-tuberculosis drugs and determinants of their serum levels. Int J Tuberc Lung Dis 11: 972-978.

van den Boogaard J, Kibiki GS, Kisanga ER, et al (2009) New drugs against tuberculosis: problems, progress, and evaluation of agents in clinical development. Antimicrob Agents Chemother 53:849–62. doi: 10.1128/AAC.00749-08

van Ingen J, Aarnoutse RE, Donald PR, et al (2011) Why do we use 600 mg of rifampicin in tuberculosis treatment? Clin Infect Dis 52:e194–9. doi: 10.1093/cid/cir184

Wallis RS, Vinhas SA, Johnson JL, et al (2003) Whole blood bactericidal activity during treatment of pulmonary tuberculosis. J Infect Dis 187:270–278. doi: 10.1086/346053

Wayne L, Hayes L (1996) An in vitro model for sequential study of shiftdown of *Mycobacterium tuberculosis* through two stages of nonreplicating persistence. Infect Immun 64:2062–2069.

Weber W, Hein D (1979) Clinical pharmacokinetics of isoniazid. Clin Pharmacokinet 4:401–422.

Werngren J, Sturegård E, Juréen P, et al (2012) Reevaluation of the critical concentration for drug susceptibility testing of *Mycobacterium tuberculosis* against pyrazinamide using wild-type MIC distributions and pncA gene sequencing. Antimicrob Agents Chemother 56:1253–1257. doi: 10.1128/AAC.05894-11

West GB, Brown JH, Enquist BJ (1997) A general model for the origin of allometric scaling laws in biology. Science (80-) 276:122–6. doi: 10.1126/science.276.5309.122

West GB, Enquist BJ, Brown JH (1999) The fourth dimension of life: fractal geometry and allometric scaling of organisms. Science (80-) 284:1677–1679. doi: 10.1126/science.284.5420.1677

Wilby KJ, Ensom MHH, Marra F (2014) Review of evidence for measuring drug concentrations of first-line antitubercular agents in adults. Clin Pharmacokinet 53:873–90. doi: 10.1007/s40262-014-0170-1

Wilkins JJ, Langdon G, McIlleron H, et al (2011) Variability in the population pharmacokinetics of isoniazid in South African tuberculosis patients. Br J Clin Pharmacol 72:51–62. doi: 10.1111/j.1365-2125.2011.03940.x

Wilkins JJ, Langdon G, McIlleron H, et al (2006) Variability in the population pharmacokinetics of pyrazinamide in South African tuberculosis patients. Eur J Clin Pharmacol 62:727–35. doi: 10.1007/s00228-006-0141-z

Wilkins JJ, Savic RM, Karlsson MO, et al (2008) Population pharmacokinetics of rifampin in pulmonary tuberculosis patients, including a semimechanistic model to describe variable absorption. Antimicrob Agents Chemother 52:2138–48. doi: 10.1128/AAC.00461-07

World Health Organization (2006) Guidelines for the programmatic management of drug-resistant tuberculosis.

World Health Organization (2010) Treatment of tuberculosis: guidelines.

World Health Organization (2011) Global Tuberculosis Control.

World Health Organization (2013) Global Tuberculosis Report 2013.

World Health Organization (2014a) Guidelines on the management of latent tuberculosis infection.

World Health Organization (2014b) Global Tuberculosis Report 2014.

World Health Organization (2015) Global Tuberculosis Report 2015.

World Health Organization (2016) The shorter MDR-TB regimen.

Zhang Y (2004) Persistent and dormant tubercle bacilli and latent tuberculosis. Front Biosci 1:113611–56.

Zhang Y, Mitchison D (2002) The curious characteristics of pyrazinamide: a review. Int J Tuberc Lung Dis 7:6–21.

Zhang Y, Scorpio A, Nikaido H, Sun Z (1999) Role of acid pH and deficient efflux of pyrazinoic acid in unique susceptibility of *Mycobacterium tuberculosis* to pyrazinamide. J Bacteriol 181:2044–2049.

Zhu M, Burman WJ, Starke JR, et al (2004) Pharmacokinetics of ethambutol in children and adults with tuberculosis. Int J Tuberc Lung Dis 8:1360–1367.

Zhu R, Kiser JJ, Seifart HI, et al (2012) The pharmacogenetics of NAT2 enzyme maturation in perinatally HIV exposed infants receiving isoniazid. J Clin Pharmacol 52:511–9. doi: 10.1177/0091270011402826

Zumla A, Nahid P, Cole ST (2013) Advances in the development of new tuberculosis drugs and treatment regimens. Nat Rev Drug Discov 12:388–404. doi: 10.1038/nrd4001

Zvada SP, Van Der Walt J-S, Smith PJ, et al (2010) Effects of four different meal types on the population pharmacokinetics of single-dose rifapentine in healthy male volunteers. Antimicrob Agents Chemother 54:3390–3394. doi: 10.1128/AAC.00345-10